IAEA
International Atomic Energy Agency

INDC(KAS)-0001
Distr. NC

INDC International Nuclear Data Committee

Proceedings of the

Fourth Asian Nuclear Reaction Database Development Workshop

al-Farabi Kazakh National University, Almaty, Kazakhstan

23 – 25 October 2013

Edited by

Nurgaly Takibayev[1], Naohiko Otsuka[2], Nurzat Kenzhebayev[1]

[1]al-Farabi Kazakh National University, Almaty, Kazakhstan
[2]Nuclear Data Section, International Atomic Energy Agency, Vienna, Austria

February 2014

IAEA Nuclear Data Section, Vienna International Centre, A-1400 Vienna, Austria

Selected INDC documents may be downloaded in electronic form from
http://www-nds.iaea.org/publications/
or sent as an e-mail attachment.
Requests for hardcopy or e-mail transmittal should be directed to
nds.contact-point@iaea.org
or to:

Nuclear Data Section
International Atomic Energy Agency
Vienna International Centre
PO Box 100
A-1400 Vienna
Austria

Produced by the IAEA in Austria
February 2014

INDC (KAS)-0001
Distr. G+NC

Proceedings of the

Fourth Asian Nuclear Reaction Database Development Workshop

al-Farabi Kazakh National University, Almaty, Kazakhstan

23 – 25 October 2013

Edited by

Nurgaly Takibayev[1], Naohiko Otsuka[2], Nurzat Kenzhebayev[1]

[1]al-Farabi Kazakh National University, Almaty, Kazakhstan
[2]Nuclear Data Section, International Atomic Energy Agency, Vienna, Austria

February 2014

Abstract

This report summarizes the Fourth Asian Nuclear Reaction Database Development Workshop held at the al-Farabi Kazakh National University in Almaty, Kazakhstan from 23 to 25 October 2013. The workshop was attended by 36 participants from five countries and one international organization. Furthermore the workshop was attended by students and interested specialists. The approved program of the workshop has been slightly modified during its work. A summary of each presentation is given in this report.

The 4th Asian Nuclear Reaction Database Development Workshop

Honorable Committee

Mutanov G.M. - Rector of al-Farabi Kazakh National University (al-Farabi KazNU);
Kozhamkulov T.A. - Academician of Kazakh National Academy of Sciences (Kaz NAS);
Zhantikin T.M. - Head of Atomic Energy Committee of Republic of Kazakhstan (AEC RK);
Batyrbekov E.G. – Director General of National Nuclear Center of Republic of Kazakhstan (NNC RK);
Salikhbaev U.S. – Director of Institute of Nuclear Physics of Uzbekistan Academy of Sciences (INP Uzb AS).

Program Organizers

Aikawa M., Hokkaido University, Japan
Artemov S., INP Uzb AS, Uzbekistan
Burtebaev N., Nuclear Physics Institute, Kazakhstan
Davaa S., National University of Mongolia
Ge Z., China Institute of Atomic Energy
Kato K., Hokkaido University, Japan
Kim G., Kyungpook National Univ., South Korea
Lee Y., Korea Atomic Energy Research Institute
Otsuka N., International Atomic Energy Agency, Austria
Saxena A., Bhabha Atomic Research Centre, India
Semkova V., International Atomic Energy Agency, Austria
Takibayev N., al-Farabi KazNU, Kazakhstan
Varlamov V., Moscow State University, Russia
Yarmukhamedov R., INP Uzb AS

Local Organizers

Burkitbaev M.M.; Ramazanov T.S.; Abishev M.E.; Davletov A.E.; Takibayev N.Zh. – chairman;
Workshop secretariat: Zhumabekova V.N., Kurmangalieva V.O., Kenzhebayev N.B.;
Tel.: +(7-727)-377-34-14; +(7-727)-377-34-58;
E-mail: ca.nrdb@gmail.com
Mailing address:
Physico-Technical Faculty, al-Farabi ave., 71, al-Farabi KazNU, Almaty 050040, Kazakhstan

Contents

The 4th Asian Nuclear Reaction Database Development Workshop

al-Farabi Kazakh National University, Almaty, Kazakhstan, 23-25 October, 2013; E-mail: ca.nrdb@gmail.com

TOPICS:

- Asian Nuclear Data Center Activity
- EXFOR Compilation
- Development of the Asian Nuclear Reaction Database Network
- Nuclear Reaction Experiments & Nuclear Reaction Evaluation
- Computational Simulation on Nuclear Reactions and Accelerator Facilities

Date	Time	Program
Oct.23 (Wen)	09：00-09：30	Registration
	09：30-10：00	Opening Ceremony
	Chairpersons : G. Mutanov (rector of al-Farabi Kazakh National University), N. Otsuka (IAEA, Vien, Austria)	
	10:00 – 10:20	M. Aikawa (Hokkaido University) International and Asian Collaboration on Nuclear Data
	10:20 – 10:50	G. Chen, Zh. GE, et al (CNDC), Recent EXFOR Compilation in CNDC
	10:50 – 11:20	N. Otsuka (IAEA), A. Saxena (BARC, India), Measurement and compilation of nuclear reaction data in India
	11;20-11;40	M. Takibayeva, M. Bakabayev, et al (al-Farabi KazNU), The Features and the Development of Central Asia Nuclear Reaction Database at al-Farabi University
	11:40-12：00 Coffee Break	

Date	Time	Program
Oct.23 （Wen)		Chairpersons: Y. O. LEE (NDC, Korea Atomic Energy Research Institute) , M. Burkitbaev (al-Farabi Kazakh National University);
	11:50 – 12:20	S. Yang, Y. O. Lee, et al. (KAERI), EXFOR Activity and Measurement of KAERI/NDC
	12:20 – 12:50	J. Yoo (KAERI), Overview of Nuclear Structure and Decay Data Evaluation Activities at KAERI
	12:50 – 13:20	M. Burkitbaev (al-Farabi KazNU), Work Performed by the al-Farabi University on Environmental Radioactivity in Central Asia
		13:20-14:30 Lunch
		Chairpersons: K. Kato (Hokkaido University, Japan), T. Ramazanov (al- Farabi Kazakh National University);
	14:30-14:50	S.V. Artemov (INP UzbAS) Possibility of Experimental Studies of Nuclear Reactions in Uzbekistan
	14:50-15:05	Ch. Omarov (AFIF, Almaty), Development of astronomy in Kazakhstan: from new ground-based telescopes to space ones

Date	Time	Program
	15:05-15:20	A. Davletov (al-Farabi KazNU), The present and future research and innovative activities of the Physical and Technical Department
	15:20-15:50	A. Makinaga (Hokkaido University) JCPRG-RIKEN Nuclear Data Project and Asian Collaborations
Oct.23 (Wen)	Chairpersons: J.G. Yoo (Korea Atomic Energy Research Institute), E. Batyrbekov (Nuclear National Center of Kazakhstan)	
	16:10 – 16:40	J. Wang (CNDC), The Systematic of Thermal Neutron Fission Cross Sections
	16:40 – 17:10	K. Kato (Hokkaido University), Electro-magnetic dissociations of neutron-rich nuclei
	17:10-17:40	S.Zaitsev (IMT RAS, Chernogolovka, Russia), Modern technologies of nanostructuring and applications
	18:00-21:00 Banquet	

Date	Time	Program	
Inst. of Nuclear Physics Oct.24 (Wen)	**Visit to Institute of Nuclear Physics**		
	08:00-08:15	Hotels: Shamshirack, Best Western Plus, Almaty - Places of gathering for the trip to Institute of Nuclear Physics	
	09:00	Arrival time to the Institute of Nuclear Physics	
	09:15-12:00	Excursion on facilities and acquaintance with the laboratories	
	13:00- 14:00	Lunch	
	Chairpersons: N. Otsuka (IAEA, Vien, Austria), N. Chakrov (Institute of Nuclear Physics, Almaty, Kazakhstan) The Scientific Program of Presentations at INP is still in development		
	14:00 – 14:30	N. Chakrov (INP) Recent Experiments at Institute of Nuclear Physics	
	14:30-15:00	N. Otsuka (IAEA) International Experimental Nuclear Reaction Data Library (EXFOR) and Central Asian Countries	
	15:00 – 15:30	N. Burtebaev (INP RK) The new experimental data on the elastic scattering of protons by ^{10}B at low energies.	
	15:30 – 16:20	Discussions and other	

Date	Time	Program	
Oct.25 (Wen)	Chairpersons: Zh. GE (China Nuclear Data Center), A. Davletov (al-Farabi Kazakh National University)		
	09:00 – 09:30	Y. O. LEE (KAERI), Photo-neutron Source at KAERI	
	09:30 – 10:00	R. Yarmukhamedov (INP UzbAS) On the new Modern Approaches and their application for Nuclear Astrophysics	
	10:00 – 10:30	S. Ebata (Hokkaido University), Systematic study of electric dipole excited states utilizing the linear response method	
	10:30-11：00	V. Zhumabekova, G. Spanova, M. Takibayeva (al-Farabi KazNU), Research of Metalic Berillium Properties - JAEA-KazNU Agreement	
	11:00 – 11:30	R. Beisembayev et al., (Lebedev PIAS and al-Farabi KazNU) , Experiments of Tian Shan Station of Cosmic Rays	
	11:30-11：50	Coffee Break	
	Chairpersons: G. Chen (CNDC, China), M. Abishev (al-Farabi KazNU)		
	11:50 – 12:20	G. Chen et al (CNDC) “Introduction of the digitization software Gdgraph”	

Date	Time	Program	
	12:20 – 12:40	M.Odsuren (Hokkaido University), Scattering Phase Shifts of Two-Three Body Systems in the Complex Scaling Method	
	12:40 – 13:00	N. Takibayev (al-Farabi KazNU), Recent studies of Be9 as a reflector material	
Oct.25 (Wen)	13:00-14:30	Lunch	
	Chairpersons: M. Aikawa (Hokkaido University, Japan) R. Yarmukhamedov (Institute of Nuclear Physics, Uzbekistan),		
	14:30-15:00	A. Makinaga, (Hokkaido University), Photo neutron experiment by using activation method at Hokkaido University electron linac facility	
	15:00-15:30	S. Kunakov et al. (al-Farabi KazNU, ITT Univ.) Researches of accumulation of tritium and helium from the beryllium reflector under reactor irradiation	
	15:30-15-50	M. Abishev (al-Farabi KazNU), On Medical Physics and Nuclear Medicine Development in Kazakhstan	
	15:50-16：20	Coffee Break	

Date	Time	Program	
Oct.25 (Wen)	Chairpersons: N. Otsuka (IAEA, Austria), Y.O. Lee (KAERI) Zh. GE (CNDC), , K. Kato (Hokkaido University, Japan)		
	16:20- 16：50	**Round Table: Asian Nuclear Reaction Database Development**	
	16:50- 17:10	N. Takibayev, (al-Farabi KazNU), - CA-NRDB - Appointment of advisors and Steering committee. - Proposal to issue NRDB scientific journal.	
	Conclusion remarks: Kato K., Chen G., Otsuka N. , Ge Ch., Lee Y.O., Yarmuchamedov R. et al.		
	Closing of the 4th ANRDDW		
	Visiting National Theater. Sightseeing.		

INTRODUCTION TO THE 4th ASIAN NUCLEAR REACTION DATABASE DEVELOPMENT WORKSHOP

The 4th Annual Asian Database Nuclear Reactions Workshop (4th ANRDDW) was held from 23 to 25 October 2013 in Kazakhstan, Almaty. 4th ANRDDW organizers were physical-technical faculty of the al-Farabi Kazakh National University (al-Farabi KazNU) and the science team of the Central Asian Nuclear Reactions Database (CA-NRDB), based at the University.

4th ANRDDW continued the series of Asian nuclear reactions databases workshops, following the workshops at the Hokkaido University (Japan, 2010), Beijing (China, 2011) and Pohang Accelerator Center (Republic of Korea, 2012).

Representatives of nuclear reactions databases from Japan, Korea, Russia, Uzbekistan, and from the IAEA (Austria), which oversees an international network of nuclear reactions databases, took part in the work of 4th ANRDDW.

Scientific reports were presented by scientists of the following research centers: JCPRG, KAERI, National Nuclear Center of the Republic of Kazakhstan, Institute of Nuclear Physics of Uzbekistan Academy of Sciences, Institute of Nuclear Physics of Kazakhstan, Moscow State University (Russia), Fesenkov Astrophysical Institute of Kazakhstan, al-Farabi KazNU, etc.

The results of experimental studies, theoretical analysis and calculations regarding various problems of nuclear physics and nuclear astrophysics were presented at the Workshop. The problems of the safe operation of nuclear facilities and nuclear power plants, radio-ecological problems in Central Asia, as well as application of modern nuclear physics methods in medicine and various human activities were discussed.

The meeting was concluded with a round-table discussion which outlined further goals and objectives of the international network of databases on the nuclear reactions. The parties discussed development of the nuclear reactions databases in Asia.

After the 4th ANRDDW was finished, N. Otsuka, leading specialist of IAEA, held a short course for young specialists: training on the procedure for compilation of nuclear data in EXFOR. The training was very useful for young professionals.

Now CA-NRDB is actively working to strengthen cooperation between Asian and Russian national centers of nuclear reactions databases, and with an international network of nuclear data (NRDC) at the IAEA.

For that purpose, a Center for nuclear reactions data has been established in Kazakhstan (CA-NRDB, Central Asia Nuclear Reaction Database), to develop the first in Central Asia database of nuclear reactions and to incorporate this resource into international network of nuclear data bases under auspices of IAEA. It is implied that CA-NRDB would serve not only as a library of nuclear data but as an interactive educational portal for junior scientists and students fostering interest in nuclear physics and astrophysics, nuclear power production, radio-ecology and nuclear medicine, geology and other areas of knowledge.

Development of the nuclear reactions database is an important strategic task for Kazakhstan: providing free access to nuclear reactions data for specialists, junior scientists and students contributes to the image of Kazakhstan as a country with peaceful use and development of nuclear energy.

Electro-magnetic dissociation of neutron-rich nuclei – Nuclear data evaluations of ^{9}Be –

Kiyoshi Katō
Nuclear Reaction Data Centre, Faculty of Science, Hokkaido University,
Sapporo 060-0810, Japan

Abstract

The electro-magnetic dissociation reactions including two- and three-body final states are investigated using the complex scaling method. This method is applied to the two-neutron halo nuclei, ^{6}He and ^{11}Li, and it is shown that the observed three-body photo-dissociation cross sections can be well described. The recently observed ^{9}Be(γ, n) reaction cross section is also investigated applying this method to an $\alpha + \alpha + n$ three-body model.

1 Introduction

The (n, γ) or its inverse (γ, n) reactions are the most interesting ones in nuclear science. In nuclear reactor physics and astro-nuclear physics, nuclear data of those reactions are indispensable. However, our knowledge and understanding particularly for light nuclei are not yet complete. Furthermore, recent developments of unstable nuclear physics have provided us a new challenging field of nuclear data studies. The so-called Borromean nuclei, being the typical unstable nuclei, are easily broken into three clusters by a small perturbation of an external electro-magnetic field because a three-body decay channel is the lowest threshold in these nuclei.

To study such problems, we have developed the complex scaling method (CSM) [1] describing resonance and continuum states separately. This method is very promising for studying the bound and unbound states in a unified way. The details of the method is given in the review paper [2] and recent results of the application studies are presented in the article [3]. The main subject of this talk is concerning with the electro-magnetic dissociation reactions such as (n, γ) or its inverse (γ, n) reactions.

Recently a new observation of the ^{9}Be(γ, n) reaction cross section has been reported by Arnold *et al.* [4]. This new data are pointed to be not consistent with old data. For evaluation of these data, it is desired to study the photo-dissociation of ^{9}Be theoretically. Because the ^{9}Be nucleus is considered to have a $\alpha + \alpha + n$ cluster structure in the low-energy region, three-body calculation is necessary for the bound ground state and also the unbound resonance states.

In section 2, the present method is briefly explained. In section 3, the Coulomb breakup reactions of ^{6}He and ^{11}Li are discussed and shown to be well explained by theoretical calculations. In section 4, the ground state and excited resonant states are calculated within the complex scaling for the $\alpha + \alpha + n$ cluster model.

2 The complex scaling method

For the Hamiltonian $H = T + V$, the complex scaled Schrödinger equation [2] is expressed as

$$H(\theta)\Psi(\theta) = E\Psi(\theta), \tag{1}$$

where $H(\theta) = U(\theta)HU^{-1}(\theta)$ and $\Psi(\theta) = U(\theta)\Psi$ with the transformation $U(\theta)$ [1] defined by

$$U(\theta); \qquad \vec{r}_i \to \vec{r}_i e^{i\theta} \quad \text{and} \quad \vec{k}_i \to \vec{k}_i e^{-i\theta} \quad \text{for } i = 1, 2 \cdots, f. \tag{2}$$

The degree of freedom of a system is expressed by $f = n - 1$ for an n-body system. The wave function Ψ of this system is described as an expansion of a basis set of L^2 functions;

$$\Psi(\theta) = \sum_{j=1}^{N} c_j(\theta)\psi_j. \tag{3}$$

The eigenvalues and eigenstates of the complex scaled Schrödinger equation (1) are classified as

$$(E_\alpha, \Psi^\alpha) = \begin{cases} (E_B,\ \Psi^B) & B = 1, \cdots, N_B & ;\text{ bound states,} \\ (E_R,\ \Psi^R) & R = 1, \cdots, N_R(\theta) & ;\text{ resonance states,} \\ (E_c(\theta),\ \Psi^c) & c = 1, \cdots, N - N_B - N_R(\theta) & ;\text{ continuum states,} \end{cases} \tag{4}$$

where N_B and $N_R(\theta)$ are the number of bound states and the θ-dependent number of resonant states, respectively. The energies of resonant states are independent of $\theta > \left(\tan^{-1}\left(\Gamma^R/2E_r^R\right)\right)$ because of the intrinsic quantities of the system; $E_R = E_r^R - i\Gamma^R$. But the discretized energies $E_c(\theta)$ of continuum states are θ-dependent and expressed as $E_c = \epsilon_r^c - i\epsilon_i^c$.

3 Coulomb breakup reactions of ^{6}He and ^{11}Li

The Coulomb breakup experiment is a unique method to investigate the exotic properties of neutron halo nuclei, which are weakly bound systems. Many studies have been done on the two-neutron halo nuclei ^{6}He and ^{11}Li, but a satisfactory understanding of the relation between the exotic structure and characteristic reaction mechanism has not been obtained yet. Since the final states of the two-neutron halo breakup are three-body continuum states, it is very appropriate to apply CSM to the Coulomb breakup reactions.

The breakup cross section of the Coulomb response is assumed to be determined by $E1$ transitions and is described as

$$\frac{d\sigma}{dE} = \frac{16\pi^3}{9\hbar c} N_{E1}(E_\gamma) \frac{dB(E1)}{dE}, \tag{5}$$

where $N_{E1}(E_\gamma)$ is the virtual photon number and

$$\begin{aligned} \frac{dB(E1)}{dE} &= \frac{1}{2J_{gr}+1} \sum_\nu \left\langle \tilde{\Psi}_{gr} | \hat{E}1 | \Psi_\nu \right\rangle \left\langle \tilde{\Psi}_\nu | \hat{E}1 | \Psi_i \right\rangle \delta(E - E_\nu) \\ &= -\frac{1}{\pi} \mathrm{Im} \left[\frac{1}{2J_{gr}+1} \sum_\nu \frac{\left(\Psi_{gr}^\theta | \hat{E}1(\theta) | \Psi_\nu^\theta\right) \left(\Psi_\nu^\theta | \hat{E}1(\theta) | \Psi_i^\theta\right)}{E - E_\nu^\theta} \right]. \end{aligned} \tag{6}$$

.

The last equation is calculated with CSM, where Ψ_ν^θ are solutions belonging to the eigen-energy E_ν^θ and satisfy the outgoing boundary condition. It should be noted that the result is independent of the parameter θ.

In Fig. 1, we show the result of the calculated Coulomb breakup cross section for the two-neutron halo nucleus ^{6}He using a ^{4}He$+n+n$ model [6]. In the left-hand panel, the eigen-energy distribution obtained with $\theta = 30°$ is shown. The contribution from the continuum states of ^{5}He$(3/2^-)+n$ is dominant in the cross section. The similar results for ^{11}Li has been obtained [7, 8]

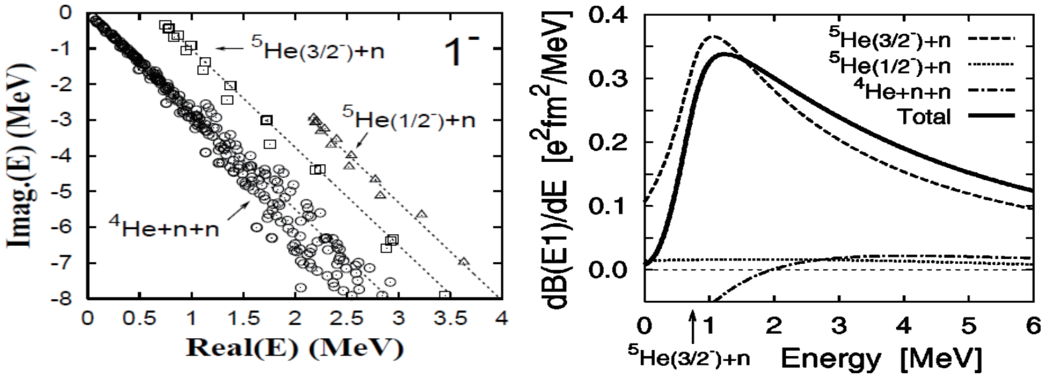

Figure 1: The 1^- energy eigenvalue distribution (left-hand panel) in the complex-scaled ^{4}He$+n+n$ model and the Coulomb breakup reaction cross section (right-hand panel) calculated with the use of the complex-scaled Green's function.

4 $(\gamma,\ n)$ reaction cross sections of ^{9}Be

Recently, Arnold *et al.* [4] have performed the new experiment of ^{9}Be$(\gamma,\ n)$, which indicates some breakup cross sections inconsistent with the previous data. We employ a three-body model of $\alpha+\alpha+n$ and calculate the energy spectrum of ^{9}Be. The α-α interaction is a folding potential which has been used in the three-α cluster model for ^{12}C [9] and the α-n interaction is the same as one used in the ^{4}He$+n+n$ calculation [6].

The calculated energy spectrum of ^{9}Be is presented in Fig. 2 comparing with the experimental data [10]. We see that the calculated result well reproduces the observed data, but the first excited $1/2^+$ state cannot be reproduced. It is explained for the reason that the resonance width of this state is so large as not to be reproduced within CSM. This understanding can be confirmed by a calculation of $\alpha+\alpha+p$ within CSM, which indicates a resonant state of $1/2^+$ due to the Coulomb potential barrier. We can estimate the resonance position of the $1/2^+$ state in ^{9}Be applying the analytical continuation method where the electric charge of the valence proton is reduced to zero. The result predicts that the resonance energy is 0.911 MeV and the width 1.47 MeV. This result is compared with the recent observation of $E_r = 0.174$ MeV and $\Gamma = 0.283$ MeV [4].

The resonance mechanism and the structure of the $1/2^+$ state in ^{9}Be is still not clear. To solve this problem, the study of a ^{8}Be$+n$ model is in progress as a joint project with the Almaty group.

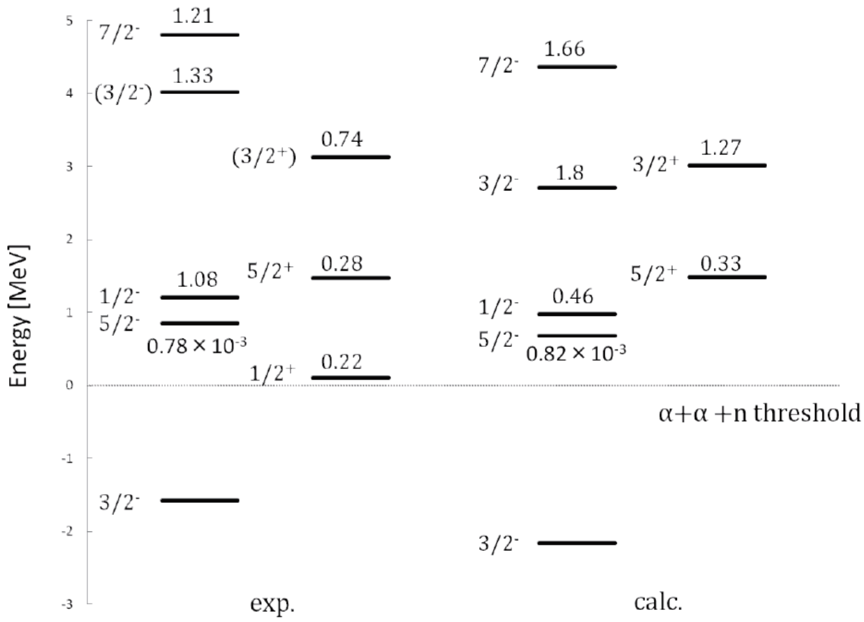

Figure 2: The observed and calculated energy spectra of ^{9}Be.

5 Summary

We have presented a new approach to evaluate the nuclear reaction data of the low energy $(n,\ \gamma)$ and $(\gamma,\ n)$ reactions using the complex scaling method. This method has been show to explain the photo-dissociation cross sections of two-neutron halo nuclei, ^{6}He and ^{11}Li. To evaluate the recent data of ^{9}Be$(\gamma,\ n)$ reaction cross section, the $\alpha+\alpha+n$ model calculation starts and the preliminary result has been reported.

References

[1] J. Aguilar and J.M. Combes, Commun. Math. Phys. **22**, 269 (1971); E. Balslev and J. M. Combes, Commun. Math. Phys. **22**, 280 (1971).

[2] S. Aoyama, T. Myo, K. Katō and K. Ikeda, Prog. Theor. Phys. **116**, 1 (2006).

[3] H. Horiuchi, K. Ikeda and K. Katō, Prog. Theor. Phys. Suppl. **192**, 1, (2012).

[4] C. W. Arnold, T. B. Clegg, C. Iliadis, H. J. Karwowski, G. C. Rich, and J. R. Tompkins, Phys. Rev. C **85**, 044605 (2012).

[5] T. Myo, A. Ohnishi and K. Katō, Prog. Theor. Phys. **99**, 801 (1998).

[6] T. Myo, K. Katō, S. Aoyama and K. Ikeda, Phys. Rev. **C 63**, 054313 (2001).

[7] T. Myo, K. Katō, H. Toki, and K. Ikeda, Phys. Rev. C **76**, 024305 (2007).

[8] Y. Kikuchi, T. Myo and K. Katō and K. Ikeda, Phys. Rev. C **87**, 034606 (2013).

[9] C. Kurokawa and K. Katō, Nucl. Phys. A **792** (2007), 87.

[10] TUNL Nuclear Data Evaluation, http://www.tunl.duke.edu/nucldata/

JCPRG-RIKEN Nuclear Data Project

A. Makinaga[1], M. Aikawa[1], K. Katō[1], A. Kohama[2], H. Otsu[2], H. Sakurai[2,3]
[1]*Faculty of Science, Hokkaido University, N10W8, Kita-ku, Sapporo 060-0810, Japan*
[2]*RIKEN Nishina Center, RIKEN, Hirosawa, Wako, Saitama 351-0198, Japan*
[3]*Department of physics, University of Tokyo, Tokyo 113-0033, Japan*

Since 2006, RI beam factory (RIBF) at RIKEN Nishina Center has actively produced new elements and the first observables in the field of unstable nuclei. Those new data should be stored in an international experimental database (EXFOR) in collaboration with the Nuclear Reaction Data Centre (NRDC) network centering on IAEA. The Hokkaido University Nuclear Data Centre (JCPRG) and RIKEN Nishina center established the "JCPRG-RIKEN Nuclear Data Project" to compile data obtained in RIBF.

1. Introduction

An nuclear reaction database is a powerful tool in nuclear physics, astrophysics, nuclear engineering, and medical physics. The JCPRG-RIKEN Nuclear Data Project started in 2010 to distribute the new-fangled RIBF experimental data to all over the world via the EXFOR database. With the progress of globalization for RIBF experiments, collaborative relationship for the compilation process with world experimentalists has been built successfully. We have also an annual RIBF mini-workshop in order to share the compilation status and to discuss some topics such as a database format, new physical quantities and information engineering to share the experimental data files effectively. In this paper, we report on the current status of the compilation process and information disclosure on the webpage.

2. Nuclear data from RIBF facility

Main accelerators in RIBF are a heavy – ion linac (RILAC), AVF cyclotron (AVF), ring cyclotron (RRC). In addition, newly developed ring cyclotron (fRC and IRC) and superconducting ring cyclotron (SRC), are available. Downstream equipments of SRC (BigRIPS, RIPS, SAMURAI, SHARAQ, SCRIT) make it possible to perform various kinds of experiments by using unstable beams. GARIS, which is settled on the downstream of RILAC, is used to find super heavy elements. Experimental details are described on the RIBF webpage [1].

Figure 1. Statistics of EXFOR entries compiled in Japan

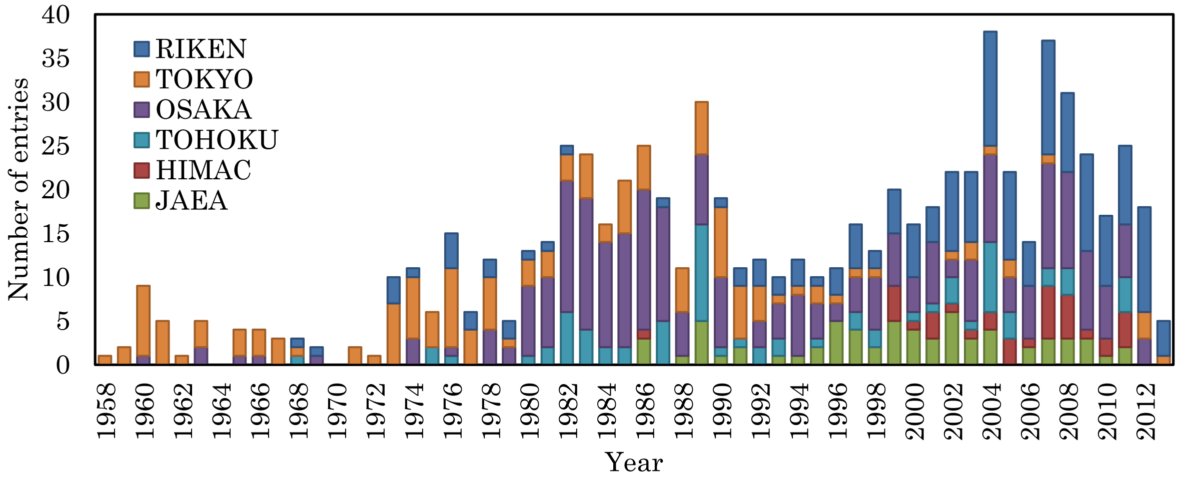

Table 1. The list of compiled papers published from 2008 to 2013 with their EXFOR accession entry number

	2008	2009	2010	2011	2012	2013
entry	E2107 [8] E2116 [9] E2120 [10] E2122 [11] E2124 [12] E2125 [13] E2127 [14]	E2132 [15] E2133 [16] E2137 [17] E2139 [18]	E2147 [19] E2173 [20] E2174 [21] E2280 [22] E2286 [23] E2287 [24] E2290 [25]	E2324 [26] E2325 [27] E2326 [28] E2327 [29] E2346 [30] E2350 [31] E2360 [32] E2364 [33]	E2368 [34] E2369 [35] E2370 [36] E2371 [37] E2375 [38] E2376 [39] E2378 [40] E2382 [41] E2416 [42]	E2404 [43] E2405 [44] E2406 [45] E2407 [46] E2430 [47] E2431 [48] E2434 [49] E2438 [50] E2439 [51] E2440 [52]
total	7	4	7	8	9	10

3. Distribution of the RIBF data in the world

Figure 1 shows the statistics of EXFOR entries compiled by JCPRG. In Table 1, we summarized the list of compiled papers published from 2008 to 2013. After establishment of the JCPRG-RIKEN Nuclear Data Project in 2010, the compilation activity for RIBF experimental data has been grown rapidly. To distribute the compilation results, we opened the webpage in both JCPRG [2] and RIKEN (Figure 2). This webpage shows the RIBF data quickly without using a database search system. Information, such as of Title, Reference, Reaction and numerical data is available. We also distribute the compilation status to RIBF researchers via RIKEN Nishina Center news once a month. The IAEA website is also available to search the RIKEN data files.

Figure 2. JCPRG-RIKEN webpage. Right: JCPRG side webpage [2]. Left: RIKEN sideweb page (http://www.nishina.riken.jp/researcher/archive/index_e.html).

4. Summary

Since 2010, the JCPRG-RIKEN Nuclear Data Project has successfully compiled RIKEN RIBF nuclear data in the databases such as EXFOR. Information of the status of the database is opened on the webpage for every user in the world. Further contributions of the compilation activity will be continued.

Acknowledgement

This work was supported by the Hokkaido University Support program for research exchange with inter-university foreign partners and by JCPRG-RIKEN Nuclear Data project.

References

[1] http://www.nishina.riken.jp/RIBF/accelerator/overview.html

[2] http://www.jcprg.org/riken/

[3] K. Kato *et al.*, RIKEN Accel. Prog. Rep. **43**, 62 (2010).

[4] K. Tsubakihara *et al.*, RIKEN Accel. Prog. Rep. **44**, 58 (2011).

[5] N. Furutachi *et al.*, RIKEN Accel. Prog. Rep. **45**, 48 (2012).

[6] N. Furutachi *et al.*, RIKEN Accel. Prog. Rep. **46**, 56 (2013).

[7] A. Makinaga *et al.*, RIKEN Accel. Prog. Rep. **47** (2014). submitted.

[8] J. J. He *et al.*, Eur. Phys. J. A **36**, 1 (2008).; E2107 in EXFOR.

[9] T. Ohnishi *et al.*, J. Phys. Soc. Jpn. **77**, 083201 (2008).; E2116 in EXFOR.

[10] S. Ota *et al.*, Phys. Lett. B **666**, 311 (2008).; E2120 in EXFOR.

[11] H. Iwasaki *et al.*, Phys. Rev. C **78**, 021304(R) (2008).; E2122 in EXFOR.

[12] A. Ozawa *et al.*, Phys. Rev. C **78**, 054313 (2008).; E2124 in EXFOR.

[13] M. Janek *et al.*, Phys. of At. Nucl. **71**, 1495 (2008).; E2125 in EXFOR.

[14] J. Gibelin *et al.*, Phys. Rev. Lett. **101**, 212503 (2008).; E2127 in EXFOR.

[15] Y. Kondo *et al.*, Phys. Rev. C **79**, 014602 (2009).; E2132 in EXFOR

[16] H. Yamaguchi *et al*., Phys. Lett. B **672**, 230 (2009).; E2133 in EXFOR.
[17] D. Kaji *et al*., J. Phys. Soc. Jpn. **78**, 035003 (2009).; E2137 in EXFOR.
[18] T. Nakamura *et al*., Phys. Rev. C **79**, 035805 (2009).; E2139 in EXFOR.
[19] S. Takeuchi *et al*., Phys. Rev. C **79**, 054319 (2010).; E2147 in EXFOR.
[20] Y. Kondo *et al*., Phys. Lett. B **690**, 245 (2010).; E2173 in EXFOR.
[21] K. Tanaka et al., Phys. Rev. Lett. **104**, 062701 (2010).; E2174 in EXFOR.
[22] E. Yu. Nikolskii *et al*., Phys. Rev. C **81**, 064606 (2010).,;E2280 in EXFOR.
[23] J-Q. Faisal *et al*., Chin. Phys. Lett **27**, 092501 (2010).; E2286 in EXFOR.
[24] T. Uesaka *et al*., Phys. Rev. C **82**, 021602 (2010).; E2287 in EXFOR.
[25] K. Tanaka *et al*., Phys. Rev. C **82**, 044309 (2010).; E2290 in EXFOR.
[26] H. Haba *et al*., Phys. Rev. C **83**, 034602 (2011).; E2324 in EXFOR.
[27] Y. Satoh *et al*., Phys. Lett. B **697**, 459 (2011).; E2325 in EXFOR.
[28] H. Yamaguchi *et al*., Phys. rev. C **83**, 034306 (2011).; E2326 in EXFOR.
[29] J. L. Lou *et al*., Phys. Rev. C **83**, 034612 (2011).; E2327 in EXFOR.
[30] K. Sekiguchi *et al*., Phys. Rev. C **83**, 061001(R) (2011).; E2346 in EXFOR.
[31] T. Yamaguchi *et al*., Nucl. Phys. A **864**, 1 (2011).; E2350 in EXFOR.
[32] N. Sato *et al*., J. Phys. Soc. Jpn. **80**, 094201 (2011).; E2360 in EXFOR.
[33] A. Ozawa *et al*., Phys. Rev. C **84**, 064315 (2011).; E2364 in EXFOR.
[34] M. Takechi *et al*., Phys. Lett. B **707**, 357 (2012).; E2368 in EXFOR.
[35] J. Chen *et al*., Phys. Rev. C **85**, 015805 (2012).; E2369 in EXFOR.
[36] Z. X. Cao *et al*., Phys. Lett. B **707**, 46 (2012).; E2370 in EXFOR.
[37] H. Haba *et al*., Phys. Rev. C **85**, 024611 (2012).; E2371 in EXFOR.
[38] N. Imai *et al*., Phys. Rev. C **85**, 034313 (2012).; E2375 in EXFOR.
[39] L. H. Lv *et al*., J. Phys. G: Nucl. Part. Phys. **39**, 065102 (2012).; E2376 in EXFOR
[40] Y. Togano *et al*., Phys. Rev. Lett. **108**, 222501 (2012).; E2378 in EXFOR
[41] K. Miki *et al*., Phys. Rev. Lett. **108,** 262503 (2012).; E2382 in EXFOR.
[42] LI Kuo-Ang *et al*., Chin. Phys. Lett. **29**, 102301 (2012).; E2416 in EXFOR.
[43] M. U. Khandaker *et al*., Nucl. Instrum. Meethods B **296**, 14 (2013).; E2404 in EXFOR
[44] B. Guo *et al*., Phys. Rev. C **87**, 015803 (2013).; E2405 in EXFOR.
[45] T. Sumita *et al*., J. Phys. Soc. Jpn. **82**, 024202 (2013).; E2406 in EXFOR.
[46] S. Sakaguchi *et al*., Phys. Rev. C **87**, 021601(R) (2013).; E2407 in EXFOR.
[47] A. K. Kurilkin *et al*., Phys. Rev. C **87**, 051001 (2013).; E2430 in EXFOR.
[48] H. Yamaguchi *et al*., Phys. Rev. C **87**, 034303 (2013).; E2431 in EXFOR.
[49] J. J. He *et al*., Phys. Rev. C **88**, 012801 (2013).; E2434 in EXFOR.
[50] M. Murakami *et al*., Phys. Rev. C **88**, 024618 (2013).; E2438 in EXFOR.
[51] M. U. Khandaker *et al*., Nucl. Instrum. Methods B **316**, 33 (2013).; E2439 in EXFOR.
[52] S. J. Jin *et al*., Phys. Rev. C **88**, 035801 (2013).; E2440 in EXFOR.

Activity of the photon induced activation experiments with 45 MeV electron linear accelerator at Hokkaido University

A. Makinaga[1], H. Akimune[2], H. Otsu[3], T. Kamiyama[4], K. Kino[4], Y. Kiyanagi[4], G. N. Kim[5], M-W. Lee[6], S-G. Shin[7], M. Aikawa[1] and K. Kato[1]

[1]*Faculty of Science, Hokkaido University, N10W8, Kita-ku, Sapporo 060-0810, Japan*
[2]*Department of Physics, Konan University, Kobe 658-8501, Japan*
[3]*RIKEN Nishina Center, RIKEN, Hirosawa, Wako 351-0198, Japan*
[4]*Faculty of Engineering, Hokkaido University, Sapporo 060-8628, Japan*
[5]*Center for High Energy Physics, Kyungpook National University, Daegu 702-701, Korea*
[6]*Research Center, Dongnam Institute of Radiological and Medical Science, Busan 619-953, Korea*
[7]*Division of Advanced Nuclear Engineering, Pohang University of Science and Technology, Pohang 790-784, Korea*

Nuclear data measurements are one of the greatest interests to the nuclear power field, such as the nuclear transmutation techniques by using the accelerator-driven system (ADS), as well as the nuclear astrophysics. We report on the activities of the neutron and the photon induced experiments by using the 45 MeV pulsed electron linear accelerator at Hokkaido University.

1. Introduction

A nuclear reaction database is a powerful tool in the nuclear physics, the astrophysics, the nuclear engineering, and the medical physics. Since 2010, the Hokkaido University Nuclear Data Center (JCPRG) has been partly developed the neutron and the photon experimental techniques for the nuclear data measurements by using the Hokkaido University electron linear accelerator facility under the "Asia-Africa Science Platform Program (AASPP) " by Japan Society for the Promotion of Science [1].

Figure 1. A group photo of the experimental group under the AASPP project.

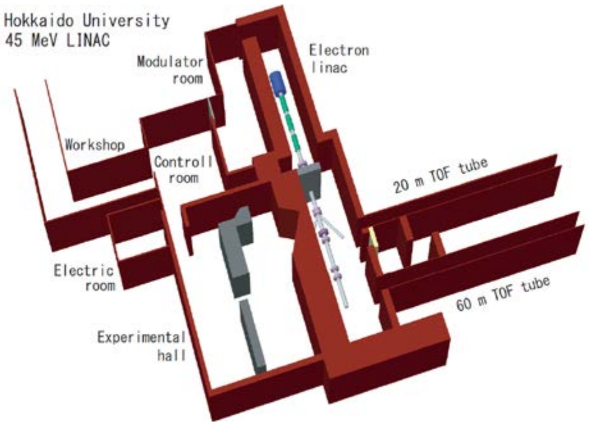

Figure 2. Layout of the 45 MeV electron linear accelerator facility at Hokkaido University. Three main beam lines are available. RIGHT: Pulsed cold neutron beam line. CENTER: Pulsed thermal neutron, electron or photon beam line. LEFT: Fast neutron beam line.

Electron Linac	S-band
Maximum energy	45 MeV
Maximum current	140 μA
Repetiation rate	10 pps to 200 pps
Pulse width	10 ns to 3μs

Table 1. Basic performance of the 45 MeV electron linear accelerator.

We report here on the current status of the photo activation experiment at Hokkaido University.

2. Photon activation experiment

In a photon activation experiment [2-4], the activity of the sample during the irradiation period is described as:

$$\frac{dN(t)}{dt} = N_t \int_{S_{th}} \sigma(E) I(t, E) dE - \lambda N(t)$$

Where, N(t) is the number of daughter nuclei, N_t is the area density of the target, S_{th} is the particle threshold, σ(E) is the cross section, I(t, E) is the gamma flux and λ is the decay constant of daughter nuclei. After irradiation, β-, β+, EC and IT decay from the activated sample can be observed as following equation:

$$\text{Yield} = \int_{t_{start}}^{t_{stop}} \lambda N(t_{ir}) e^{-\lambda t} hi\varepsilon(E) dt$$

Where, t_{start} is the start time of the measurement, t_{stop} is the stop time of the measurement, *h* is the emission probability, *i* is the self absorption in the sample and ε(E) is the efficiency of the gamma detector.

$$\int_{S_{th}} \sigma(E) n_\gamma(E) dE = \frac{\text{Yield}\, e^{\lambda t_{ir}}}{N_t hi\varepsilon(E)(e^{-\lambda t_{start}} - e^{-\lambda t_{stop}})} \cdot \frac{\int_0^{t_{ir}} K(t) dt}{\int_0^{t_{ir}} K(t)\, e^{\lambda t} dt}$$

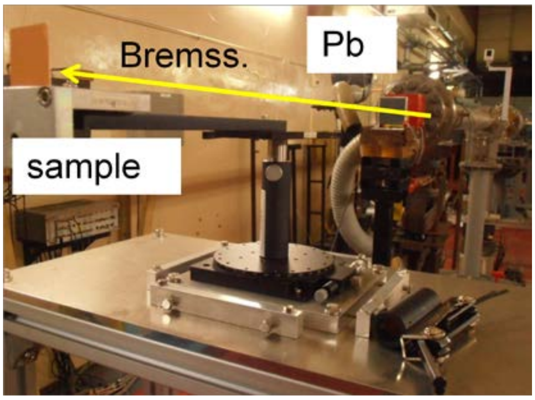

Figure 3. Experimental set up for the photo activation method.

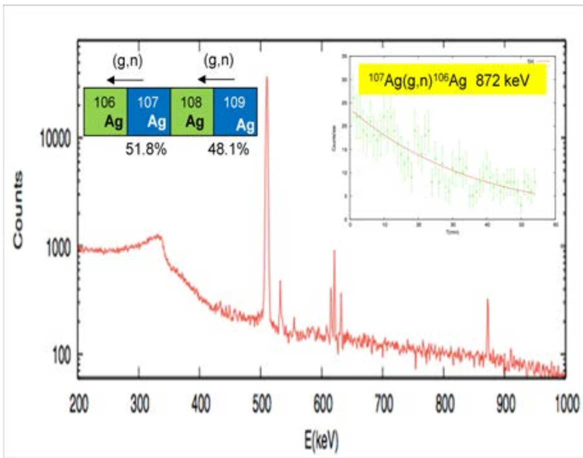

Figure 4. Gamma ray spectrum from the ^{nat}Ag after the irradiation of the photon beam. An inlet figure shows the measured decay time of the ~872 keV peak, which are emitted from ^{106}Ag.

$$n_\gamma(E) = \int_0^{t_{ir}} I(t,E)dt = \int_0^{t_{ir}} K(t)J(E)dt$$

Where, t_{ir} is the irradiation time.

The experiment was performed at the 45 MeV electron linear accelerator at Hokkaido University by using bremsstrahlung photons (Figure 2). Bremsstrahlung was produced by hitting a 2 mm lead radiator with an electron beam of ~24 MeV kinetic energy. The average current was 0.5 μA and the electron pulse width was 0.2 μs. Typical fluctuation of the electron beam current is less than 1% [5]. The intensities of the bremsstrahlung were monitored by using the iron block (Figure 3). As activation targets, we used 0.1 mm natural Pb, Mo, Ag and Cu samples. After irradiation, the activated samples were measured with HPGe detector with coaxial HPGe detector with a crystal geometry of d 48.8 mm diameter and 66.4 mm height. Typical energy resolution of the FWHM (full width at half maximum) at 1.33 MeV and 5.9 keV are 1.90 keV and 650 eV, respectively. Relative detection efficiency at 1.33 MeV is 20 %. Figure 4 shows an example of the gamma ray energy spectrum from the activated ^{nat}Ag sample. Now, we are analyzing the experimental data. Detailed discussion will be performed in near future.

3. Summary

Since 2010, the Hokkaido University Nuclear Data Center (JCPRG) has been partly developed the neutron and the photon experimental techniques for the nuclear data measurement by using the Hokkaido University electron linear accelerator facility under the "Asia-Africa Science Platform Program" by Japan Society for the Promotion of Science.

Acknowledgement

The authors would like to thank the staffs of the Hokkaido University 45 MeV electron linear accelerator facility for their cooperation during the experiment. A. M thanks Dr. N. Otsuka (IAEA) for their discussion about nuclear data experiments. A. M also thanks Prof. M. Fujiwara (Osaka University) for his teaching in the early stage of this experiment. This work was partly supported by “'R&D' Platform Formation of Nuclear Reaction Data in Asian Countries (2010-2013)”, Asia-Africa Science Platform Program and Grant-in-Aid for Publication of Scientific Research Results (No. 257005), Japan Society for the Promotion of Science (JSPS), and by the Hokkaido University Support program for research exchange with inter-university foreign partners.

References

[1] A. Makinaga et al., JCPRG Annual Report, No.1, 44 (2012).
[2] S. Goko et al., Phys. Rev. Lett. 96, 192501 (2006).
[3] C. Nair et al., Phys. Rev. C 78, 055802 (2008).
[4] H. Naik et al., Nucl. Instrum. Methods B, 269, 1417 (2011).
[5] K. Kosako et al., J. Nucl. Sci. Technol., 48 [2], 227-236 (2011).

SCATTERING PHASE SHIFTS OF TWO-BODY SYSTEMS USING THE COMPLEX SCALING METHOD

M.Odsuren[1,2] , K.Katō[3] , M.Aikawa[3] and T.Myo[4,5]
[1]*Meme Media Laboratory, Hokkaido University, Sapporo 060-8628, Japan*
[2]*Nuclear Research Center, National University of Mongolia, Ulaanbaatar 210646, Mongolia*
[3]*Nuclear Reaction Data Centre, Faculty of Science, Hokkaido University, Sapporo 060-0810, Japan*
[4]*General Education, Faculty of Engineering, Osaka Institute of Technology, Osaka 535-8585, Japan*
[5]*Research Center for Nuclear Physics (RCNP), Osaka University, Ibaraki 567-0047, Japan*

We investigate the scattering phase shifts by using the complex scaling method and extract the individual contributions of several resonances in the phase shifts. We show the cases using a simple schematic potential with the 0^+ and 1^- partial waves. We also investigate scattering phase shifts for low-lying partial waves of the α-α system to see the effect of the resonances.

Introduction

The complex scaling method (CSM) [1-4] is one of the well-established techniques in wide areas of physics, especially in resonance studies in nuclear physics. At the beginning, its advantage was mainly explained by the superior description of the resonances of the composite systems. Nowadays, it is successfully utilized for getting information on the unbound and scattering states in the observables.

In the present framework, the complex scaled orthogonality condition model (CSOCM) [3] and the extended completeness relation [4] are used. The scattering phase shifts have been investigated as important scattering quantities from the continuum level density (CLD) [2] obtained using the CSM.

The CSOCM can be used for obtaining scattering phase shifts of the many resonance system. In order to investigate effects of the many resonances for such system, we applied a simple schematic potential [4,5] for the $J^\pi = 0^+$ and 1^- partial waves. In addition, we discuss characteristics of the decomposed scattering phase shifts of the α-α system.

Schematic Potential Scattering

We investigate the scattering phase shifts using a simple schematic potential to produce many resonances. The relative wave functions are expanded in terms of the L^2 basis states with finite numbers in each system. The weight of the each basis state is determined by diagonalizing the complex-scaled Hamiltonian matrix elements.

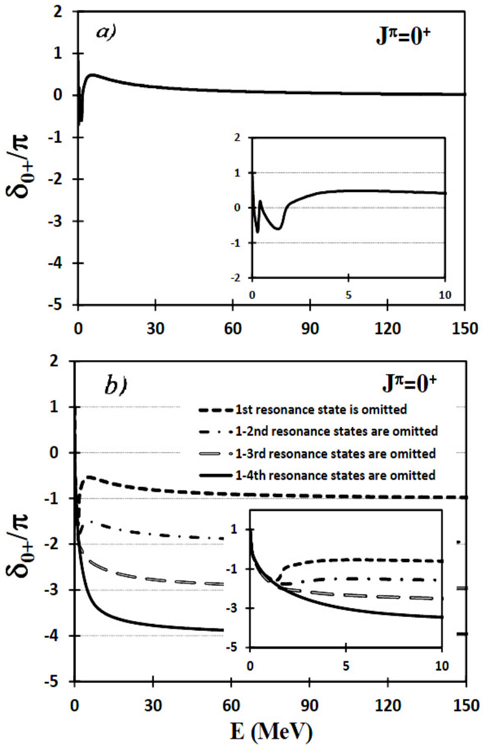

Fig. 1. The phase shifts (with and without resonances and bound state) as a function of energy with the $J^{\pi} = 0^{+}$ partial wave. *a)* the solid curve is calculated with four resonances and one bound state. *b)* the effects of the bound and resonances are omitted one by one in the each calculation which are drawn four types of lines.

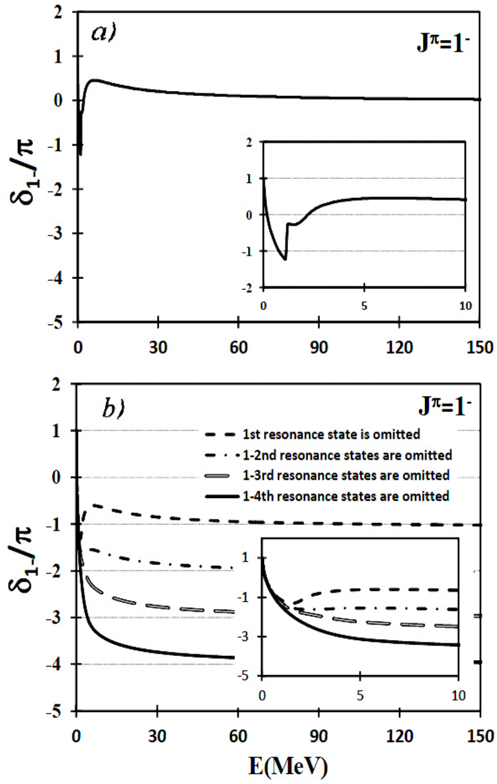

Fig. 2. The phase shifts (with and without resonances and bound state) as a function of energy with the $J^{\pi} = 1^{-}$ partial wave. In the upper and lower panels, same analysis is performed as done in Fig.1.

Table I. Bound and resonance eigen energies for the $J^{\pi} = 0^{+}$ and 1^{-} partial waves.

0^{+} wave		1^{-} wave	
E(MeV)	**state**	**E(MeV)**	**state**
-1.922782	bound	-0.674647	bound
$0.3101+i10^{-6}$	resonance	$1.1710-i4.948\times10^{-3}$	resonance
$1.6322+i0.1228$	resonance	$2.0309-i4.8944\times10^{-1}$	resonance
$2.2493-i1.0397$	resonance	$2.8318-i1.1986$	resonance
$2.8542-i2.5699$	resonance	$3.9341-i1.7885$	resonance

We use a simple expression of Hamiltonian for the schematic potential model, in order to obtain several resonances, which is given as

$$H = T + V(r),$$

where $T = -(\hbar^2 / 2\mu)\nabla^2$,$V(r)$=$-8.0exp(-0.16r^2)+4.0exp(-0.04r^2)$ and $\hbar^2 / 2\mu = 1$ (MeV fm^2) for simplicity. In the present case, one bound state and four resonances are obtained for the 0^+ and 1^- partial waves.

Fig. 1 *a)* shows the phase shifts including all resonant and bound states as a function of the energy for the $J^\pi = 0^+$ partial wave. In Fig. 1 *b)*, the effects of the 1st, 2nd, 3rd and 4th resonances are omitted one by one in the each calculation which are drawn in dashed, dotted-dashed, long-dashed and solid-curves, respectively. Note that the scale of the graph was magnified in the insets of Fig.1 *a)* and *b)*. We can see from the inset of Fig.1 *a)* a very sharp peak appears at low energy region (0.3 MeV). We clearly identify the sharp peak corresponding to the 1st resonance state of the 0^+ partial wave from the inset of Fig.1 *b)* which is given dashed-curve. Moreover, in Fig.1 *b)*, we check that the behavior of the continuum contribution for the 0^+ wave by omitting the observed resonance contributions which are drawn as other three-types of curves. Similarly the scattering phase shifts of the $J^\pi = 1^-$ partial wave are given in Fig. 2 and the same technique is used as the J^π=0^+ partial wave. The observed bound and resonance states at the J^π=0^+ and 1^- partial waves by using the schematic potential model are summarized in the Table I. Table I contains one bound and four resonance energies with decay widths at each partial waves.

Scattering Phase Shifts of the Alpha-Alpha System

We investigate the scattering phenomena of the α-α system. In our calculations, the decomposed scattering phase shifts into the resonance and continuum terms are shown by applying CSM and the extended completeness relation.

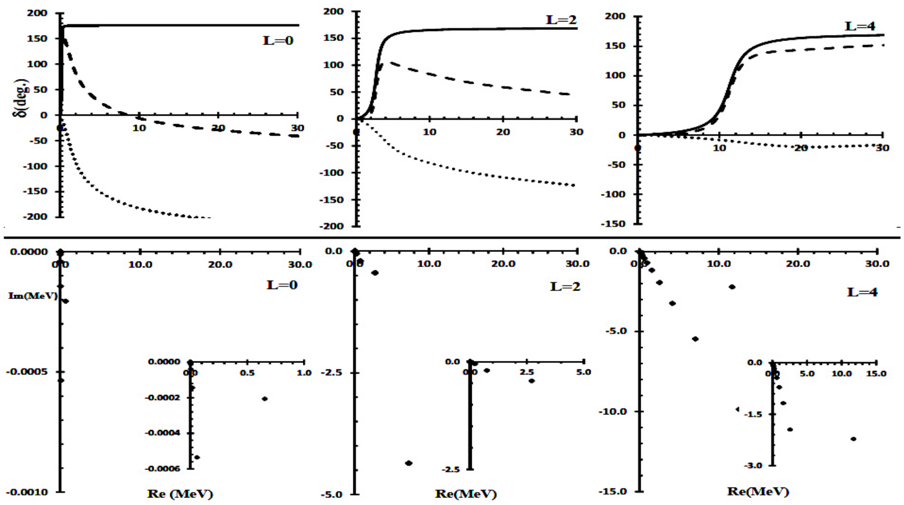

Fig. 3. Decomposed scattering phase shifts of the α-α systems for L=0^+, 2^+ and 4^+ states. The solid and dotted lines represent the contributions of the resonance and continuum terms. The dashed lines describe the total scattering phase shifts. In the lower parts of the panel, the distributions of the calculated eigenvalues are given in the complex energy plane, measured from the α-α threshold energy.

Figure 3 displays the scattering phase shifts decomposed into the single resonance and the residual continuum terms for the α-α system in each partial wave state. The extended completeness relation is applied and this method provides us with the information on the decomposition of the scattering phase shifts into the resonance and continuum terms. In Fig. 3, we plot not only the scattering phase shifts but also the contributions of the resonance and scattering terms. The dashed-lines indicate scattering phase shifts, and the solid-curves, dotted-lines show the behaviors of resonance and continuum contributions. As is seen Fig. 3, it is important to keep in mind that the total contributions in the low energy region mainly arise from the resonance terms. In the calculations we integrate the continuum level density to obtain the contributions of each eigenstates to the scattering phase shifts. In this sense, we describe the phase shifts by using the discrete eigenvalues obtained within the finite number of the L^2 basis states. In the lower part of Fig. 3, the schematic distributions of eigenvalues are displayed in the complex energy plane where one resonance state is obtained in the each partial wave.

From the results including a schematic potential case, it could be said that the continuum contributions of the phase shifts give repulsive characteristics even the system consists of several resonances. Thereby, other systems could be generally analyzed by this method.

Summary

We have presented that CSM is a useful method for obtaining the resonant states and the scattering quantities such as the phase shifts. The phase shifts of the α-α system have been investigated in the present method, in which the contributions of the one resonance and residual continuum states are exhibited. Furthermore, we presented the scattering phase shifts using the schematic potential model which shows the several resonances. We can clearly confirm the resonance and continuum contributions in the phase shifts without ambiguity.

Acknowledgement

The authors are grateful for the support by “'R&D' Platform Formation of Nuclear Reaction Data in Asian Countries (2010-2013)”, Asia-Africa Science Platform Program, Japan Society for the Promotion of Science (JSPS).

References

1. Y. K. Ho, Phys. Rep. 99, 1 (1983).
2. R. Suzuki, T. Myo, and K. Katō, Prog. Theor. Phys. 113, 1273 (2005).
3. A. T. Kruppa and K. Katō, Prog. Theor. Phys. 84, 1145 (1990).
4. T. Myo, A. Ohnishi and K. Katō, Prog. Theor. Phys. 99, 801 (1998).
5. A. Csótó, B. Gyarmati, A. T. Kruppa, K. F. Pál, and N. Moiseyev, Phys. Rev. A41, 3469 (1990).

Neutron-Nuclear Reaction Data Analysis at the Nuclear Research Center, National University of Mongolia

M.Odsuren[1,2*], G.Khuukhenkhuu[1], S.Davaa[1], J.Munkhsaikhan[1] and Ts.Zolbadral[1]

[1]*Nuclear Research Center, National University of Mongolia, Ulaanbaatar 210646, Mongolia*
[2]*Meme Media Laboratory, Hokkaido University, Sapporo 060-8628, Japan*

1. INTRODUCTION

Since 1990 we have been studying fast neutron induced charged particle emission reactions in collaboration with the Frank Laboratory of Neutron Physics, JINR, Dubna, Russia and the Institute of Heavy Ion Physics, Peking University, P.R. China. Our investigation is carried out in the two directions of neutron cross section systematical analysis and experimental study of the fast neutron induced (n,p) and (n,α) reactions [1,2].

Some systematical regulatory of the cross sections on the relative neutron excess parameter (N-Z)/A for the target isotope was observed in the wide energy range of incident neutrons. This dependence is termed in the literature as the isotopic effect. In the framework of the statistical model, exciton model and PWBA were deduced formulae to explain the isotopic effect [3-5].

The experimental study of the fast neutron induced charged particle emission reactions was performed on the Van de Graaff accelerator of the Institute of Heavy Ion Physics, Peking University, P.R. China for wide mass range of the target nuclei [6-10].

In this work the recent results of the systematical analysis for fission neutron spectrum averaged (n,α) reaction cross sections and experimental study of the $^{57}Fe(n,\alpha)^{54}Cr$ reaction [11] are presented.

2. Systematical Analysis of (n,α) Cross Sections Averaged Over the Fission Neutron Spectrum

2.1. Formulae

The direct and pre-equilibrium mechanisms are neglected for fission neutrons and the compound mechanism can be considered, only. Then, neglecting the γ-emission and using the Weizsacker formula of binding energy, the (n,α) cross section for fast neutrons can be written as follows [5]:

$$\sigma(n,\alpha) = C_\alpha \pi (R + \lambda_n / 2\pi)^2 e^{-K_\alpha \frac{N-Z+0.5}{A}} \tag{1}$$

where

$$C_\alpha = 2\exp\sqrt{\frac{A}{13.5(E_n + Q_{n\alpha})}}\left(-3\alpha + \gamma\left(\frac{4Z}{A^{1/3}}\right) + \varepsilon_\alpha - 2.058\frac{Z}{A^{1/3}}\right) \quad \text{and} \quad K_\alpha = 2\xi\sqrt{\frac{A}{13.5(E_n + Q_{n\alpha})}} \tag{2}$$

Here: E_n is the incident neutron energy; $Q_{n\alpha}$ is the (n,α) reactions energy; Z, N and A are the proton, neutron and mass numbers of the target nucleus; α, γ, and ξ are the Weizsacker formula constants; ε_α is the internal binding energy of α-particle; λ_n is the wave length of the neutrons; R is the radius of the target nucleus.

The parameters K_α and C_α in formula (1) can be fitted and determined as the constant for all isotopes.

*Corresponding author: odsuren@nucl.sci.hokudai.ac.jp

2.2. Systematical Analysis of the Cross Sections

The effective average neutron energy is important for theoretical analysis of averaged over the continuum neutron spectrum cross sections. Average energy for fission neutrons is, usually, around 2 MeV [12]. So, the parameters K_α and C_α in formula (1) are found at E_n=2 MeV by fitting to known experimental data (Fig.1).

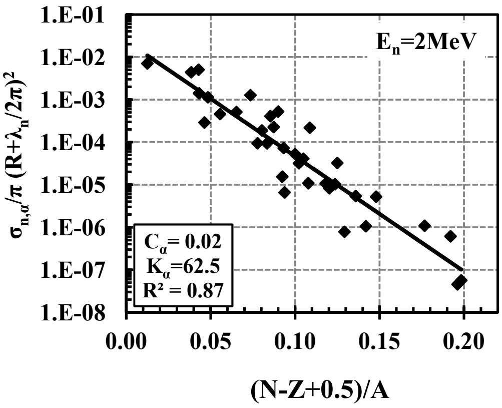

Fig.1. Theoretical cross section (solid line) and experimental data (black points).

In addition, energy dependence K_α and C_α parameters were obtained in the wide neutron energy range of E_n=6-20 MeV [5]. If we consider the energy dependence of K_α and C_α parameters for E_n=2-20 MeV, both parameters at 2 MeV have different tendency from E_n=6-20 MeV range (Fig.2 and 3). This fact, perhaps, shows effective average energy of fission neutron spectrum for (n,α) reaction is different from 2 MeV because threshold energy of (n,α) reactions for most of isotopes lies in the E_n≈2-5 MeV region [13].

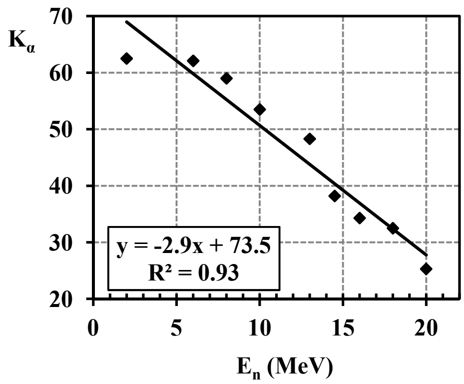

Fig.2. Energy dependence for K_α parameter

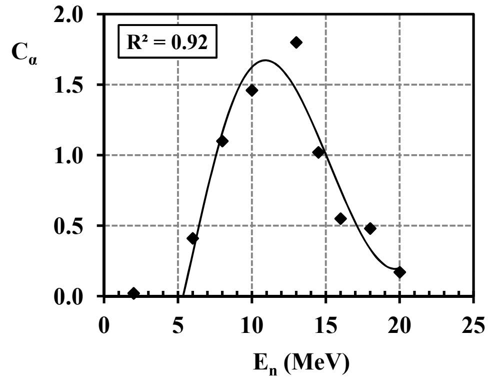

Fig.3. Energy dependence for C_α parameter

Therefore, from the tendency of energy dependence for parameters K_α and C_α can be obtained the values of K_α=66, C_α=0.2 and $\langle E_n \rangle \approx 5$ MeV (Fig.4 and 5).

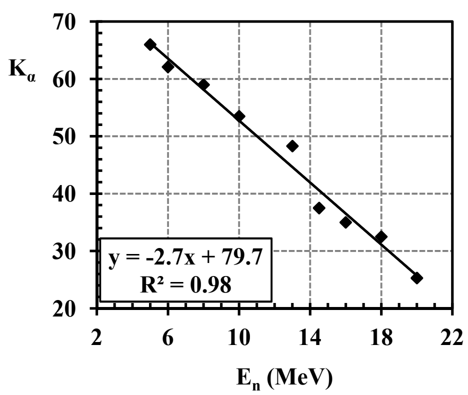

Fig.4. The same as in Fig.2 after fitting of K_α for fission neutrons

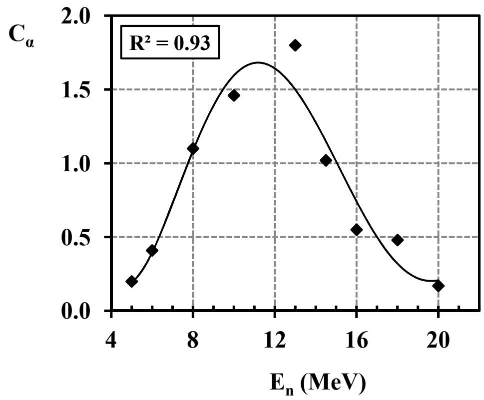

Fig.5. The same as in Fig.3 after fitting of C_α for fission neutrons

The theoretical cross sections calculated by formula (1) with fitted parameters of K_α=66, C_α=0.2 for average neutron energy $\langle E_n \rangle \approx 5$ MeV of fission spectrum are compared with known experimental values in Fig.6 where experimental data are taken from [14,15]. It can been seen that statistical model formula gives overestimated values for (n,α) cross sections.

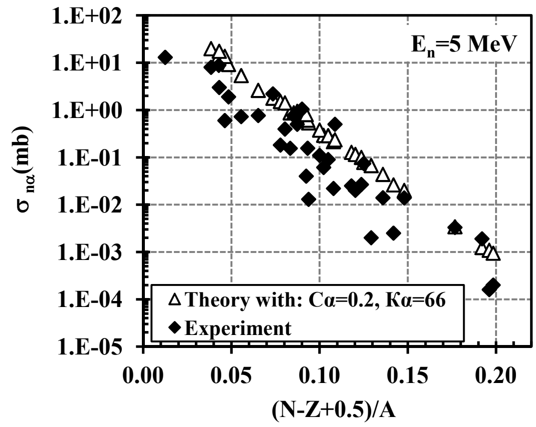

Fig.6. Theoretical and experimental (n,α) cross sections without α-clusterization effect.

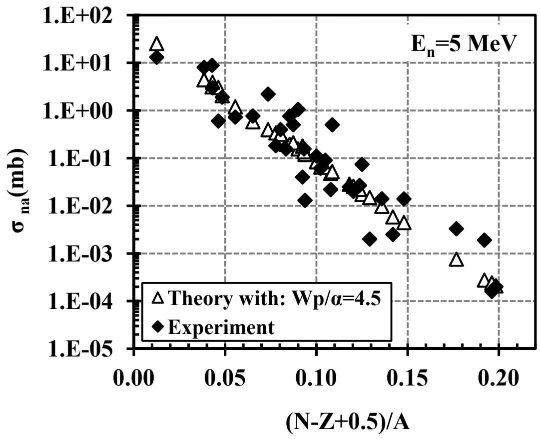

Fig.7. The same as in Fig.6 with α-clusterization factor $W_{p/\alpha}$=4.5.

At the same time, our statistical model formula was in agreement with experimental (n,p) cross sections averaged over the fission neutron spectrum [16]. So, observed disagreement between the theoretical and experimental data is, perhaps, caused by the α-clusterization effect (α-particle formation probability) on the surface of nuclei. We assume the ratio of nucleon emission probability to α-particle emission one from the compound nucleus is 4.5 [5,17]. It can been seen that (Fig.7) the statistical formula (1) with the α-clusterization factor $W_{p/\alpha}$=4.5 and average energy $\langle E_n \rangle \approx 5$ MeV for fission neutrons satisfactorily describes the systematic dependence of known experimental data for (n,α) cross sections on the relative neutron excess parameter (N-Z+0.5)/A.

3. The Study of the ^{57}Fe(n,α)^{54}Cr Reaction in the MeV Neutron Energy Region

3.1. Experimental methods

Measurements were performed at the Van de Graaff accelerator of Peking University, P.R. China. Experimental setups are composed of three parts: the neutron source, the α-particle detector, and the neutron flux monitor.

Neutrons were produced through the ^{2}H(*d,n*)^{3}He reaction using a deuterium gas target. The beam current was about 3.0 μA and the energies of produced neutrons were 5.0, 5.5, 6.0 and 6.5MeV, with energy spreads of 0.38, 0.33, 0.27 and 0.24 MeV, respectively.

The α-particle detector is a two section-gridded ionization chamber with common cathode [7-10]. A sample changer was set in the common cathode of the ionization chamber with five sample positions. The ^{57}Fe samples were prepared using press method with enriched ^{57}Fe (95.9%) metal, were attached to tantalum backings and were placed on the cathode of the ionization chamber.

Neutron flux was determined by ^{238}U (99.999%) which was placed in the ionization chamber also. In addition, for neutron flux monitor was used a BF_3 long counter.

3.2. Results and discussions

Two dimensional and linear energy spectra of the α-particles from the $^{57}Fe(n,\alpha)^{54}Cr$ reaction were obtained using the data acquisition system. From the α-particle energy spectra were determined (n,α) cross sections at neutron energy of 5.0, 5.5, 6.0 and 6.5 MeV.

The experimental (n,α) cross sections of the $^{57}Fe(n,\alpha)^{54}Cr$ reaction are compared with existing evaluations [18] and TALYS code calculation (Figs.8. and 9). It can be seen that our experimental data are in agreement with the TENDL-2012 and TALYS-1.4 calculations.

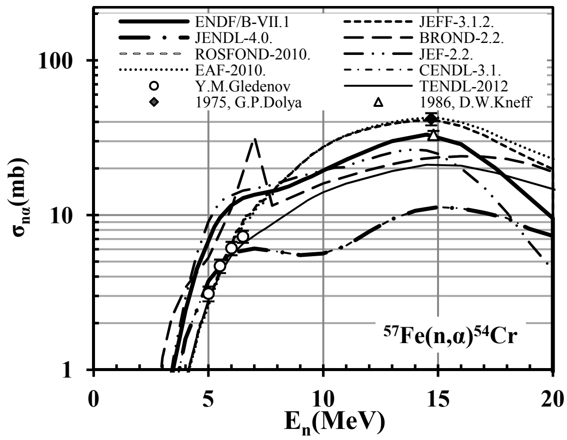

Fig.8. Present cross sections of the $^{57}Fe(n,\alpha)^{54}Cr$ reaction compared with existing evaluations.

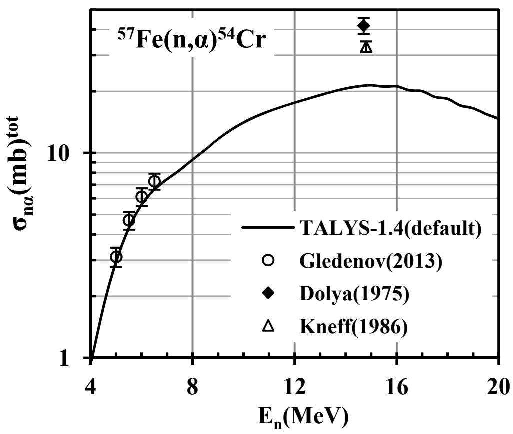

Fig.9. Experimental cross sections of the $^{57}Fe(n,\alpha)^{54}Cr$ reaction and TALYS code calculation.

References

1. G.Khuukhenkhuu *et al.,* JINR Communication, E3-93-466, (1993), Dubna.
2. G.Khuukhenkhuu *et al.,* In book: Proc. of the Intern. Conf. on Nucl. Data for Sci. and Tech., May 19-24, 1997, Trieste, Italy, Bologna, 1997, p.934, and p.514.
3. G. Khuukhenkhuu *et al.,* Nucl. Sci. Tech., Supplement 2, v.1, 2002, p.782.
4. G.Khuukhenkhuu *et al.,* JINR Communications, E3-2007-25, 26, 27, Dubna, 2007.
5. G.Khuukhenkhuu *et al.,* In book: Proc. of the XX Intern. Seminar on Interaction of Neutron with Nuclei., ISINN-20, JINR, Dubna, 2013, p.173.
6. Yu.M.Gledenov *et al.,* In Book: Proc. of the 8th Intern. Simposium on "Capture Gamma-Ray Spectroscopy and Related Topics", Fribourg Switzerland, 1994, p.587.
7. Guohui Zhang *et al.,* Nucl. Instr. Meth., v.566, N2, 2006, p.615.
8. Guohui Zhang *et al.,* Nucl. Sci. Eng., v. 160, N1, 2008, p.123.
9. Yu.M. Gledenov *et al.,* Phys. Rev. C, v.80, N4, 2009, p.044602-1-5.
10. Guohui Zhang *et al.,* Phys. Rev. Lett., v.107,Issue.25, 2011, p.252502-1-5.
11. Yu.G.Gledenov *et al.,* Proc. of the XXI Intern. Seminar on Interaction of Neutron with Nuclear, ISINN-21, May 20-25, 2013, JINR, Dubna, (in press).
12. B.I. Starostov *et al.,*Yadernye Konstanty, 2, 1980, p.3.
13. V.N. Manokhin *et al.,* Handbook on Nuclear Activation Data. IAEA, Tech. Rep. Ser., N273, 1987, p.305.
14. A. Calamand, Handbook on Nuclear Activation Cross Sections, IAEA, Tech. Rep. Ser., N156, 1974, p.273.
15. E.M. Gryntakis, J. Radional. Chem., 52, 1979, p.219.
16. G. Khuukhenkhuu *et al.,* Jour. of the Korean Phys. Soc., 59 (2), 2011, p.851.
17. Yu.P. Popov, W.I.Furman, In book: III School of Neutron Physics, JINR, Dubna, D3-11787, 1978, p.390.
18. EXFOR, www-nds.iaea.org.

ISOTOPIC SIGNATURES OF URANIUM ACTIVITY RATIOS IN THE NATURAL WATER ENVIRONMENT OF CENTRAL ASIAN URANIUM SITES

M.Burkitbayev, B.Uralbekov
al-Farabi Kazakh National University

Uranium ore mining and milling operations were conducted in the Central Asian Republics from the mid-1950s as part of the nuclear weapons and nuclear energy programmes of the former Soviet Union. As a result of these past ore mining and processing activities, large volumes of low-level radioactive waste in the form of spoil heaps and tailing materials were left behind at different sites within this area. The impact of these wastes on local settlements and main irrigation channels (e.g., Shu and Syr-Daria valleys) have received increased attention in recent years, as concerns have been expressed by local populations on the possible health effects arising from potential contamination. Despite some efforts to evaluate the radiological situation of these sites, large knowledge gaps still remain. In particular, there is a lack of analytical data in many environmental compartments, and the status of drinking waters is largely unknown.

In this study, we report on the seasonal and spatial variability of $^{234}U/^{238}U$ activity ratios in the natural waters from U mining sites of Central Asia and provide interpretation to explain the variations and potential impacts to downstream water quality. In addition, we demonstrate the use of uranium disequilibria as a natural tracer to calculate fractional hydrologic and hydrochemical contributions of main tributaries to the Shu River.

In course of this work, a wide range of advanced radioanalytical techniques (alpha-beta and gamma –spectrometry) were used to determine radionuclide concentrations in the water samples referred to above. Surface waters were sampled in the course of 16 field expeditions to the selected U legacy sites. The exact position of each sampling site was determined with a portable global positioning system (Garmin GPS 12 XL).

New data on the concentration of key uranium series radionulides in water samples from Central Asian U legacy sites have been presented and interpreted using advanced radioanalytical approaches. Our interest in making these measurements was to obtain baseline information on the isotopic signatures of these at the TENORM sites of Central Asia, which could of use to better interpret measurements elsewhere.

The Kurdai site $^{234}U/^{238}U$ isotope ratios vary from 1.03 to 1.63 depending on the degree of influence from U-bearing materials and proximity to the U pit lake – a tool for studying migration. Furthermore, analysis of uranium isotopic ratios show the presence of technogenic uranium inputs into the Shu river from the Karasu point, as evidence by a decrease in the measured $^{234}U/^{238}U$ ratio from 1.63 in uncontaminated sites to 1.22 in sites affected by past mining activities.

$^{234}U/^{234}U$ isotope ratios were determined along the former uranium mining sites of central Asia was used to identify source of uranium and contribution of main tributaries to the river by using mixing calculations of uranium-234 equivalent. Our results showed that uranium activity ratio can be utilized as natural tracers as tributary mixing processes in arid zones of Central Asia. Obtained results can be used in the further radiological studies of the main irrigation channels in Central Asian region.

Study of elastic and inelastic scattering of ^{4}He from ^{11}B at energies 29, 40 and 50.5 MeV

N. Burtebayev[1], Sh. Hamada[2], Y. Mukhamejanov[3], M. Nassurlla[3], A. Morzabayev[4], S. Sakhiyev[4], W.Trzaska[5], A.Demyanova[6], A. Ogloblin[6]
[1] Institute of Nuclear Physics, Almaty, Kazakhstan.
[2] Faculty of Science, Tanta University, Tanta, Egypt.
[3] Al-Farabi Kazakh National University, Almaty, Kazakhstan.
[4] Eurasia National University, Astana, Kazakhstan.
[5]University of Jyväskylä, Jyväskylä, Finland.
[6]NRC Kurchatov Institute, Moscow, Russia

Study of nuclear reaction is of a special interest as it could provide us with useful information about the nuclear structure, potential parameters, deformation, and transition probabilities. The α-nucleus interaction is an essential tool for the understanding of nuclear structure and nuclear reactions. The concept of the α-particle mean field has been widely used to unify the bound and scattering α-particle states in a similar way to use of the nuclear mean field to calculate the properties of bound single particle states and also the scattering of unbound nucleons by nuclei.

We have measured the angular distributions for the elastic and inelastic scattering of ^{4}He from ^{11}B in the isochronous cyclotron U-105 M INP RK. The extracted α-particles beam has been accelerated to energies 29, 40 and 50.5 MeV and then directed to ^{11}B target of thickness ~ 32.9 μg/cm^{2}. The experimental results were analysed within the framework of both the optical model using different complex potential and the double folding potential obtained with different density-dependent NN interactions which give the corresponding values of the nuclear incompressibility K in the Hartree-Fock calculation of nuclear matter. The theoretical calculations for the concerned excited states were performed using the CC coupled channel method implemented in code FRESCO. We extracted the optimal deformation parameters for the $5/2^{-}$ and $7/2^{-}$ states.

On the new methods of determination of the asymptotic normalization coefficients and their application for nuclear astrophysics

R. Yarmukhamedov*

November 4, 2013

Institute of Nuclear Physics, Uzbekistan Academy of Sciences, 100214 Tashkent, Uzbekistan
**Corresponding author, E-mail: rakhim@inp.uz*

1 Introduction

In the present review report, we will briefly present the some methods of determination of asymptotic normalization coefficients (ANC) for $A + a \to B$ [1] and their application for the extrapolation of the astrophysical S factors to the solar energy region for some specific radiative capture reactions. The results of the analysis of the specific experimental astrophysical S factors for some nuclear astrophysical reactions are also presented (see, the recent review [2] also).

2 ANC from proton transfer reactions

One of such methods uses the modified DWBA approach for nuclear reactions of manifest peripheral character. The DWBA cross section for reaction A(x, y)B with particle a transferring is expressed in terms of product of the ANCs for $y + a \to x$ and $A + a \to$ (e.g., see [2] and references therein)

If the reaction under consideration is peripheral and the ANC value for $y + a \to x$ is know, this expression can be applied for determination of the "indirect determined" ANC value for $A + a \to B$ by means of the analysis of the experimental differential cross section of the peripheral transfer reaction under consideration.

The ANC for $^{12}\mathrm{C}+p\to{}^{13}\mathrm{N}$. The analysis of the experimental differential cross sections for the $^{12}\mathrm{C}(^3\mathrm{He},d)^{13}\mathrm{N}$ reaction for two the energies of the $^3\mathrm{He}$ projectile has been performed in Refs. [3] within the "post"-approximation of the modified DWBA. The "indirect determined" ANC value for $^{12}\mathrm{C}+p\to{}^{13}\mathrm{N}$ was found to be $C^2_{^{12}\mathrm{C}p}$=2.1±0.2 fm^{-1} [3], respectively.

3 $^{208}\mathrm{Pb}(^6\mathrm{Li},\alpha d)^{208}\mathrm{Pb}$ and the ANC for $\alpha+d\to{}^6\mathrm{Li}$

According to [4], the triple differential cross section (TDCS) of the $^{208}\mathrm{Pb}(^6\mathrm{Li},\alpha d)^{208}\mathrm{Pb}$ with taking into account the contributions from the E1- and E2-multipolarites in a correct manner can be expressed in terms of the ANC for $\alpha+d\to{}^6\mathrm{Li}$.

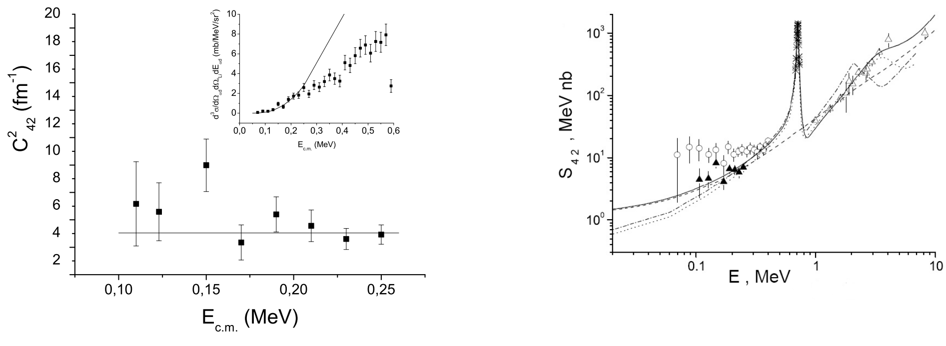

Figure 1: In the left hand site, the ANC values for $\alpha+d\to{}^6\mathrm{Li}$ ($C^2_{42}\equiv C^2_{\alpha d}$, full square symbols), their weighted mean(the straight line) and its uncertainty(the band width) [4, 5] as well as the TDCS for the $^{208}\mathrm{Pb}(^6\mathrm{Li},\alpha d)^{208}\mathrm{Pb}$ Coulomb breakup reaction in the inset (the experimental data are taken from [6] and the solid line is the result of calculation obtained in [4]). In the right hand site, the $d(\alpha,\gamma)^6\mathrm{Li}$ astrophysical S factor. The experimental astrophysical S factors are taken from [4](full triangle symbols), [6](open cycle symbols), [7](open triangle symbols) and [8](star symbols). The solid (dashed) line corresponds to the total (direct) astrophysical S factor obtained in [4, 5], whereas the dotted (dash–dotted) line is taken from [9] for the MN (V2) form of the NN potential.

The "indirect determined" ANC values for $\alpha+d\to{}^6\mathrm{Li}$, deduced in [4] separately from the experimental TDCS [6] for each experimental point of energy E within the range 107 $\lesssim E \lesssim$ 250 keV for which the calculated TDCS reproduces fairly well the absolute values of the experimental data (the inset in Fig. 1), are presented in the left hand side of Fig. 1. The weighted mean of the ANC obtained from all the experimental point of energy E is found to be $C^2_{\alpha d}$=5.24±0.51 fm^{-1} [4, 5] (see, Ref. [2] also), which is in an excellent agreement with $C^2_{\alpha d}$=5.37±0.26 and 5.24±0.77 fm^{-1}, deduced in [10] and [11] from the analysis of the elastic

$d\alpha$-scattering and the d^6Li-exchanged reaction, respectively, and reproduces well the absolute values of the experimental TDCS within the range $90 \lesssim E \lesssim 250$ keV (the solid line in the inset of Fig. 1).

4 Modified R-matrix approach for the radiative capture $A(a,\gamma)B$ reaction and ANC for $A + a \to B$

In the modified R-matrix approach (see, Refs. [2, 12] and references therein), the direct amplitude $M_{Il}^{(D;EI,M1)}(E)$ is determined only by the channel radius r_c and the ANC C_{Aa}, and the single resonance pole amplitude $M_I^{(R)}(E)$ is determined by a resonance energy $E^{(R)}$, the channel radius r_c, ANC for $A + a \to B$, the partial widths for the particle a and γ-ray.

The ^{12}C$(p,\gamma)^{13}$N reaction. The results of the analysis of the ^{12}C$(p,\gamma)^{13}$N astrophysical S factor and the reaction rate performed within the modified R-matrix approach in [12] using the "indirectly determined" ANC value for $^{12}\mathrm{C} + p \to {}^{13}\mathrm{N}$ aforementioned above are presented in fig. 2. In [12]. The new value has been obtained for the γ-width for the first resonance

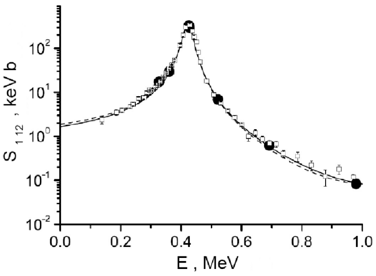

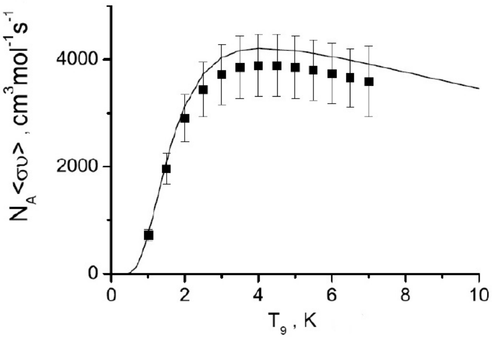

Figure 2: The astrophysical S factors (the left hand site) and the rate (the right hand site) for the ^{12}C$(p,\gamma)^{13}$N reaction. The experimental data for the astrophysical S factors are taken from Refs. [12](black points) and [13] (open points), and those for the rate are taken from Ref. [14]. The curves are the results of calculations taken from [12].

state of ^{13}N (E^*=2.365 MeV; J^π=1/2$^-$) (Γ^γ=0.65±0.07 eV), which differs noticeably from the values of Γ^γ=0.50±0.04 eV recommended in [15, 16] being obtained with the underestimated value of the cross section in the first resonance peak. The values of the astrophysical S factors at two most astrophysically important energies E=0 and 25 keV recommended in [12] are $S_{1\,12}(0)$=1.62±0.20 keV b and $S_{1\,12}(25$ keV) =1.75±0.22 keV b. It should be noted that the value of $S_{1\,12}$(25 keV) is in a good agreement within the uncertainty with that recommended in [13, 15].

The $d(\alpha,\gamma)^6$Li **reaction.** The result for the experimental $d(\alpha,\gamma)^6$Li astrophysical S factors (full triangle symbols), which has been obtained in [4, 5] within the energy region 100$\lesssim E \lesssim$ 600 keV using the ANC values of $C^2_{\alpha d}$ plotted in the left hand site of Fig. 1 (full square symbols), and its comparison with that of [6] are displayed in the right hand site of Fig. 1. As is seen from here, the rather large uncertainties (from 26% to 50%) for the $S^{exp}_{42}(E)$ obtained in [4, 5] occur for the energy region $E \leq$ 190 keV. It is connected with the aforementioned uncertainties for the $C^2_{\alpha d}$, which are conditioned by the large uncertainties in the experimental TDCS [6].

Note that, in [6], the $S^{exp}_{42}(E)$ were determined in the energy region 100$\lesssim E \lesssim$ 600 keV from the analysis of the experimental TDCS ^{208}Pb(^{6}Li$, \alpha d)^{208}$Pb Coulomb breakup with taking into account only the contribution of the E2-multipole (see, the open cycle symbols in the right hand side of Fig. 1), which results in reality overestimated values of $S^{exp}_{42}(E)$ in the energy region $E \leq$ 250 keV [4]. Therefore, the resulting $S_{42}(0)$ recommended in [4, 17, 18], which is equal to 1.30 MeV nb, differs also considerably on $S_{42}(0)$=9.10$\pm$ 1.80 MeV nb recommended [6]. It should be noted that the new data for $S^{exp}_{42}(E)$ obtained in [4] are in a good agreement with the theoretical predictions [17, 18]. Therefore, the $S^{exp}_{42}(E)$ values obtained in [4] at $E \leq$ 250 keV could so far be considered as the “best values” of the experimental $S^{exp}_{42}(E)$.

5 Conclusion

We now have at our disposal the different indirect methods for determination of the “indirect determined” ANC values. In particular, the modified R-matrix approach is a good tool of both obtaining the valuable information about ANCs being astrophysical interest and the reliable extrapolation of the astrophysical S factor $S_{aA}(E)$ for the radiative capture A(a,γ)B reaction at stellar energies E with uncertainty not exceeding the experimental one.

The work has been supported by the Academy of Sciences of the Republic of Uzbekistan (grant No. FA–F2–F177).

References

[1] L. D. Blokhintsev, I. Borbely, E. I. Dolinskii. Sov. J. Part. Nucl. **8**, 485 (1977).

[2] R. Yarmukhamedov and Q. I. Tursunmahatov. The Universe Evolution: Astrophysical and Nuclear Aspects (Nova Publishers, New York, USA), Chapter 6, 2013, pp.219–270.

[3] S. V. Artemov, et al. Izv.RAN.Ser.Fiz. **66**, 60 (2002).

[4] S. B. Igamov and R. Yarmukhamedov, Nucl.Phys.A **673**, 509 (2000)

[5] R. Yarmukhamedov, *et al.* Uzb.J.Phys. **12**,No.4–6, 233 (2010).

[6] J. Kiener, et al. Phys.Rev.C **44**, 2195 (1991).

[7] R. Robertson, *et al.*. Phys.Rev.Lett. **47**, 1867 (1981).

[8] P. Mohr, *et al.*. Phys.Rev.C **50**, 1543 (1993).

[9] A. Kharbch, P. Descouvmont, Phys.Rev.C **.58** (1998) 1066.

[10] L. D. Blokhintsev, et al.. Phys.Rev. C **48** 2390 (1993).

[11] G. V. Avakov et al. Sov.J.Nucl.Phys. **43**, 524 (1986).

[12] N. Burtebaev, et al. Phys.Rev. **C78**, 035802 (2008).

[13] C.Rolfs and R.E.Azuma. Nucl. Phys. A227 (1974) 291.

[14] N.A. Roughton, et al. Atomic Data and Nuclear Data Tables. **23**, 177 (1979).

[15] G. Barker, N. Ferdous. Aust.J. Phys. **33**, 3 (1980); private communication (2008).

[16] F. Ajenberg-Selove. S.Nucl.Phys. **A523**, 1 (1991).

[17] S.B. Igamov, R. Yarmukhamedov. Phys.At Nucl. **58** (1995) 1317.

[18] A. M. Mukhamedzhanov, *et al.* Phys.Rev.C **52** (1995) 3483.

POSSIBILITY OF EXPERIMENTAL STUDIES OF NUCLEAR REACTIONS IN UZBEKISTAN

S.V. Artemov, U.S. Salikhbaev
Institute of Nuclear Physics, Academy of Sciences. Tashkent, Uzbekistan

Scientific institutions of the Republic Uzbekistan are possessed of various modern facilities for carrying out the experiments in actual directions of basic and applied nuclear physics.

The most large research center is the Institute of Nuclear Physics Uzbekistan Academy of Sciences which has the Research Nuclear Reactor of WWR-SM type (power ~10 MWt), two Cyclotrons U-150-II and U-115 (energies 10–20 MeV/nucleon), Gamma-facility based on Co-60 irradiation, Neutron Generator NG-150 (E_n=14 MeV, flux up to 10^{11} $n/4\pi$ s). Either of them is equipped by the specific experimental set-up.

The researches of heavy nuclei fission under action of thermal neutrons are carried out at the mass-spectrometer placed in the main hall of the Nuclear Reactor WWR-SM. New data on mass distributions of heavy fraction of fission fragments were obtained.

The experimental technique is developed for extraction and study the radioactive neutron-excess nuclei, based on extraction of radioactive isotopes by the recoil method. Investigation of structure of neutron-excess nuclei within middle A-mass region is carried out with use the (E-E-t) - spectrometer and autocorrelated single-crystal time spectrometer of the delayed coincidences.

The external beams of the Cyclotron U-150-II can serve several basic installations. Two reaction chambers of specific design equipped by semiconductor ΔE-E –telescopes with appropriate electronics and software are meant for measurement of the nuclear reaction products. A cycle of investigations of the nucleon transferring reactions with the lightest projectile and light nuclei was fulfilled and the unique spectroscopic information was obtained with use of the set-up. The time-of-flight method is available for study the reactions with neutron escape and the multichannel magnet spectrometer is intended for high energy resolution experiments.

The specific set-up with 3-detector semiconductor ΔE-E –telescopes is used at the flux of fast neutrons from Neutron Generator NG-150. Some interesting results were obtained at few-body (n+d, n+t) interactions, and precise measuring the nucleon transferring reactions is done.

The probabilities of excitation of isomeric states, parameters of level density and mechanism of reactions (n,2n) and (γ,n) on 110<A<144 nuclei above the giant dipole resonance are studied at the neutron and γ-quanta fluxes of the NG-150 and Betatron SB-50 of National University of Uzbekistan.

The original new method has been developed at the electrostatic Accelerator EG-2 “SOKOL” of the Institute of Applied Physics National University of Uzbekistan in cooperation with physicists of INP AS RU for measurement the yields and astrophysical S-factors of the charged particle radiative capture at rather low energies. Both “activation” and ‘prompt” methods are used simultaneously to increase the accuracy of measurements. The pilot results have been obtained.

Products of photo fission heavy nuclei were studied using the bremsstrahlung beam of electrons E_e=13MeV of Microtron MT-22C (Nuclear Physics Laboratory at the State University, Samarkand) using the methods of multidimensional analysis of $\gamma\gamma$T(t) coincidences.

The experimental information accumulated at the aforesaid scientific directions may be useful for development of the Asian Reaction Database.

Systematic Study of Electric Dipole Excited States using Linear Response Method

Shuichiro Ebata
Meme Media Laboratory, Hokkaido University, N13W8, Kita-ku, Sapporo 060-8628, Japan

Systematic investigation of electric dipole (*E1*) excited states of finite nuclear system is carried out with a linear response method. The liner response calculation has been executed through the time-dependent mean field theory which can describe effects of nuclear pairing and of deformed shape of the system in nuclear dynamics. We focus on the low-lying *E1* mode which is often called Pygmy dipole resonance (PDR), and investigate the behavior of PDR as a function of neutron number. The systematic investigation without restrictions of the particle number and shape of the system is important to promote study of unstable nuclear physics and astrophysics.

1. Introduction

Electric dipole (*E1*) excited mode is one of most important response to investigate basic properties of nuclear system. The nucleus composes of proton and neutron which are charged and neutral, respectively. The *E1* mode is induced by the fluctuation of protons in the nucleus, due to the Coulomb force basically. In other words, it is the nuclear excited state of the absorption of photons or gamma-ray, and should be reflected by the proton distribution.

To derive the properties of unstable nuclei, we investigate the most basic reaction, such as *E1* excitation. It is well-known that the characteristic structure appears in neutron-rich nuclei far from stability line, which has a large difference between neutron and proton distribution [1]. We use the *E1* response to know the difference between the distributions. The response of unstable nuclei is an important probe to understand the growth and emergence of their characteristic structure, from a view point of nuclear physics. Furthermore, the systematic information of the nuclear reaction is essential to evaluate the element distribution of the solar system in astrophysics [2]. Especially, the data of unstable nuclei are important, because the nuclei have major roles of the nucleosynthesis on the rapid neutron capture process path.

We apply the linear response method with using the time-dependent mean field theory to the investigation of *E1* modes. In order to study excited states systematically, the method should describe several effects which are deformation and nuclear pairing correlation of open shell nucleus. We suggest a feasible time-dependent mean field theory [3] that includes above effects, and apply it to *E1* response for about 350 kinds of even-even nuclei. We report the application to *E1* modes and perspectives of our method in a nuclear database.

2. Theoretical Method and Results

Our time-dependent method is named the canonical-basis time-dependent Hartree-Fock -Bogoliubov theory (Cb-TDHFB) which can include nuclear pairing correlation while nuclear dynamics and can be executed in the three-dimensional Cartesian coordinate space, due to the small numerical cost. Then our method can describe the effects of any deformation, also. We calculate the linear response of nucleus using the Cb-TDHFB. The procedure of linear response calculation for *E1* mode with time-dependent scheme is that we prepare the ground state as initial state of time-evolution, and add a weak instantaneous *E1* external field to the initial state, and compute the time-evolution of nuclear density fluctuation, then obtain a spectra of *E1* mode through the Fourie transformation of time-dependent expectation value of *E1* operator. This method can be extended to other excited mode.

Figure 1 shows the photo-absorption reaction cross section of ^{172}Yb as an example of linear response calculation using Cb-TDHFB. ^{172}Yb is relatively heavy, deformed and open shell nucleus. The cross section has a characteristic giant dipole peak of deformed nucleus which composes two parts, in both theoretical (lines) and experimental (points) results. ^{172}Yb has a prolate shape in its ground state, and the fluctuations along long (K=0) and short (K=1) axes appear in its *E1* excited states, which is reported in Ref.[4]. Figure 2 shows the ratios of the low-lying *E1* strength below 10 MeV in the total *E1* strength as a function of neutron number. The low-lying strengths are recognized as PDR. We can see the characteristic kinks of PDR ratio at N=50, 82 and 60, 72 that are corresponding to magic numbers and shape transition points, respectively. We can regard that PDR is sensitive the individual structure of each nucleus, and can expect that the mechanism of PDR is not simple.

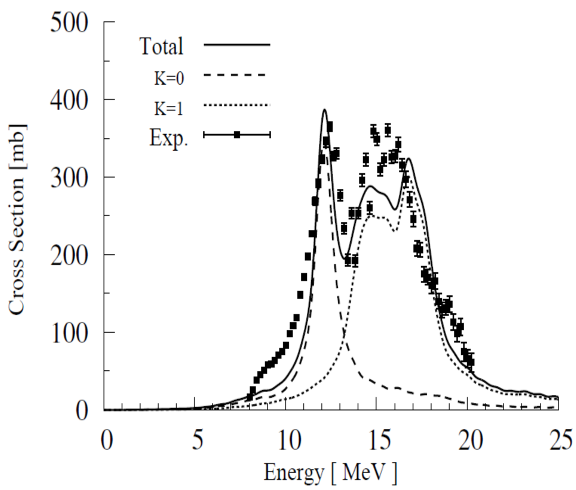

Figure 1: Photo-absorption reaction cross section of ^{172}Yb. The experimental data is taken from Ref.[5].

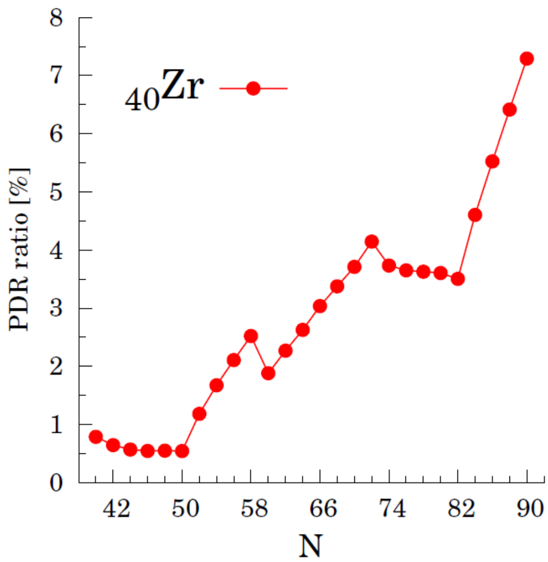

Figure 2: Neutron number dependence of PDR strength ratio in the total *E1* strength.

3. Summary

We carried out the systematic study of *E1* modes using the linear response method with the Cb-TDHFB, which include the effects of nuclear pairing correlation and deformation. We can reproduce the photo-nuclear reaction cross section of ^{172}Yb, which indicates that our method express the excited states of deformed heavy nuclei. We focus on the low-lying *E1* mode which is often called PDR especially which has an important role to evaluate the elements distributions of the solar system, and show the behavior of PDR as a function of neutron number, that is reflected the shell structure and deformation of initial state.

Currently, we are developing the database of our theoretical results in order to apply the systematic data to the network calculation of the nucleosyntesis. We plan to extend the method to other excited states (for magnetic dipole mode, electric quadrupole mode, etc.).

Acknowledgement

This work was supported in part by High Performance Computing Infrastructure Strategic Program Field 5. The numerical calculation was supported by the high performance computing system at Research Center for Nuclear Physics, Osaka University, the RIKEN Integrated Cluster of Clusters (RICC) and the SR16000 at YITP in Kyoto University.

Reference

[1] I. Tanihata, et al., *Phys. Rev. Lett.* **55** (1985) 2676.
[2] Z. Y. Bao, et al., *At. Data Nucl. Data Tables* **76** (2000) 70.
[3] S. Ebata, et al., *Phys. Rev.* C**82** (2010) 034306.
[4] S. Ebata, et al., *RIKEN Accel. Prog. Rep.* **44**, (2010) iv.
[5] A. M. Goryachev and G. N. Zalesnyy, Vopr. Teor. Yad. Fiz. **5**, (1976) 42.

STUDIES OF METALLIC BERYLLIUM

V.N. Zhumabekova[1], G.A. Spanova[2], M.N. Takibayeva[1]

[1]al-Farabi Kazakh National University, Almaty, Kazakhstan
[2]Abai Kazakh National Pedagogical University, Almaty, Kazakhstan

Influence of low-energy neutron flows on microstructure, physical and mechanical properties for some reactor-grade beryllium samples has been studied. Beryllium has low capture section for thermal neutrons what in combination with its low mass assured wide application of beryllium and its compositions in nuclear power installations and in research reactors as neutron moderator and reflector. For the same reasons, beryllium and its oxide are used in a variety of research reactors. Application of beryllium as neutron reflector makes it possible to reduce reactor core dimensions, increase working temperature, assure uniform distribution of neutron flows and increase reactor yield [1].

Beryllium irradiation with fast particles results in generation and accumulation of radiation defects there as well as to formation of helium and tritium nuclei in nuclear reactions of neutrons with beryllium nuclei. At certain parameters of irradiation, these effects can cause considerable changes in such physical and mechanical properties of the material as strength and plasticity. For instance, high-dose neutron irradiation of beryllium leads to lower strength down to 500-800% compared to its initial state and to higher micro hardness up to 500% [2]. Still, structure changes in various type beryllium materials remain poorly studied. In other cases, thermal neutrons show discrepancy between measured and calculated scattering cross-sections at reflectors of metallic beryllium [3].

In al-Farabi KazNU group the calculations are carried out using variety approaches including Monte Carlo method. But the important and topical task of determination of structure defects due to thermal neutron fluxes remains unsolved yet. Our team is working in collaboration with JAEA and scientists from the Hokkaido University, where our young scientists held a short internship. Our first results concern the study of the properties of beryllium and its compounds. Revealing of the mentioned above relation and understanding of the structure effects will foster development of new materials, encourage material studies not only in nuclear applications, but in other industries such as space or fission engineering where protection from nuclear radiation flows is key for further development. Our research project (E-13) is supported by the fund of Ministry of Education and Sciences of Republic of Kazakhstan.

1. Galtsev V.P., Sernyaev G.A., Chechetkina Z.I. Radiation material science of beryllium. Minsk, “Nauka I Technika”, 1977, 96pp.- in Russian.
2. Chakin V.P., Kazakov V.A., Teykovtsev A.A.: High dose neutron irradiation damage in beryllium as blanket material (21-st Symposium on Fusion Technology, September 11-15, 2000, Madrid, Spain) // Fusion Engineering and Design, 2001, V. 58-59, P. 535-541.
3. Tsuchiya K., Status of Beryllium Study in JAEA, The 7th Specialist Meeting on Recycling of Irradiated Beryllium, October 22, 2012, Holiday Inn Executive Center, Columbia, MO, USA; http://www.murr.missouri.edu/ismtr/papercall.

THE FEATURES AND DEVELOPMENT OF CENTRAL ASIA NUCLEAR REACTION DATABASE AT AL-FARABI KAZAKH NATIONAL UNIVERSITY

Takibayev N.Zh., Kurmangalieva V., Bakabayev M.
al-Farabi KazNU, Almaty, Kazakhstan

Description of the Central Asia Nuclear Reactions DataBase (CA_NRDB) structure is presented along with its main objectives; the general relations and software features, main charts and information flows that determine the key relations are described. SQL- interrogation samples are presented to describe data reading from the tables and getting answers to the questions asked.

Main page of the CA-NRDB relates the DB to the Republic of Kazakhstan and al-Farabi KazNU. The CA-NRDB was designed to work in the international network of nuclear databases under IAEA auspices.

Local link of the CA-NRDB to Kazakhstan and al-Farabi KazNU follows one more important objective – to create a specialized database for nuclear physics for all Central Asian countries and Kazakhstan with access open for scientists and, particularly, to students and junior researchers. The CA-NRDB interface is therefore provided in three languages English, Kazakh and Russian with reference and educational units embedded.

In general, the CA-NRDB is a client-server software application. Developing this application ASP.NET and ADO.NET Microsoft technologies were utilized. Integrated development environment (IDE) Visual Studio 2010 (MS VS 2010) has been used at the development of the database. Another Microsoft product, Microsoft SQL Server 2008 R2 (MS SQL Server 2008 R2), has been used as DBMS.

The database has been developed as a relational system with data charts on specialized issues and with a log on tasks performed and system resources. Main console for work with the lower-level units is the Operations Console at the main page with the links to subunits of the DB.

Categories and units related to information on distinguished physicists of Kazakhstan and those who contributed to development of science in Kazakhstan is a feature of CA-NRDB. Several large units contain educational and lecture materials as well as reference data on nuclear physics. There is a subunit with information on international conferences and important scientific events. A photo gallery introduces Kazakhstan, Almaty and al-Farabi Kazakh National University and we believe this is an important part in forming our image.

A key to convenient operation with the DB is autonomous access to the international network of IAEA databases on nuclear reactions with capabilities to work within this network.

CA-NRDB assures direct access to our partner DBs – the DB of photonuclear reactions SRINP at Moscow State University (Russia) and to the nuclear DB of Hokkaido University (Japan). Collaboration with these universities with their half-century experience in specialized data base development is very fruitful for our junior team and contributes a lot to the development of the first in Central Asia database on nuclear reactions.

CA-NRDB today is an effective and convenient tool with continuously growing and improving massive of specialized data. CA-NRDB project (ITT-8) is supported by the fund of Ministry of Education and Sciences of Republic of Kazakhstan.

NUCLEAR DATABASES FOR SCIETIFIC RESEARCH AND EDUCATION AT THE MSU SINP CDFE

V.V.Varlamov
Lomonosov Moscow State University, Skobeltsyn Institute of Nuclear Physics
Centre for Photonuclear Experiments Data
119991 Moscow, Russia

The Centre for Photonuclear Experiments Data (Centr Dannykh Fotoyadernykh Eksperimentov – CDFE) was organized at the Skobeltsyn Institute of Nuclear Physics of Lomonosov Moscow State University with the task of informational support of scientific research and education process. The CDFE is specialized in development of various nuclear databases (DB) available through Internet (http://cdfe.sinp.msu.ru).

The main field of CDFE activity is participation as specialized center the International Atomic Energy Agency (IAEA) Nuclear Reaction Data Centres (NRDC) Network [1]. The main aim is to develop and maintain international EXFOR database contained experimental data on nuclear reactions with various incident projectiles. The field of CDFE responsibility is compilation, evaluation and dissemination of photonuclear data.

Therefore the main CDFE database is “Nuclear Reaction Database (EXFOR)” maintained in cooperation with the IAEA NRDC Network: many data for reactions induced by photons, neutrons, charge particles and heavy ions.

The “Complete Nuclear Spectroscopy Database "Relational ENSDF" contains many nuclear spectroscopy data for all known (~3200) nuclides from the well-known international fund ENSDF (Evaluated Nuclear Structure Data File), produced and maintained by USA National Nuclear Data Center (NNDC) and NSDD cooperation.

The “Nuclear Physics Publications ("NSR" Database)” is the really relational CDFE produced DB using the NSR (Nuclear Science References) data fund maintained by USA NNDC.

The “Nucleus Ground and Isomeric State Parameters” DB is based on many various sources of data and combines many useful information on the nucleus as whole and its ground and isomeric states properties (masses, binding energy, nucleon separation energy, decay mode, energy of various decays, etc).

Other databases are CDFE-produced and maintained:

- digital “Chart of Giant Dipole Resonance Main Parameters” contains data on main parameters (energy position, amplitude, width, integrated cross section) of GDR for many nuclei;

- digital “Chart of Nucleus Shape and Size Parameters” contains data on quadrupole moments, parameters of quadrupole deformation and charge radii for many nuclei;

- “Calculator and Graph Engine for Atomic nuclei Parameters and Nuclear reactions and Radioactive Decays Features” gives to one possibility for convenient calculation of: i) nucleus binding energy, ii) nucleon and nucleus separation energy, iii) decay energy, iv) reaction threshold and energy, v) nucleus fission parameters; graphical presentation of A-dependencies of data calculated is possible.

All databases maintained by CDFE are widely used for scientific research, primarily for investigation of systematical disagreements between the results of various photonuclear experiments and are the base for education of MSU Physics Faculty students.

The work was partially supported by several Russia Foundation for Basic Research (RFBR) Grants (now is supported by Grant N13-02-00124).

[1] International Network of Nuclear Reaction Data Centres, Prepared by Naohiko Otsuka and Svetlana Dunaeva, IAEA International Nuclear Data Committee, INDC(NDS)-0401, Rev.5, IAEA, Vienna, Austria, 2010.

Introduction of the digitization software GDgraph

Chen Guochang Jin Yongli Wang Jimin
China Nuclear Data Center, China Institute of Atomic Energy, Beijing, 102413, China

1. Introduction

The evaluators and experimenters always desire to have full and latest experimental data sets. However, the data are often published as figures without any numerical values for some publications or journals. Furthermore, the quality of figures is not always good enough, especially for some figures scanned from the hard copy of old publications. On the other hand, the researchers would like to retrieve the data directly from EXFOR database. Digitization of figures is only one method to obtain the numerical data and correlative uncertainty, when there are only figures available from publications. Therefore we need a digitization software to fit the requirements from evaluation, measurement and EXFOR compilation in CNDC.

Before 2000, there have no common software to digitize experimental and evaluated data. And the quality of digitization results can not fit the requirements of evaluation and measurement using the traditional coordinate paper or rule. The end of twenty century, the PC was developed so quickly that to develop a software for digitization purpose become possible. Since 1997, CNDC devotes to design and develop a software for digitization. Four years later, the first version of digitization software GDGraph was developed using VC++ and released in CNDC. Although, the functions of the 1st version of GDGraph is fit the basic requirements of digitization only, in which can digitize one group data excluding data error, BMP image format only, and it can not randomly delete digitizing data points. However, it obtains higher quality digitizing results and efficiency than the traditional method.

Five years late, we collected some feedback information and suggestion on update of this software. The 2nd version of GDGraph software was released at 2006, in which the whole software was re-written using Perl to obtain more comfortable conditions for programming and updating. The version 3.0, 4.0 and 5.0 of GDGraph is released at 2011, 2012 and 2013, respectively.

2. Main feature of GDGraph5.0

Main features of GDGraph5.0 is listed below:

(1) Operating system: WindowsXP or the higher version of Windows.
(2) Intuitive and light GUI: Provide Chinese and English version GUI.
(3) Supports image format: such as PNG, GIF, BMP and JPEG etc.
(4) The image can be automatically fit to the GUI window, and zoom-in or zoom-out manually together with the digitizing X, Y axis.
(5) Allow to rotate the image and set a rotation angle with degree unit.
(6) The maximum digitizing data group number is three, and the color, size and shape of each group can be defined by user using “Settings” function.
(7) Randomly add the digitizing point and move it by mouse or cursor keys.
(8) Output data can be saved as a data file or at clipboard.
(9) Import data function is enable to reuse the former digitizing data or compare with other data group easily.
(10) X, Y axes: Select or set a unit for X, Y data by user is available. Allow to digitize X, Y error with symmetry or asymmetry mode and move it using mouse or cursor keys, and set a fix value with relative (%) or absolute mode.
(11) Magnifying glass function: It magnify the local area of the image, and the window size can be set from 200% to 800% and move it by mouse. The partial image in the magnifying glass window can be magnified 2 or 4 times.
(12) Setting the color, size and shape of digitizing point, the background with or without gridding lines, output digitizing numerical data format is available.
(13) Project function: It is used to save image, digitizing results with other settings as a project

file *.GDP for checking and modification in the future.

(14) Remark function is applied to keep some marks and memo text for checking, modification and memory by user.

3. Basic Functions of GDGraph5.0

3.1 Installing GDGraph5.0

Recently GDGraph5.0 can be used in WINDOWS operation system only such as WindowsXp or the higher versions. To download the installation file “GDGraph5.0.msi” from the website as “www.nuclear.nsdc.cn/gdgraph”.

Double clicks “GDGraph5.0.msi” file to start installing GDGraph in your computer. Click “Next” button to continue install. The “Custom” mode of installation allows to choose the installation directory, and the “Install” mode use the default installation directory as “C:\Program Files\CNDC\GDGraph\”. You can find the short cut execution link at Windows start program menu as “CNDC” or you can have a shortcut link at desktop.

3.2 Loading the image file

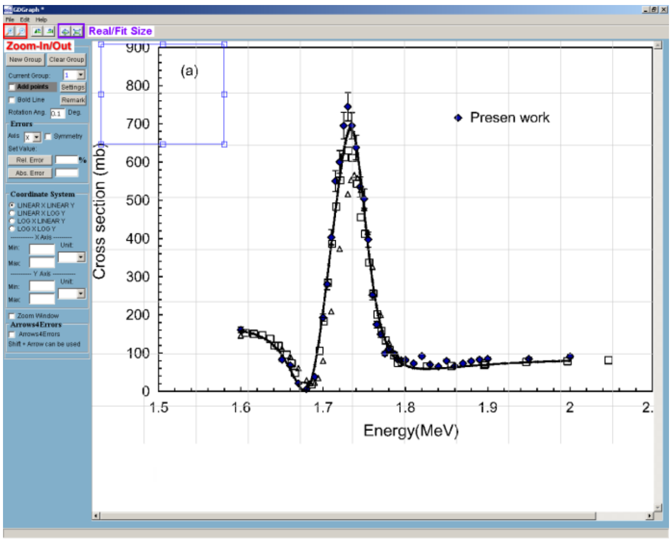

Figure 1 An image loads on the main panel.

There have some options to load an image. One is using “Load Graph File” from the “File” menu in the menu bar. Select an image file (as PNG, GIF, BMP or JPEG) from a file dialog box in a new window and the image with original size is default. Another one can directly copy an image using clipboard from other file such as MS Word, PDF, etc. If the image file is successfully loaded, the image is displayed on the main panel as shown in Figure 1.

3.3 Setting axes

Use cross lines to set the X-Y axes of image, and adjust the square symbols of the starting, middle and ending positions of X-Y axes to fit the image one. Then select the X-Y axes type as Linear-Linear, Linear-Log, Log-Linear and Log-Log. According to the cross line positions, fill in the starting and ending value of X-Y axes, and select or fill in unit for X-Y axes at “Coordinate System” in “Control Panel”, respectively. When we set or adjust the positions of axis, there exist an orthogonal cross lines to assist confirming the position of axes. When you finish setting the axes, you will see a window as shown in Figure 2.

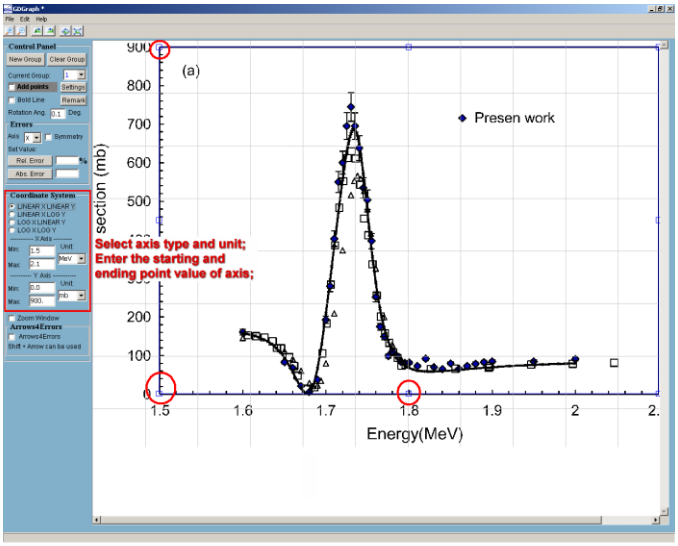

Figure 2 Window after setting axes with squares.

3.4 Reading the data and error

Activate the check box "Add points" to start digitizing data points. If there exist more than one group digitizing data, please select which group you want to add new points or modify the original digitizing results. If you click on the image in the data input mode, a data point is added on the image. Continue to click the image until all the data points are added. When you finish adding the data points, you will see a window as shown in Figure 3(a).

Digitizing data point error is possible now. First of all, disable the "Add points" mode. Then, to select the error mode of X-Y with asymmetric or symmetric. The default error mode of X-Y is asymmetric. To set a symmetric error for X or Y, first select X-axis or Y-axis at "Axis" list box in "Errors" part, then click "Symmetric" check box. After that, click a data point to activate it which will appear 4 red square symbols around it. In this mode, it realize to move data point by mouse or cursor keys or set X-Y error. The left and right square symbols represent X-Err-/X-Err+, and the bottom and top symbols represent Y-Err-/Y-Err+. If you obtain the information of X-Y uncertainty from paper or other ways, you can directly fill in a fix value as X-Y uncertainty with relative (%, in percent) or absolute mode. You can directly use mouse to pull one of four red squares to obtain X-Y error. On the other hand, you can apply "Arrows4Errors" function to realize using cursor keys to move one of four red squares to proper position. After inputting errors, you will see a window as shown in Figure 3(b).

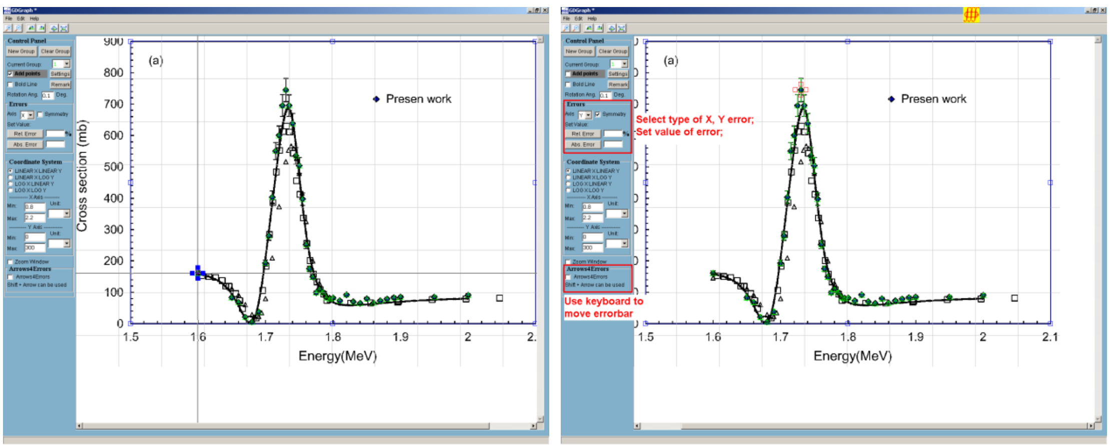

(a) Reading the data points (b) Reading the data errors

Figure 3 Window after reading the data points and errors.

3.5 Outputting the numerical data

Select “Save Data File” from the “File” menu or directly use “Ctrl+C” to copy all digitizing data to clipboard and paste to other applications. The output data is in exponent or float format, and the number of digits can be set at “Settings” function. Each data can be set as 11 columns to fit EXFOR format requirements. The output file contains the information of each group No., number of data points, name of each column and digitizing data. Each group output contains X, Y, Y-Err+, Y-Err-, X-Err-, and X-Err+ as shown in Figure 4.

```
!!######group 1 ####(39 points) ############
!#     X(MeV)        Y(mb)         dY+          dY-          dX-          dX+
  1.03415E+00 5.34411E+01 2.63429E+00 2.63429E+00 0.00000E+00 0.00000E+00
  1.15063E+00 2.73492E+01 3.13606E+00 3.13606E+00 0.00000E+00 0.00000E+00
  1.17425E+00 2.24569E+01 2.38340E+00 2.38340E+00 0.00000E+00 0.00000E+00
  1.19746E+00 6.65120E+00 2.50884E+00 2.50884E+00 0.00000E+00 0.00000E+00
  1.22109E+00 1.63351E+00 1.63075E+00 1.63075E+00 0.00000E+00 0.00000E+00
  1.24430E+00 1.22961E+01 2.88517E+00 2.88517E+00 0.00000E+00 0.00000E+00
  1.26751E+00 6.41037E+01 3.13606E+00 3.13606E+00 0.00000E+00 0.00000E+00
  1.27932E+00 9.30809E+01 4.51592E+00 4.51592E+00 0.00000E+00 0.00000E+00
  1.29073E+00 1.34100E+02 6.77388E+00 6.77388E+00 0.00000E+00 0.00000E+00
  1.30294E+00 1.83274E+02 9.15728E+00 9.15728E+00 0.00000E+00 0.00000E+00
  1.31435E+00 1.99958E+02 1.00354E+01 1.00354E+01 0.00000E+00 0.00000E+00
  1.32616E+00 2.31695E+02 1.15407E+01 1.15407E+01 0.00000E+00 0.00000E+00
  1.33780E+00 2.48260E+02 1.20897E+01 1.20897E+01 0.00000E+00 0.00000E+00
  1.34937E+00 2.31569E+02 1.16661E+01 1.16661E+01 0.00000E+00 0.00000E+00
  1.36118E+00 2.12627E+02 1.07880E+01 1.07880E+01 0.00000E+00 0.00000E+00
  1.37258E+00 1.78256E+02 8.90640E+00 8.90640E+00 0.00000E+00 0.00000E+00
  1.38480E+00 1.67719E+02 8.53007E+00 8.53007E+00 0.00000E+00 0.00000E+00
  1.39539E+00 1.32093E+02 6.77388E+00 6.77388E+00 0.00000E+00 0.00000E+00
  1.40802E+00 8.37982E+01 4.26504E+00 4.26504E+00 0.00000E+00 0.00000E+00
  1.41860E+00 5.79571E+01 2.88517E+00 2.88517E+00 0.00000E+00 0.00000E+00
  1.43082E+00 4.94270E+01 2.50884E+00 2.50884E+00 0.00000E+00 0.00000E+00
  1.44304E+00 3.27432E+01 1.63075E+00 1.63075E+00 0.00000E+00 0.00000E+00
  1.45404E+00 3.60047E+01 2.13252E+00 2.13252E+00 0.00000E+00 0.00000E+00
```

Figure 4 An example of outputting numerical data file.

4. Conclusion

Since 1997, the digitization software GDgraph is developed to fit the requirements of evaluation, measurement and EXFOR compilation. From the mold software to present version 5.0, GDgraph is mainly fit the requirements, although there are some aspects need to modify and add some new functions also.

Recent EXFOR Compilation in CNDC

Guochang Chen, Jimin Wang, Xi Tao, Youxiang Zhuang, Zhigang Ge
China Nuclear Data Center, China Institute of Atomic Energy, Beijing, China, 102413

1. Introduction

The EXFOR library has become the most comprehensive compilation of microscopic experimental nuclear reaction data. It contains cross sections and other nuclear reaction quantities induced by neutron, charged-particle and photon beams, etc. Currently compilation is mandatory for all low and intermediate energy neutron and light charged-particle induced reaction data. Heavy-ion and photon induced reaction data are also additionally compiled on a voluntary basis.

Currently fourteen data centers are participating in the International Network of Nuclear Reaction Data Centres (NRDC) and are collaborating mainly for compilation and exchange of experimental data by using the common Exchange Format (EXFOR Format) under the auspices of the IAEA Nuclear Data Section (NDS).

2. EXFOR Compilation in CNDC

Since China joined IAEA at 1984 and China Nuclear Data Center (CNDC) joined NRDC in 1987, we are takes part in scanning Chinese journals and compiling EXFOR entries and collaborating with NRDC. CNDC is one specialized center at NRDC as shown in Figure 1. Which the experiments are carried out by Chinese researcher, the experiments are measured in China and measurements are published in Chinese journals, compilation of bibliographic references (CINDA) to microscopic neutron reaction data and related data published in Chinese, CNDC need to scan and collect measured results and compile these data and information as EXFOR format including neutron and charge particle induced reactions. CNDC are respond more than 9 Chinese journals now such as Figure 2 and IAEA assigns EXFOR compilation task.

Country	Center	Joined
Russia	Nucl. Struc. & Nucl. Reac. Data Centre	1974
Japan	Japan Nuclear Reaction Data Center	1975
Russia	Centre for Exp. Photonuclear Data	1982
China	*China Nuclear Data Center*	*1987*
Japan	Nuclear Data Center	1991
Korea	Nuclear Data Evaluation Laboratory	2000
India	Nuclear Data Section	2008

Figure 1 The specialized center at NRDC

In 1985, IAEA and CNDC hold a working meeting about compilation in EXFOR. Fifteen charged particle EXFOR entries were transmitted to IAEA for NRDC communication at this meeting as shown in Figure 3 and started to compile neutron entries at 1989.

1. Chinese Physics C(ENG/2007;HEN)
2. Atom. Energy Sci. & Tech.(CHN/1959)
3. J. of Nucl. & Radiochemistry(CHN/1979)
4. Nuclear Physics Review(CHN/1984)
5. Nuclear Techniques(CHN/1978;+ENG/1989)
6. Com. of Nucl. Data Prog.(ENG/1989)
7. Nuclear Science and Techniques(ENG/1989)
8. Chinese Physics Letters(ENG/1984)
9. Chinese Physics B (ENG)
10. Acta Physica Sinica(ENG/1933)
11. Conference, Workshop etc.

Figure 2 List of the responsibility of CNDC

01 Li Zhichang+	Yuanzineng Kexue Jishu 3(1977)229
02 Liang Qichang+	Yuanzineng Kexue Jishu 1(1977)10
03 Mao Zhenlin+	Conf. on Low Energy Nucl. Phys.3(1972)
04 Yuan Rongfang+	Chin. J. Nucl. Phys. 3(1981)155
05 Jiang Chenglie+	Conf. on Low Energy Nucl. Phys.3(1972)
06 Sun Hancheng+	Yuanzineng Kexue Jishu 3(1984)329
07 Yan Chen+	Chin. J. Nucl. Phys. 2(1980)137
08 Sun Hancheng+	Yuanzineng Kexue Jishu 2(1981)185
09 Ma Weiyi+	Chin. J. Nucl. Phys. 2(1980)239
10 Shen Wenqen+	High Energ.Phys.Nucl.Phys.1(1977)70
11 Tao Zhenlan+	Canadian Nucl Technol.45(1987)
12 X.Long+	NST-001 (1985)
13 Long Xianguan+	NST-003 (1989)
14 Tao Zhenlan+	Chin. J. Nucl. Phys. 3(1981)242
15 Tao Zhenlan+	Yuanzineng Kexue Jishu 5(1983)506

Figure 3 CNDC provided the first 15 charged particle EXFOR entries

	No.	Ref.	Title	Vol.	Issue	Page	Lab	Publish date	Author	Status	Action	Delay date(m)	Compiler	Entry	Sub.	Memo
修改 详情	1	J,BCA	Cross section measurements for gallium in the neutron energy range of 13.5 to 14.8 MeV	100	4	231	3CPRHXU	201202	J. Luo	Allocated	Compiling	6	Youxiang ZHUANG	32704	n	Assigned this entry a …
修改 详情	2	J,IPC	Cross-sections for formation of 99mTc through nat-Ru(n, x)99mTc reaction induced by neutrons at 13.5 and 14.8 MeV	81	5	495	3CPRHXU	201201	Junhua Luo	Allocated	Compiling	7	Youxiang ZHUANG	32702	n	Assign this entry is …
修改 详情	3	J,IPC	Cross-sections for (n,2n), and (n,a) reactions on 55Mn isotope around neutron energy of 14 MeV	81	10	1563	3CPRLNZ	201204	Yanbin Zhang	Allocated	Compiling	4	Jimin YANG	32701	n	Assign this entry is …
修改 详情	4	J,JRN	Cross section measurements for 141Pr(n, g)142Pr reaction at neutron energies from 13.5 to 14.8 MeV	293	1	261	3CPRHXU	201204	Junhua Luo	Allocated	Compiling	4	Guochang CHEN	32703	n	It is assigned at Aug …
修改 详情	5	J,HFH	239Pu(nth, f)短寿命裂变产物产额测量	34	2	88	3CPRAEP	201203	刘世龙	Allocated	Compiling	5	Guochang CHEN	32700	n	It is assigned at Au …
修改 详情	6	J,EPJ/A	New determination of the astrophysical 13C(p, y)14N S(E) factors and reaction rates via the 13C(7Li, 6He)14N reaction	48	2	13	3CPRAEP	201202	Y.J.Li	Allocated	Compiling	6	Xi TAO	S0054	cp	Assigned this entry …
修改 详情	7	J,HEN	Cross section measurements for (n,p) reaction on stannum isotopes at neutron energies from 13.5 to 14.6 MeV	35	5	445-448	3CPRLZT	201105	PU Zhongsheng(蒲忠胜)	Allocated	Compiling	15	Youxiang ZHUANG	32699	n	Finish compile at Ju …
修改 详情	8	ASI	13 兆电子伏氘核所引起的一些反应的激发函数	22	2	250	3CPRNRS	196602	程晓五	Allocated	Finalized	558	Guochang CHEN	S0060	cp	Finalized this entry …
修改 详情	9	JP/CS	Fusion-fission and quasifission competition in the 32S+184W reaction	282	1	12013	3CPRAEP	201103	H.Q.Zhang	Allocated	Compiling	17	Youxiang ZHUANG		cp	This is calculation r …
修改 详情	10	J,EPJ/A	Level structures in the 114In nucleus	47	11	141	3CPRAEP	201111	C.B.Li			9			cp	This paper couldn't b …

Figure 4 EXFOR compilation managed Website

Present we have a small group to attend EXFOR compilation work. Everyone respond to scan 2 journals, collect the scanning results of all responsible journals, and assign neutron and charged particle tasks. After that, upload the information such as the assigned entry No., paper in pdf, author, publication date, delayed date, the compiler and the processing of compilation to our EXFOR compilation managed Website as shown in Figure 4.

From 2009 to 2013, CNDC compiled 59 EXFOR entries as shown in Figure 5 which is included 20 neutron and 39 charged particle entries. We can find recently the charged particle induced reaction measurement is become more and more.

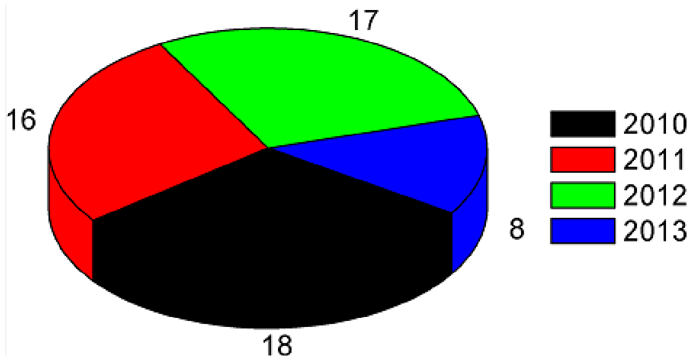

Figure 5 Compiled EXFOR entries of each year

3. Nuclear Data Service

CNDC provides the nuclear data service in China for different institute, school or other requirements. CNDC joined the developing of Chinese basic database and established a "The Database of Nuclear Physics" website as shown in Figure 6 including experimental data (EXFOR), evaluation data, decay data, nuclear structure, astrophysical data and nuclear data for medical applications for online retrieve and plotting, and the website is "www.nuclear.csdb.cn". CNDC also established the mirror site of IAEA-NDS at Aug. 31 2013, which is "www-nds.ciae.ac.cn". And the database of this mirror site is update with IAEA-NDS website at the same time. Up to now, the contents of mirror site includes EXFOR database and evaluation database as shown in Figure 7. And the contents will be enriched in the future.

Figure 6 Webpage of "The Database of Nuclear Physics"

Figure 7 Webpage of IAEA-NDS mirror site

4. Conclusion

The needs for experimental reaction data are always growing. CNDC response to scan, collect and compile the experimental information which are carried out by Chinese researcher, the experiments are measured in China and measurements are published in Chinese journals, and related data published in Chinese. Present CNDC have a small group to attend EXFOR compilation work and construct an EXFOR compilation managed Website for EXFOR compilation organization. CNDC will continue to scan, collect and compile EXFOR data and collaborate with NRDC.

International and Asian Collaboration on Nuclear Data

M. Aikawa[1], S. Ebata[2], N. Furutachi[1], D. Ichinkhorloo[2], K. Katō[1], A. Makinaga[1], V. Devi[2], M. Odsuren[2], N. Otsuka[3], M. Takibayeva[4,5] and K. Tsubakihara[6]

[1]Faculty of Science, Hokkaido University, N10W8, Kita-ku, Sapporo 060-0810, Japan
[2]Meme Media Laboratory, Hokkaido University, N13W8, Kita-ku, Sapporo 060-8628, Japan
[3]Nuclear Data Section, International Atomic Energy Agency, P.O. Box 100, A-1400 Wien, Austria
[4]Graduate School of Science, Hokkaido University, N10W8, Kita-ku, Sapporo 060-0810, Japan
[5]Institute of Experimental and Theoretical Physics, Al-Farabi Kazakh National University, Almaty 050071, Kazakhstan
[6]Department of Engineering Science, Osaka Electro-Communication University, Neyagawa 572-8530, Japan

Experimental nuclear reaction data can be obtained at enormous cost and huge researcher effort. Such data must be shared worldwide, compiled as a database, and available to the public through the Internet. The data obtained in experiments must be theoretically evaluated and then applied in many application fields, e.g. nuclear physics, astrophysics, nuclear engineering, and radiation therapy. Due to the large number of nuclear reaction data, international and Asian collaboration is important and unavoidable.

1. Introduction

Nuclear reaction is applicable in many application fields, e.g. nuclear physics, astrophysics, nuclear engineering, and radiation therapy. There are many experimental works performed worldwide to obtain nuclear reaction data, such as cross sections and product yields. The majority of such data is published in scientific journals, which may apply charges and are accessible only to researchers. In addition, nuclear reaction experiments can be performed only under enormous cost and huge researcher effort. Such data, therefore, must be common property and freely available through the Internet. Compilation of the data requires broad and long-term efforts due to a large number and variety of experiments. One of the open databases compiling experimental nuclear reaction data is the EXFOR database, which is maintained by the International Atomic Energy Agency (IAEA) and the International Network of Nuclear Reaction Data Centres (NRDC). The NRDC consists of 14 members worldwide and cooperatively compiles experimental nuclear reaction data into the EXFOR database.

2. Asian Collaboration

Nuclear reaction data is obtained in accelerators worldwide and also in Asian countries. It is preferable to compile the data in their own countries due to easy communication with the authors of published articles. In order to sustain and develop compilation activities, collaboration with the NRDC members in Asia was developed under the support of the 'R&D' Platform Formation of Nuclear Reaction Data in Asian Countries (2010-2013), the Asia-Africa Science Platform Program, the Japan Society for the Promotion of Science from April 2010 to March 2013. Since 2010, annual workshops, referred to as the Asian Nuclear Reaction Database Development Workshop, were held at Sapporo, Japan in 2010; Beijing, China in 2011; and in Pohang, and Korea in 2012. The workshops were devoted to sharing information about their activities, to strengthen collaboration among the NRDC members in Asia and to promote the dissemination and improvement of data compilation techniques. In order to improve compilation techniques, educational sessions for digitization and compilation took place.

Fortunately, even though the support had already been finished by March 2013, the 4th workshop could be held at Al-Farabi Kazakh National University, Almaty, Kazakhstan in October 2013. Central Asian countries, such as Kazakhstan and Uzbekistan, have a long history of nuclear research. During this period, a large amount of data was produced. This fact motivated them to create a database of nuclear reaction data obtained in Central Asia. Therefore, the

Central Asia Nuclear Reaction Database (CA-NRDB) was established and started to compile nuclear data obtained at their domestic facilities with the support and encouragement from the Hokkaido University Nuclear Reaction Data Centre (JCPRG) and the Centre for Photonuclear Experiments Data of the Moscow State University.

In the EXFOR database, a country's ratio of facilities where experiments were performed was shown in Table 1. The contributions of Japan and Kazakhstan are 12.03% and 0.22%, respectively. The compilation of nuclear data performed in Kazakhstan is being developed.

3. Summary

Al-Farabi Kazakh National University and Hokkaido University concluded an Inter-University Exchange Agreement in August 2011. Under the agreement, researchers in the two universities promote collaborative researches on nuclear data. As one of the collaborations, the compilation of nuclear data obtained in Kazakhstan was initiated. The collaboration is extending to nuclear data evaluation and simulations using the Monte Carlo method.

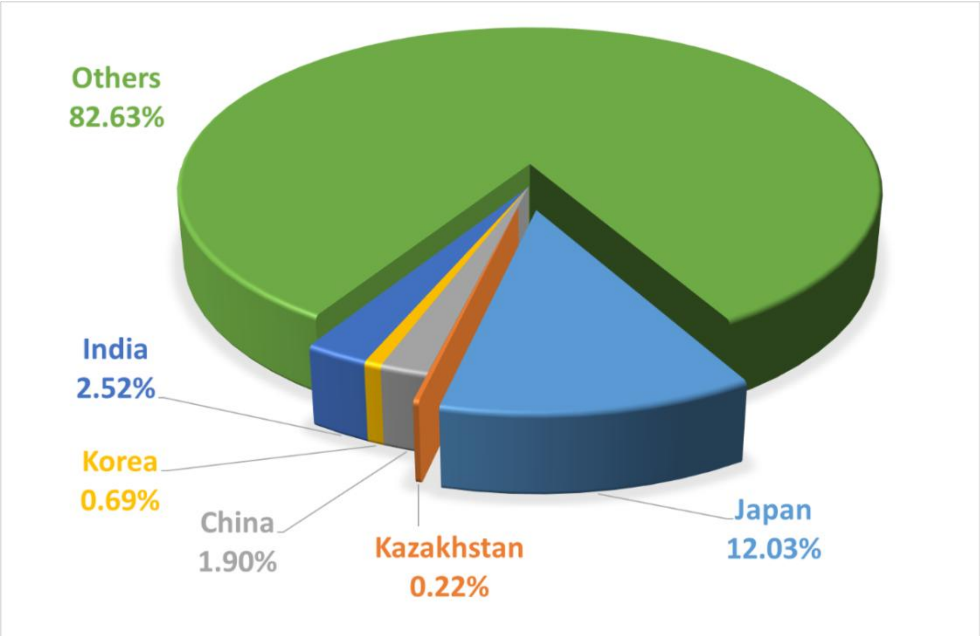

Table 1: Country's ratio of experimental facilities in the EXFOR database

Acknowledgement

The authors are grateful for the support by the ITT-8 Project of Ministry of Education and Sciences of the Republic of Kazakhstan, by "'R&D' Platform Formation of Nuclear Reaction Data in Asian Countries (2010-2013)", Asia-Africa Science Platform Program and Grant-in-Aid for Publication of Scientific Research Results (No. 257005), Japan Society for the Promotion of Science (JSPS), and by the Hokkaido University Support program for research exchange with inter-university foreign partners.

Compilation of Experimental Nuclear Reaction Data Measured in Central Asia

N. Otsuka[1], V. Semkova[1], N. Kenzhebayev[2], F. Ergashev[3], V. Kurmangalieva[2], M. Nusipalyeva[2], M. Takybayeva[2]
[1]*Nuclear Data Section, International Atomic Energy Agency, A-1400 Vienna, Austria*
[2]*Institute of Experimental and Theoretical Physics, Al-Farabi Kazakh National University, 050060 Almaty, Kazakhstan*
[3]*Institute of Nuclear Physics, Uzbekistan Academy of Sciences, 702132 Tashkent, Uzbekistan*

The Institutes of Nuclear Physics (INP) in Almaty and Tashkent been active in measurements of nuclear reaction data (**Fig. 1**). The charged-particle induced reaction data measured by the cyclotrons of the INP Almaty and Tashkent as well as the neutron-induced reaction data measured at the research reactor of the INP Almaty have been the major contributors to the current EXFOR library from these countries. The cyclotron of the INP Almaty is active, and the cyclotron of the INP Tashkent currently used for isotope production is planned to be back to nuclear reaction experiments in the near future. All experimental works from these countries and compiled in EXFOR are listed in **Appendices 1** and **2**, and have been utilized by EXFOR users. For example, proton and alpha induced reaction activation cross sections measured by V.N. Levkovskij [1] are known to show good agreements with later experimental data sets (if the original data are renormalized due to change in the monitor cross section), and it is one of the most frequently cited experimental nuclear data from Kazakhstan.

Recently the IAEA Nuclear Data Section has performed checking of EXFOR completeness for radioisotope production cross sections by using the reference lists in Landolt-Börnstein compilation [2], and found some experimental works from Kazakhstan and Uzbekistan are missing in EXFOR. All of them are published in domestic journals (Izvestiya Akademii Nauk Kazakhskii SSR Seriya Fizika i Matematiches, Izvestiya Akademii Nauk Uzbekiskoi SSR Seriya Fizika i Matematiches). Especially there is no EXFOR entry compiled from the latter journal, and the situation may indicate that systematic scanning of articles for EXFOR compilation have not been performed for these journals though it is not easy to find these journals in libraries outside these countries. Furthermore, it was mentioned during this workshop (The 4th Asian Nuclear Reaction Database Development Workshop, Almaty, Kazakhstan, 23-25 October 2013) that about half of experimental works from INP Almaty are still missing in EXFOR [3]. Appendices 1 and 2 show that digitized data are sometimes compiled instead of the original data provided by authors from Kazakhstan and Uzbekistan even for the experimental works published recently.

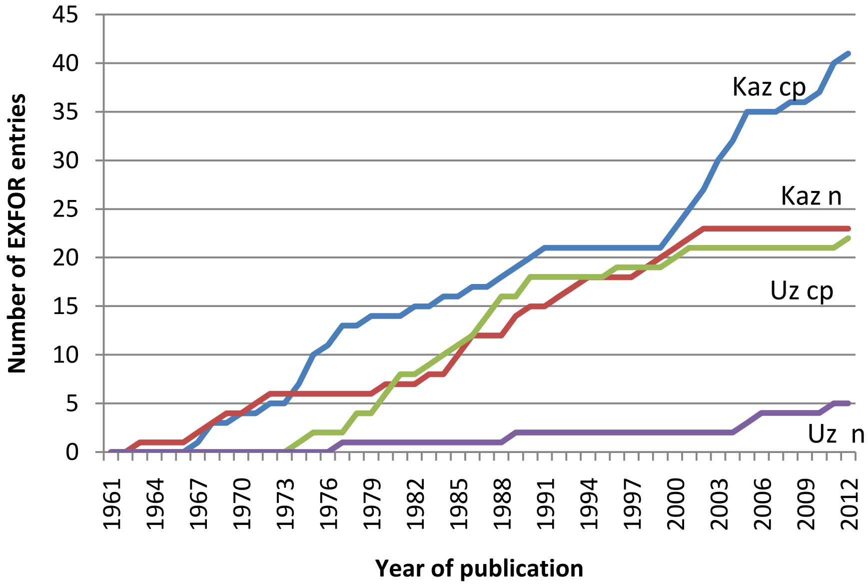

Fig. 1: Cumulative numbers of EXFOR entries for charged-particle (cp) and neutron (n) induced reactions measured in Kazakhstan (Kaz) and Uzbekistan (Uz).

The Institute of Experimental and Theoretical Physics, Al-Farabi Kazakh National University organized a three-days workshop from 28 to 30 October 2013 for young researchers from Kazakhstan and Uzbekistan in order to improve the above mentioned situation. Following some lectures on access to EXFOR and preparation of EXFOR entries, the participants searched some EXFOR entries by themselves, and also learned EXFOR compilation by using an editor (HENDEL) [4] and digitizer (GSYS) [5]. The participants finalized one new EXFOR entry for the $^{19}F(\alpha,n)^{22}Na$ excitation function measured at INP Almaty [6], and the entry was accepted by the IAEA Nuclear Data Section for transmission to other data centres. Note that there have been only two EXFOR entries reporting this (α,n) excitation function. Both of them were measured by detection of neutrons while the Kazakh experiment reports data by activation.

After the workshop, the participants finalized three more EXFOR entries for radioisotope production cross sections measured at INP Almaty [7] and Tashkent [8-9]. All Kazakh and Uzbek data identified as missing in EXFOR by checking against Landolt-Börnstein compilation will be included in EXFOR in the near future. After finalization of these entries, a new article published by researchers of Kazakh National University [10] was also compiled by us with the numerical data received from the authors. It must be also mentioned that one of us (M.T.) compiled another new article reporting data from INP Almaty [11] under supervision of JCPRG prior to the workshop in Almaty. The IAEA Nuclear Data Section plans to continue this training to investigate if the Kazakhstan-Uzbekistan group is capable to continue EXFOR compilation activity for data from these countries on a stable basis.

We acknowledge M. Aikawa, R. Forrest, K. Katō, N. Takibayev and R. Yarmukhamedov for their support to this project. S. Babykina, S. Taova and V. Varlamov kindly agree to use articles reporting data measured in these countries for this attempt, and it is appreciated. One of us (N.O.) also wants to express his thanks to the hospitality by Kazakh National University and KazAS Institute of Nuclear Physics.

References

[1] V.N. Levkovskij, Activation cross section nuclides of average masses (A = 40 - 100) by protons and alpha-particles with average energies (E = 10 - 50 MeV), Moscow, 1991. EXFOR A0510.

[2] H. Schopper (ed.), Production of Radionuclides at Intermediate Energies, Landolt-Börnstein New Series, Group I, Vol. 13, Springer Verlag, 1991 - 1999.

[3] N. Burtebayev, private communication, 2013.
[4] N. Otuka, NRDF Annual Report No.15, p.12, 2001 (in Japanese).
[5] R. Suzuki, Report INDC(NDS)-629, p.19, 2013.
[6] V.T. Gladun, G.P. Chursin, Izv. KazSSR A.N. Ser Fis.-Mat. 1980 No.4 (1980) 82. EXFOR D0723.
[7] I.N. Naustov, S.T. Tinomirova, S.D. Beizin, Izv. A.N. KazSSR Ser Fis.-Mat. 1990 No.2 (1990) 3. EXFOR D0725.
[8] A. Vasidov, G. Vakilova, S. Mukhammedov, Izv. A.N. UzSSR Ser Fis.-Mat. 1981 No.3 (1981) 93. EXFOR D0726.
[9] S. Mukhammedov, E. Pardayev, Izv. A.N. UzSSR Ser Fis.-Mat. 1985 No.5 (1985) 81. EXFOR D0727.
[10] V.V. Dyachkov, A.V. Yushkov, A.L. Shakirov, Instrum. Exp. Tech. **56** (2013) 521. EXFOR D0728.
[11] Sh. Hamada, Y. Hirabayashi, N. Burtebayev, S. Ohkubo, Phys. Rev. C**87** (2013) 024311. EXFOR D0711.

Appendix 1

Nuclear reaction data measured in Kazakhstan and compiled in EXFOR before this workshop (Italicized EXFOR entry numbers indicate inclusion of data digitized from figures.)

EXFOR	**1st Author**	**Year**	**Lab.**	**Quantity measured**
40016	V.N. Levkovskiy	1963	INP (linac?)	(n,p) and (n,α) cross section at 14 MeV
40009	G.P. Vinitskaya	1967	INP (linac)	(n,p) and (n,α) cross section at 14 MeV
F1184	V.Yu. Gonchar	1967	INP (cyclotron)	α scattering angular distribution
40223	V.N. Levkovskiy	1968	INP (CCW)	(n,p) and (n,α) cross section at 14 MeV
F0668	V.Yu. Gonchar	1968	INP (cyclotron)	^{24}Mg+α scattering angular distribution
F1168	V.Yu. Gonchar	1968	INP (cyclotron)	Ni, Pb+α scattering angular distribution
40226	V.N. Levkovskiy	1969	INP (VdG?)	(n,p) and (n,α) cross section at 14 MeV
A0647	O.A. Zhukova	1970	INP (cyclotron)	(α,n) cross section excitation function
40029	V.N. Levkovskiy	1971	INP (VdG?)	(n,p) and (n,α) cross section at 14 MeV
40125	K.E. Volodin	1972	INP (reactor)	^{249}Cf(n,f) fragment kinetic energy
A0644	O.A. Zhukova	1972	INP (cyclotron)	Co(α,x) cross section excitation function
A0695	B.G. Kiselev	1974	INP (cyclotron)	^{93}Nb+p cross section excitation function
O0627	V.N. Okolovich	1974	INP (cyclotron)	(p,f) cross section excitation function
F0865	K.B. Baktybaev	1975	INP (cyclotron)	Zn+α elastic scattering ang. distribution
F0868	N.T. Burtebaev	1975	INP (cyclotron)	^{7}Li(α,p)^{10}Be angular distribution
F1145	A.D. Duisebaev	1975	INP (cyclotron)	^{27}Al,^{59}Co(α,t+x) double diff. cross section
F0672	N.N. Pavlova	1976	INP (cyclotron)	α elastic scattering angular distribution
F1142	A.D. Duisebaev	1977	INP (cyclotron)	Al, Co, Sn(3He,α) energy spectrum
F1160	N.N. Pavlova	1977	INP (cyclotron)	Fe+α elastic scattering ang. distribution
F0670	N.N. Pavlova	1979	INP (cyclotron)	α elastic scattering angular distribution
41321	O.I. Artem'ev	1980	INP (VdG)	(n,p) and (n,α) cross section at 14 MeV
F0940	N.T. Burtebaev	1982	INP (cyclotron)	(^{3}He,cp+x) double diff. cross section
40698	E.Z. Akhmetov	1983	INP (reactor)	Cold neutron total cross sections
F0570	N.T. Burtebaev	1984	INP (cyclotorn)	(α,p) double differential cross section
40904	G.A. Dostemesova	1985	INP (reactor)	^{70}Ge(n,n'+γ)^{70}Ge gamma spectrum
40905	Yu.G. Kosyak	1985	INP (reactor)	^{74}Ge(n,n'+γ)^{74}Ge gamma spectrum

40939	G.A. Dostemesova	1986	INP (reactor)	^{78}Se(n,n'+γ)^{78}Ge gamma spectrum
40941	L.V. Chekushina	1986	INP (reactor)	^{80}Se(n,n'+γ)^{80}Se gamma spectrum
F0777	V.N. Gragin	1986	INP (cyclotron)	α scattering angular distribution
O1277	N.I. Zaika	1988	INP (cyclotron)	(^{3}He,f) angular distribution
41043	Yu.G. Kosyak	1989	INP (reactor)	Ni(n,n'+γ)Ni gamma ang. Distribution
41146	Ga. Dostemesova	1989	INP (reactor)	Se(n,n'+γ)Se gamma ang. dist.
F0497	S.Ya. Aisina	1989	INP (cyclotron)	α scattering angular distribution
41106	Yu.G. Kosyak	1990	INP (reactor)	^{73}Ge(n,n'+γ)^{73}Ge gamma spectrum
A0510	V.N. Levkovskiy	1991	INP (cyclotron)	p-, α- cross section excitation function
41136	Yu.G. Kosyak	1992	INP (reactor)	^{52}Cr(n,n'+γ)^{52}Cr gamma spectra
41140	Yu.G. Kosyak	1993	INP (reactor)	^{48}Ti(n,n'+γ)^{48}Ti gamma spectra
41176	Yu.G. Kosyak	1994	INP (reactor)	^{46}Ti(n,n'+γ)^{46}Ti gamma spectra
41408	Yu.G. Kosyak	1998	INP (reactor)	^{82}Se(n,n'+γ)^{82}Se gamma spectra
41411	Yu.G. Kosyak	1999	INP (reactor)	^{80}Se(n,n'+γ)^{80}Se gamma spectra
41412	Yu.G. Kosyak	2000	INP (reactor)	^{65}Cu(n,n'+γ)^{65}Cu gamma spectra
F0775	N. Burtebaev	2000	INP (cycloron)	^{13}C+^{3}He elastic scattering ang. dist.
O1145	A.M.Blechman	2000	INP (cyclotron)	^{197}Au(α,^{3}He+x) doub. diff. cross section
41413	Yu.G. Kosyak	2001	INP (reactor)	^{65}Cu(n,n'+γ)^{65}Cu gamma spectra
F0560	K.A. Kuterbekov	2001	INP (cyclotron)	^{120,124}Sn+α scattering ang. distribution
F0561	A.D. Duisebaev	2001	INP (cyclotron)	^{90,94}Zr+α scattering ang. distribution
41486	Yu.G. Kosyak	2002	INP (reactor)	^{72}Ge(n,n'+γ)^{72}Ge gamma spectra
F0758	N. Burtebaev	2002	INP (cyclotron)	^{10}B(α,^{3}He), ^{11}B(d,^{3}He) ang. distribution
F0759	N. Burtebaev	2002	INP (cyclotron)	9Be+α elastic angular distribution
F0766	M.K. Baktybaev	2003	INP (cyclotron)	^{28}Si+α total reaction cross section
F0767	N. Burtebaev	2003	INP (cyclotron)	^{13}C(^{3}He,t) angular distribution
O1060	A. Duisebayev	2003	INP (cyclotron)	^{90}Zr(p,p,d+x) double diff. cross section
A0851	V.Yu. Ugryumov	2004	INP (cyclotron)	^{28}Si+α total reaction cross section
F0763	N.T. Burtebaev	2004	INP (VdG)	^{14}N(p,γ)^{15}O angular distribution
41451	Yu.G. Kosyak	2005	INP (reactor)	^{74}Ge(n,n'+γ)^{74}Ge gamma spectra
F0772	N. Burtebaev	2005	INP (cyclotron)	^{11}B+α scattering angular distribution
O1307	A. Duisebayev	2005	INP (cyclotron)	^{56}Fe(p,p,α+x) double diff. cross section
A0819	N. Burtebaev	2008	INP (cyclotron)	^{12}C(p,γ)^{13}N angular distribution
A0867	N. Burtebaev	2010	INP (cyclotron)	^{6}Li+d elastic scat. angular distribution
A0886	Sh. Hamada	2011	Astana (cyclotron)	^{12}C+^{16}O elastic scat. ang. distribution
A0899	S.V. Artemov	2011	INP (cyclotron)	^{10}B(d,t) and (d,^{3}He) ang. distribution
A0907	S.B. Dubovichenko	2011	INP (Tandem)	^{6}Li+p elastic ang. distribution
F1189	V.V. Dyachkov	2012	INP (cyclotron)	Mg, C+d elastic angular distribution

Appendix 2: Nuclear reaction data measured in Uzbekistan and compiled in EXFOR before this workshop (Italicized EXFOR entry numbers indicate inclusion of data digitized from figures.)

EXFOR	1st Author	Year	Lab.	Quantity measured
A1482	U.R. Arifkhanov	1974	INP (cyclotron)	(p,n) angular distribution
A1127	S.A. Azimov	1975	INP (cyclotron)	(d,n) angular distribution
40541	S. Arynov	1977	INP (reactor)	(n,γ) gamma spectra
A1194	M.P. Gold'berg	1978	INP (cyclotron)	D(p,p)np DDX
F1140	S.V. Artemov	1978	INP (cyclotron)	^{24}Mg+p scattering excitation function

A0075	L.Ya. Arifov	1980	INP (cyclotron)	^{92}Mo(p,γ) isomeric ratio
A0085	A.V. Muminov	1980	INP (cyclotron)	(p,n) thick target isotope yield
A0104	L.Ya. Arifov	1981	INP (cyclotron)	^{92}Mo(d,n) isomeric ratio
F0892	S.V. Artemov	1981	INP (cyclotron)	^{27}Al+p scattering excitation function
A0211	G. Vakilova	1983	INP (cyclotron)	(p,n) thick target isotope yield
A0212	S. Mukhammedov	1984	INP (cyclotron)	(p,x) (d,x) thick target isotope yield
F1181	R.B. Begzhanov	1985	INP (cyclotorn)	(p,d) angular distribution
A0331	S. Mukhammedov	1986	INP (cyclotron)	(d,x) thick target isotope yield
F0403	F. Kadirov	1987	INP (cyclotron)	(d,n) angular distribution
F1171	G.S. Valiev	1987	INP (cyclotron)	(p,d) angular distribution
A1301	M.A. Kayumov	1988	INP (cyclotron)	(d,n) and (p,n) angular distribution
F0222	S.A. Goncharov	1988	INP (cyclotron)	(d,t) angular distribution
41047	A.D. Belyaev	1989	INP (reactor)	^{241}Pu(n,f) fission yields FY(A,E)
A0621	R.B. Begyanov	1990	INP (cyclotron)	^{66}Zn(α,n)^{68}Ge excitation function
F0071	I.R. Gulamov	1990	INP (cyclotron)	(d,t) angular distribution
F0821	S.V. Artemov	1996	INP (cyclotron)	(^{3}He,d) angular distribution
M0749	S.R. Palvanov	1998	NUU (betatron)	^{89}Y(γ,2n)^{87}Y isomeric ratio
M0766	S.R. Palvanov	1999	NUU (betatron)	(γ,n) (γ,p) isomeric ratio
F0698	S.V. Artemov	2000	INP (cyclotron)	(^{3}He,d) angular distribution
F0780	S.V. Artemov	2001	INP (cyclotron)	^{12,13}C+α scat. angular distribution
41465	V.P. Pikul	2005	INP (reactor)	^{235}U(n,f) fission yields FY(A,E)
41493	Yu.N. Koblik	2006	INP (reactor)	^{239}Pu(n,f) Fission yields FY(A,E)
M0743	S.R. Palvanov	2007	NUU (betatron)	^{142}Nd(γ,n)^{141}Nd isomeric ratio
41563	S.R. Palvanov	2011	INP (VdG?)	(n,2n) and (γ,n) isomeric ratio
M0812			NUU (betatron)	
A0945	S.V. Artemov	2012	INP (cyclotron)	^{14}N(p,γ)^{15}O angular distribution

Recent studies of ^{9}Be as reflector material

N. Takibayev

al-Farabi KazNU, Almaty

The ^{9}Be nuclide has been considered as a system of two alpha-particles and one neutron and it has been shown that such system can exist in "quasi-molecular" state, when the wave number of a pair of heavy particles becomes imaginary $q = i\kappa$ with the wave number of the light particle being a real quantity. That is, rescattering of light particles on the two heavy particles creates additional attraction between the heavy particles and "binds" this heavy pair. The total energy of the system becomes negative: $E = p^2/m + q^2/M < 0$, m is the mass of the light particle, and M is the mass of the heavy particle. Since $\kappa = \kappa(p)$, the total energy of the system $E(p)$ has a minimum for the variable p. The estimates were obtained in the Born-Oppenheimer approximation, where the choice of the pair potentials in separable form allows to solve the three body problem in a simple and compact form. It is shown that the additional attraction between alpha particles increases their usual pair interaction and, therefore, shifts the corresponding pole of the t-matrix from the resonance region to the area of bound states. Interaction of an additional external neutron with such three-body system could lead to displacement in the energy of the primary neutron along the curve $E(p)$ from the minimum point. If the strength of such disturbance is small for the dissociation of the three-body system, the primary neutron returns to the minimum point, throwing back the external neutron acting as an elastic wall. As we assume, this is how the reflection effect of neutrons works for the case of beryllium nucleus.

Introduction. Study and theoretical description of the ^{9}Be nucleus properties still remains one of the urgent problems in nuclear physics [1,2]. Such interest is conditioned by specific properties of this nucleus and its promising use as an effective neutron reflector. (Be-9 stands right after the first unstable nuclei with atomic number A = 8). Its reflection capability has pre-determined its widespread use in nuclear engineering [3,4].

It is known that the light nuclei are good neutron moderators and some of them are good neutron reflectors. Reflectors of thermal and intermediate neutrons are usually made from a substance of moderators used in nuclear reactors [3,4]. In heavy water reactors graphite is used as a reflector due to its availability and good diffusion properties. In light water reactors there is always a layer of water (10 cm or more) as a moderator between active zone and shell of the reactor. This layer is already a reflector and reduces the active zone size.

Intermediate reactor contains some moderator and neutrons absorbed by substance before becoming heat. The best reflector for neutrons is beryllium. Also, beryllium is the best moderator for intermediate reactors of small critical dimensions, i.e. for the reactors with high concentration of fissile material in the active zone. Ordinary water is inferior to beryllium because at energies above 0.1 MeV fast neutrons pass through water easier, than through beryllium [3,4]. Obviously, the reflective properties of beryllium material are directly related to its crystalline structure.

Three body model of the nucleus ^{9}Be. Let we analyze and calculate for a system consisting of two alpha particles and one neutron. Mathematically rigorous solution of the three-body problem was given by L.D. Faddeev [5]. The system of Faddeev equations for T-matrix elements can be written as:

$$T_{ij}(Z) = t_i \cdot \delta_{ij} + t_i G_0(Z) \sum_{l \neq i} T_{lj}(Z)\,; \qquad i, j = 1,2,3\ , \tag{1}$$

where $t_i = V_i + V_i G_0 t_i$, V_i are the pair interaction potentials, and t_i corresponding pair t-matrices. Indices i, j denote the number of the pairs, G_0 is a Green function for three free particles. The total T-matrix corresponds to the sum $T = \sum T_{ij}$.

To solve the task one needs to determine the pair t-matrices t_i, i.e. there is no need to deal with complex pair interaction potentials for the particles; this makes our analysis task easier. Within the considered model we would first consider the main peculiarities of the pair amplitudes at low energies. Such peculiarities are their resonances: for α,α-subsystem this is a very narrow resonance in S-wave at $E_{R,\alpha\alpha} \approx 91.6\, keV$ and width $\Gamma_{\alpha\alpha} \approx 6\, eV$ [6], and for (α+n)-subsystem – a resonance in P-wave at $E_R = 0.9 MeV$ and width $\Gamma = 0.6 MeV$ [7] .

Let us determine the pair t-matrixes that can generate such resonances. This can be done using simple separable potentials $V_i = \bar{\nu}_i(\vec{q}) \cdot \lambda_i \cdot \nu_i(\vec{q}\,')$, where λ_i - is the coupling constant. Then $t_i = \bar{\nu}_i(\vec{q}) \cdot \eta_i(E) \cdot \nu_i(\vec{q}\,')$, where

$$\eta_i^{-1}(E) = \lambda_i^{-1} + I(E) \quad , \qquad I(E) = -\int d\vec{q}\, \frac{\nu_i^2(q)}{E - E_s + i\gamma} \quad , \tag{2}$$

$E_s = q_i^2 / 2\mu$, μ- reduced mass in the i-subsystem, $E = q_{i0}^2 / 2\mu$. The condition $\eta_i^{-1} = 0$ determines location of pole for the pair scattering amplitude in the complex energy plane and, correspondingly, complex wave numbers.

For the α,α-subsystem we choose $\nu_i(\vec{q}) = \nu_S(\vec{q}) = N_{\alpha\alpha} t\,(t^2+1)^{-3/2} Y_{00}(\hat{\vec{q}})$, where $t = q/\beta_S$. The norm constant $N_{\alpha\alpha}^2 = 32\pi/(2\mu_{\alpha\alpha}\beta_S)$ corresponds to the normalization $I(E=0)=1$, so that $I(E) = I_S(q_0) = (1-3it_0)/(1-it_0)^3$. Dimensionless coupling constant $\lambda_S = -1+\alpha$, $\alpha = 5.78*10^{-10}$ and the parameter $\beta_S = 6.77 \cdot 10^3\, fm^{-1}$ correspond to the experimentally obtained resonance characteristics [6]. One should note that resonance in the $\alpha\alpha$ -subsystem satisfies the condition: $x^3 + 3\lambda_S x - 2\lambda_S = 0$, where $x = 1 - i \cdot t_0$.

For the (α+n)-subsystem the potential form-factor can be written as $\nu_i(\vec{p}) = \nu_P(\vec{p}) = N_{n\alpha} t\,(1+t^2)^{-1} Y_{LM}(\hat{\vec{p}})$, where $t \equiv p/\beta_P$. So, we get $I(E) = I_P(p_0) = \dfrac{1-2it_0}{(1-it_0)^2}$, where $t_0 = p_0/\beta_P$. The condition $\eta_P^{-1} = 0$ brings us to

$$\eta_P^{-1}(E) = \frac{1}{\lambda_P} + \frac{1-2it_0}{(1-it_0)^2} = \frac{1+\lambda_P - 2it_0 \cdot (1+\lambda_P) - t_0^2}{\lambda_P \cdot (1-it_0)^2} = 0 \ . \tag{3}$$

Introducing $t_0 = t_R + it_I$ we get for the case of resonance conditions $\lambda_P = -(1+t_I)$ and $t_R^2 = -t_I(1+t_I)$. As it should be, two poles symmetrical with respect to an imaginary axis $t_R = \pm\sqrt{-t_I(1+t_I)}$ correspond to the quasi-stationary state with energy $E = E_R - i\Gamma/2$. For the (α+n)-resonance with energy $E_R = 0.9 MeV$ and width $\Gamma = 0.6 MeV$ we get: $t_R = \pm 0.17$, $t_I = -0.03$, $\lambda_P = -0.97$, $\beta_P = 1.25\, fm^{-1}$.

Solution for the three interacting particles. Separating in (1) the connected term P_{ij} of amplitude with the relation $T_{ij} = t_i \cdot \delta_{ij} + |\nu_i> \eta_i\, P_{ij} \lambda_j < \nu_j|$ one can get the system of equations $P_{ij} = \Lambda_{ij} + \sum_l \Lambda_{il}\, \eta_l\, P_{lj}$. Here $\Lambda_{ij} = <\nu_i | G_0(Z) | \nu_j>,\ i \neq j$. Then, it follows for the elastic channel (i -> i) [8]:

$$P_{ii} = V_{ii}^{ef} + \sum_{i_s} V_{ii_s}^{ef}\, \eta_{i_s}\, P_{i_s i} \ , \tag{4}$$

$$V_{ii}^{ef} = \sum_{l,k} \Lambda_{il}\, \eta_l (I \cdot \eta^{-1} - \Lambda)_{lk}^{-1} \eta_k \Lambda_{ki} \ , \quad l,k \neq i \ . \tag{5}$$

The equations (4) and (5) represent a closed system of equations and are basic for the effective potential method in the three-body problem. Moreover, employing the limit $\xi = m/M \to 0$, where m - mass of a light particle, M – mass of a heavy particle, simplifies determination of the solutions. It is important that all polar peculiarities of the pair scattering amplitudes are preserved. If we accept the solution obtained within such approximation as a basic one, then corrections to it can be made based on conventional perturbation theory. The method is described in details in [8-10]. Below we present the simplified solution of the task.

The calculations show that the ^{9}Be ground state energy depends mainly on the pair resonance parameters and less depends on interactions in the non-resonant regions. The considered above (n+α)-resonance provides us with the value for bound energy of the (α+α+n)-system: E = - *1.285 MeV*. The experimentally determined value is E = - *1.665 MeV* [7]. Still, the additional (n+α) resonance with energy E_R = *4.6 MeV* and width Γ = *4 MeV* [7] amplifies the bound energy up to E= - *1.775 MeV*. But at the following parameters of this resonance E_R = *2.0 MeV*, and Γ = *5.0 MeV* [11], total bound energy is even higher: E = - *2.366 MeV*.

Conclusion. Considered above configuration of the system of three particles is, quite possibly, not typical for bound nuclear systems, but it fits the general scattering theory for three particles. One can say that (α+α+n)-system represents a "quasi-molecular" state where the wave number of a pair of heavy particles becomes imaginary $q = i\kappa$, and the wave number of a light particle p remains real. This happens because multiple scattering of a light particle at two heavy ones creates additional attraction between these particles which "couples" these heavy particles. Non-linear dependence $\kappa = \kappa(p)$ determines the coupling strength of heavy particles as a function of the light particle wave number. Total energy of the system $E = \frac{p^2}{2m} - \kappa^2/M$ becomes negative only at certain range of p values and shows a minimum over this variable (see Fig.1). Such state is known in the scattering theory of few particles as a bound state of a subsystem recessed within a continuous spectrum of an adjacent subsystem. Possibly, namely this state pre-determines the uniqueness ^{9}Be of nucleus as a neutron reflector.

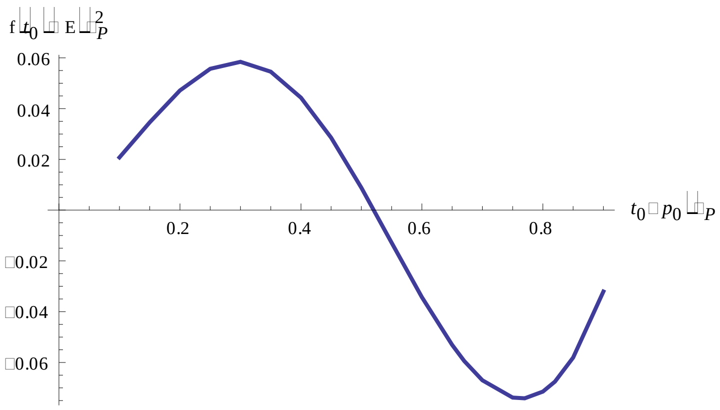

Fig. 1 $E/\beta_P^2 = f(t_0)$ curve

An additional external neutron scattered at such "flexible" coupled system can result in a shift of initial neutron energy along the curve *E(p)* away from the maximum point. If the disturbing force is low to decouple the three-particle system, the initial neutron returns back to the minimum point and kicks off the external neutron like an elastic wall. Moreover, Pauli Exclusion Principle can be applicable here preventing overlapping of the wave functions from identical neutrons what would also generate additional repulsion.

References:

1. H. Horiuchi, K. Ikeda, K. Kato, Recent Developments in Nuclear Cluster Physics, Progress of Theoretical Physics Supplement, 192, 1, 2012

2. T.A.Tomberlin, Beryllium – A Unique Material In Nuclear Applications, INEEL/CON-04-01869 PREPRINT, 36th International SAMPE Technical Conference, 2004
3. V. Chakin, A. Moeslang et al, Beryllium Application for Fission and Fusion, Proceedings of the International Symposium on Materials Testing Reactors, JAEA Oarai R@D Center, Japan, 107-116, 2008
4. V.E. Levin, Nuclear Physics and Nuclear Reactors, Moscow, Atomizdat, 1979
5. L.D. Faddeev, Mathematical Aspects of the Three Body Problem in Quantum Scattering Theory, New York, 1965.
6. J.P.Day, J.E. McEwen, et al, The α-α-fishbone potential revisited, California State University, USA, arXiv: 1105.6050v1 [nucl.-ph.], 30 May 2011
7. F. Ajzenberg-Selone, Energy levels of light nuclei, Nuclear Physics, A490, V1, 1988
8. N. Zh. Takibayev, Class of Model Problems in Three-Body Quantum Mechanics That Admit Exact Solutions, Physics of Atomic Nuclei, 2008, Vol. 71, No. 3, pp. 460–468.
9. N.Zh. Takibayev, Exact Analytical Solutions in Three-Body Problems and Model of Neutrino Generator, EPJ Web of Conferences 3, 05028 (2010), DOI:10.1051/epjconf/20103005028
10. N. Zh. Takibayev, Neutron Resonances in Systems of Few Nuclei and Their Possible Role in Radiation of Overdense Stars, Few-Body Syst (2011) 50: 311–314, DOI 10.1007/s00601-010-0207-4
11. S.F. Mughabghab, M. Divadeenam, N.E. Holden, Neutron Cross Sections, Vol. 1, Neutron Resonance Parameters and Thermal Cross Sections, Part A, Z = 1-60, Academic Press, New York, 1981.

Filtered Neutron Capture Cross Section of $^{186}W(n,\gamma)^{187}W$ Reaction at 24 keV

Pham Ngoc Son, Vuong Huu Tan
[1)] *Nuclear Research Institute, 01-Nguyen Tu Luc, Dalat, Vietnam*
[2)] *Vietnam Agency for Radiation and Nuclear Safety, 113-Tran Duy Hung, Hanoi, Vietnam*

Abstract: The neutron radiative capture cross sections of the $^{186}W(n,\gamma)^{187}W$ reaction has been measured by the activation method with filtered neutron beam of 24 keV at the Dalat nuclear research reactor. The cross sections were determined relative to the standard capture cross sections of ^{197}Au $(n,\gamma)^{198}Au$ reaction. A high efficient HPGe detector was used for the gamma rays measurements from the irradiated samples; the absolute efficiency curve of the HPGe detector is calibrated by using a set of standard radioisotope sources. The present results were compared with the previous measurements extracted from the EXFOR data library, the evaluated data in ENDF/B-VII and JENDL 4.0.

I. Introduction

Average radiactive neutron capture cross sections in the keV energy region are important in the safety analysis and design of reactors as well as in the studies of nuclear physics, the s-process for nucleosynthesis in astrophysics [1]. At present, the published experimental data is quite discrepant in different experiments, and it is still not satisfied in quality and quantity. That is the reason why new experimental data, theoretical predictions for more accurate parameters and improvement of neutron radiactive capture cross sections are necessary. In this study, the radiactive neutron capture cross section for the reactions of $^{186}W(n, \gamma)^{187}W$ at energy region of 24 keV has been measured by the activation method with the filtered neutron beam at the Dalat nuclear research reactor. A gamma spectroscopy, ORTEC DSPEC^{js}, with a high relative efficiency of 58% HPGe detector was used to measure gamma rays from the irradiated samples. The capture cross sections were obtained relative to the standard capture cross sections of ^{197}Au, and compared with the previous experimental data and the evaluated cross sections in ENDF/B-VII and JENDL 4.0.

II. Experimental

The neutron beams were derived, from the horizontal channel No.4 of the research reactor at the Dalat Nuclear Research Institute (DNRI), by the neutron filter technique [1-2], using the compositional materials as given in Table 1. The neutron energy resolution, FWHM, of each beam is 1.8 keV. The physical parameters of each neutron beam is given in Table 2.

Table 1. *The materials and sizes of neutron filters at the Dalat research reactor*

En (keV)	Compositional materials and sizes for neutron filters
24	0.2g/cm^{2} ^{10}B + 20cmFe + 30cmAl + 35g/cm^{2}S

Table 2. *The physical parameters of filtered neutron beam at the Dalat research reactor*

Energy (keV)	ΔEn (keV)	Neutron flux (n/cm^2/s)	Relative intensity (%)
24	1.8	2.6×10^5	96.72

The neutron beams were collimated to 3cm in diameter by using the usual materials of LiF, Cd, B_4C, Pb and borated paraffin. The calculated energy spectrum of the 24 keV neutron beam are shown in Fig. 1.

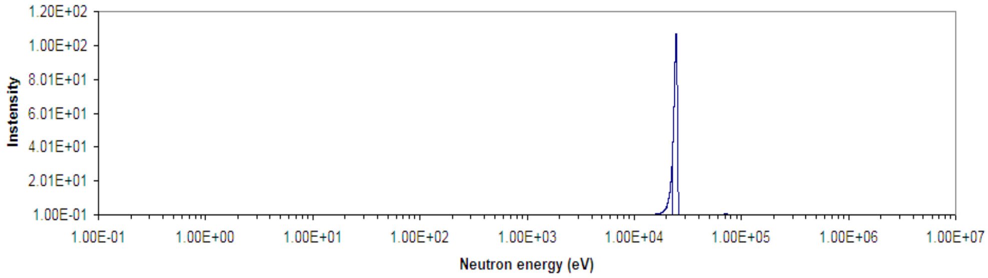

Fig. 1. *Energy spectrum of the 24 keV neutron filtered beam*

The samples were prepared from the high purity metal foils of Au (99.99%, 1.27cm in diameter, 0.05mm in thickness) as a standard for neutron flux monitor, and high purity metal foils of W (99.98%, 1.27cm in diameter, 0.05mm in thickness) provided by Shieldwerx, LLC. Each W sample was sandwiched between two Au foils, and the sample groups were wrapped in Cd-covers (0.5mm in thickness) with aim to reject most of thermal neutron background. The irradiation time was 48 hours for every sample group. The specific activities of the targets and the gold disks were measured by using a DSP-base gamma-ray spectrometer with a HPGe detector (58% efficiency, 2.5keV energy resolution at 1.332 MeV of ^{60}Co). The detector was calibrated by using a set of standard radioisotope sources: ^{152}Eu, ^{60}Co, ^{57}Co, ^{137}Cs, ^{241}Am, ^{113}Sn and ^{88}Y. In addition to the corrections for neutron multi-scattering and self-shielding in irradiated samples, it is important to concern that the large resonance capture cross sections of the standards and samples, in the slow neutron background region above the Cd-Cutoff energy, may strongly contribute to the uncertainty of the experimental results. Therefore, the correction factors for slow neutron resonance capture in this measurement were calculated by the Monte Carlo method using the MCNP5 code [3].

III. Data Analysis

During irradiation in a neutron beam with energy spectrum $\phi(E)$, the capture reaction rate, R, of samples with neutron is defined as follows:

$$R = N\int \phi(E)\sigma_a(E)dE\,, \qquad (1)$$

where N is the number of nuclei in sample, and $\sigma_a(E)$ is the neutron capture cross section as a function of neutron energy E. The average neutron capture cross section, $<\sigma_a>$, and neutron flux, $<\Phi>$, are defined as following:

$$<\sigma_a>=\frac{\int \sigma_a(E)\phi(E)dE}{\int \phi(E)dE};<\Phi>=\int \phi(E)dE. \qquad (2)$$

Applying these average quantities, the integrating eq. (1) can be rewritten as follows:

$$R = N<\sigma_a><\Phi>. \qquad (3)$$

The activity, A, of the irradiated sample at the end of neutron irradiation is determined by expressions:

$$A = R(1-e^{-\lambda t_1}),\ \text{and}\quad A=\frac{Cf_c\lambda}{\varepsilon_\gamma I_\gamma e^{-\lambda t_2}(1-e^{-\lambda t_3})}, \qquad (4)$$

where C denotes the net counts of the corresponding gamma peak, t_1, t_2 and t_3 are irradiating, cooling and measuring times, respectively. λ is the decay constant of the product nucleus, ε_γ the detection efficiency of detector, I_γ the intensity of interesting γ-ray. f_c is the correction factor which is account for self-shielding, multiple scattering, and background resonance capture of neutron in the irradiation sample. Finally, from Eqs. (2-4), the averages capture cross sections, $<\sigma_a>^x$, for nuclide x at average neutron spectrum $<\Phi>$ can be determined relative to that of ^{197}Au standard by the following relations:

$$< \sigma_a > = \frac{C^x f(\lambda,t)^x f_c^x I_\gamma^{Au} \varepsilon_\gamma^{Au} N^{Au} < \sigma_a >^{Au}}{C^{Au} f(\lambda,t)^{Au} f_c^{Au} I_\gamma^x \varepsilon_\gamma^x N^x}; \tag{5}$$

$$f(\lambda,t) = \frac{\lambda}{(1-e^{-\lambda t_1})e^{-\lambda t_2}(1-e^{-\lambda t_3})}, \tag{6}$$

where the superscript 'x' denotes the nucleus of sample. The average standard capture cross sections of ^{197}Au respects to the energy of filtered neutron beam are extracted from the reference [4]. The relevant decay data of product nuclei used in this work are given in Table 3.

Table 3. *Decay properties of the activation product nuclei [11]*

Activation products	Half-life	γ-ray (keV)	Intensity (%)
^{198}Au	2.6952±0.0002 d	411.8	95.6±0.1
^{187}W	3.7183±0.0011 d	137.157	9.42±0.06

IV. Results and Discussion

The capture cross sections of ^{186}W was obtained to be 0.2199 ± 0.0118 barn at average neutron energies of 24 keV, as given in Table 5. The present results are compared with previous measurements and the evaluated data, as shown in Figs. 2. In the present work, the errors of the measured cross section are about 6.5%. The uncertainties in the present measurements are mainly due to the statistical errors (0.5-4.0%), the uncertainties of γ-ray detection efficiency (2.0%), the reference cross section (3.0%) and the correction factors for neutron resonance capture, self-shielding and multiple scattering effects (1.0%). In comparisons with the previous measurements and the evaluated data for the case of ^{186}W, the present results are in good agreement with the previous measurements of S.V.Kapchigashev [8], and it is about 15,7 % higher than the evaluated data of JENDL 4.0 [12] and ENDF/B-VII [13].

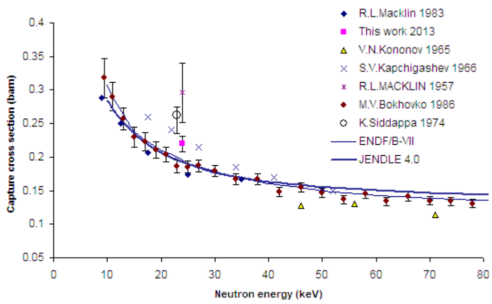

Fig. 2. *Neutron capture cross section of ^{186}W(n,γ)^{187}W reaction*

Table 6. *Measured neutron capture cross section of ^{186}W*

Average neutron energy (keV)	Cross section of ^{186}W(n,γ)^{187}W (barn)
24 ± 1.8	0.2199 ± 0.0118

V. Conclusion

The neutron capture cross section of ^{186}W(n,γ)^{187}W reaction at average incident neutron energy of 24 keV has been measured by means of the activation method, using the filtered neutron beam at the Dalat research reactor. The results, shown in Table 6, was obtained relative to the standard neutron capture cross section of ^{197}Au (0.6448 barn). The uncertainties of the measured values in the present measurement are about 6.5%, and the energy resolution of the 24 keV filtered neutron beam is 1.8 keV.

Acknowledgments

This research is funded by Vietnam National Foundation for Science and Technology Development (NAFOSTED) under grant number “103.04-2012.59”.

References

[1] V. P. Vertebnyj, et al., Filtered Medium and Thermal Neutron Beams and Their Use, “Properties of Neutron Sources”, *IAEA-TECDOC-401*, (1986).

[2] O. O. Gritzay, et al., Neutron Filters at Kyiv Research Reactor, *KIRN-01-6* (2001).

[3] X-5 Monte CarloTeam, MCNP-A General Monte Carlo N-Particle Transport Code, Version 5, Manual, *LA-UR-03-1987*, Los Alamos National Laboratory, (2004).

[4] IAEA, International Evaluation of Neutron Cross-Section Standards, 2007 (ISBN 92-0-100807-4).

[5] R.L. Macklin,N.H. Lazar,W.S. Lyon, Physical Review, Vol.107, p.504 (1957)

[6] V.N.Kononov, Ju.Ja.Stavisskij, V.E.Kolesov, A.G.Dovbenko.S.Nesterenko,V.I.Moroka, Fiz.-Energ Institut, Obninsk Reports No.29, 1965.

[7] S.V.Kapchigashev, Ju.P.Popov, F.L.Shapiro, Private communication Name.Kapchigashev, 1966 (EXFOR https://www-nds.iaea.org/exfor/exfor.htm).

[8] R.L. Macklin, N.H. Lazar, W.S. Lyon, Physical Review, Vol.107, p.504 (1957)

[9] M.V.Bokhovko, L.E.Kazakov, V.N.Kononov, E.D.Poletaev, V.M.Timokhov, A.A.Voevodskij, Vop. At.Nauki i Tekhn.,Ser.Yadernye Konstanty Issue.1, p.39 1986.

[10] K.Siddappa, M.SriramachandraMurty, J.RamaRao, Annals of Physics (New York) Vol.83, p.355 1974.

[11] Nudat 2.2 Database, http://www.nndc.bnl.gov/nudat2/

[12] K. Shibata, O. Iwamoto, T. Nakagawa, N. Iwamoto, A. Ichihara, S. Kunieda, S. Chiba, K. Furutaka, N. Otuka, T. Ohsawa, T. Murata, H. Matsunobu, A. Zukeran, S. Kamada, and J. Katakura: "JENDL-4.0: A New Library for Nuclear Science and Engineering," *J. Nucl. Sci. Technol.*. **48**(1), 1-30 (2011).

[13] M. B. Chadwick, M. Herman, P. Oblozinsky, et al., "ENDF/B-VII.1 nuclear data for science and technology: Cross sections, covariances, fission product yields and decay data", Nuclear Data Sheets, 112(12):2887-2996 (2011).

The Systematics of Thermal Neutron Fission Cross Sections for actinides

WANG Jimin, WU Haicheng, ZHANG Jingshang, CHEN Guochang, GE Zhigang
(China Nuclear Data Center, China Institute of Atomic Energy, Beijing, China, 102413)

Abstract: Based on the fission theory, the systematics formulae of thermal neutron fission cross sections have been established, for building the evaluation methods and means of some nuclei that the measured data are scare and scattered. On the basis of the recommended thermal neutron fission cross sections and the height of the fission barrier, the correlations between thermal neutron fission cross sections and the excitation energy of saddle point have been studied, the parameters of every nuclei corresponding to Z have been obtained by fitting. Then, the systematics behaviors of these parameters with Z have been studied also, and the parity relations have been found. The overall systematics formulae of thermal neutron fission cross sections have been established by fitting. The results indicate that there are the correlations between thermal neutron fission cross sections and proton number.

Key words: thermal energy neutron, fission cross sections, systematics

I. INTRODUCTION

The thermal neutron fission cross sections of actinides are important for design of the nuclear installation, nuclear energy application and understanding of nuclear fission. However, the measured data are scarce and scattered for some nuclei. Generally, the systematics are convenient and reliable for prediction of the neutron induced reaction cross sections, compared to model theory calculations when experimental data are scarce.

Earlier works on systematics of thermal neutron fission cross sections of actinides were performed by H.Diamond et al.[1] and GU Fuhua et al.[2]. The former was for the odd-odd nuclide, and the later have obtained the correlation between the fission cross sections and the mass number A, but the predicted cross sections were deviated because the experimental data have been used in the work are incomplete measured data of the thermal neutron fission cross sections.

More and more new measurements have been performed with the development of the conditions and technology of experiment. In present work, the systematics formulae of thermal neutron fission cross sections of actinides have been established, the systematics behaviours of thermal neutron fission cross sections of actinides have been studied.

II. FORMULAE

Based on the fission theory [3], the fission cross sections can be written as

$$\sigma_f \approx \sigma_r \frac{\Gamma_f}{\Gamma} = \sigma_r \frac{\Gamma_f}{\Gamma_f + \Gamma_n} \tag{1}$$

Where, Γ is the total width, Γ_f is the fission width and Γ_n is the neutron width. On basis of the Hill-Wheeler formula, the Γ_f can be solved by the following

$$\Gamma_f(E) = \frac{1}{2\pi\rho(E)} \int_0^\infty \rho_f(E - V_f - \varepsilon) T(E) d\varepsilon \tag{2}$$

Where, ρ_f is the level density of the saddle point, E is the excited energy of compound nucleus, V_f is the height of single-humped fission barrier and $T(E)$ is the transmission coefficient of barrier.

$$T(E) = \left\{1 + \exp\left[-2\pi(E - V_f)/\hbar\omega\right]\right\}^{-1} \tag{3}$$

Defining, $$x \equiv E - V_f + c \tag{4}$$

In Eq.(4), c is the systematics parameter. For the thermal neutron fission cross sections, the excited energy of compound nucleus include mainly the neutron binding energy B_N and the pairing correction Δ, then

$$x = B_N - \Delta - V_f + c \tag{5}$$

Where,

$$\begin{aligned} \Delta &= 12 / A^{1/2} \quad & even-even \\ &= 0 & odd \\ &= -12 / A^{1/2} & odd-odd \end{aligned} \tag{6}$$

Based on the Eq.(2), the systematics formulae of thermal neutron fission cross sections of actinides can be expressed approximately as

$$\ln \sigma_f = bF(x) + a \tag{7}$$

In Eq.(7), a and b are the systematics parameters, $F(x)$ denotes the function of the excited energy of the saddle point.

III. DATA SELECTION

The experimental data for thermal neutron fission cross sections were taken from EXFOR. For some nuclei, the evaluated data were used in this work and taken from BNL-325[4], ENDF/B-VII.0[5], CENDL-3.1[6] and JENDL-4.0[7]. There are 70 thermal neutron fission cross sections with the uncertainty have been recommended from ^{227}Th to ^{254}Cf.

In Eq.(4) and (5), the height of single-humped fission barrier is important to calculate the x. Based on the CENDL-3.1, the work of Moller et al[8]., RIPL[9] and JENDL-4.0, the height of single-humped fission barrier for 70 nuclei from ^{227}Th to ^{254}Cf have been recommended.

IV. PARAMETER CORRELATIONS

Firstly, the thermal neutron fission cross sections have been studied on the different proton number. For fitting conveniently and ensuring $x > 0$, the parameter c was supposed as 3. Then, on the basis of the fitted parameters, the correlations between the parameters and proton number can be expressed as simple functions.

$$\ln \sigma_f = b(Z) \times \ln(B_N - \Delta - V_f + 3) + a(Z) \tag{8}$$

$$a(Z) = \begin{cases} 3.709(Z - 97.73), & odd\ \ Z \\ (Z - 93.32)^2 - 17.39, & even\ Z \end{cases} \qquad b(Z) = \begin{cases} 2.425(Z - 100.1), & odd\ Z \\ 0.3166(Z - 93.89)^2 - 32.32, & even\ Z \end{cases}$$

V. RESULTS AND DISCUSSION

Using the regional parameters, the thermal neutron fission cross sections of actinides have been calculated. The results are shown in Figs.1 through 5, in which the blue square points are predicted values, the red points are evaluated values, the black square points are

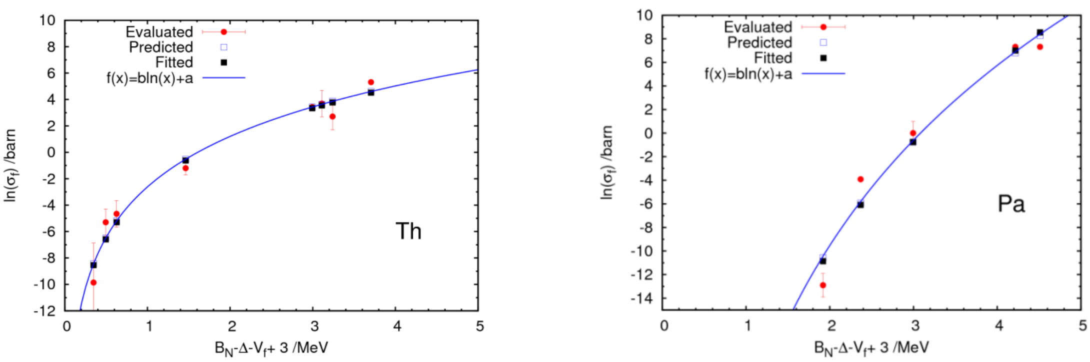

Fig.1 Comparison of predicted values with evaluated and fitted for Th and Pa

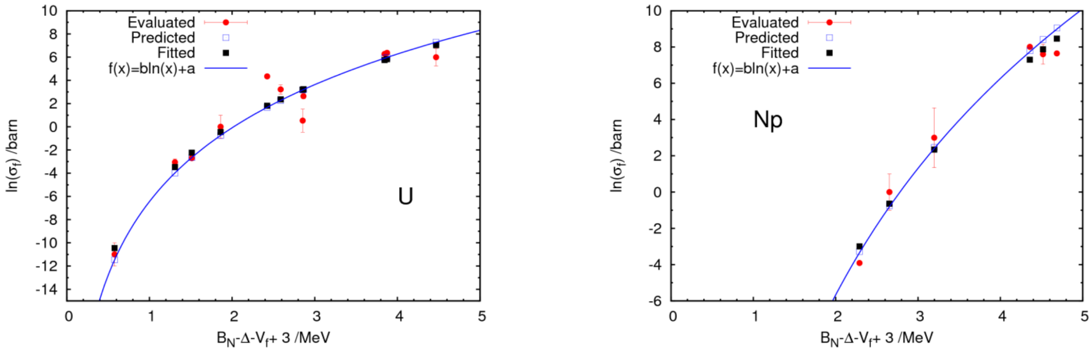

Fig.2 Comparison of predicted values with evaluated and fitted for U and Np

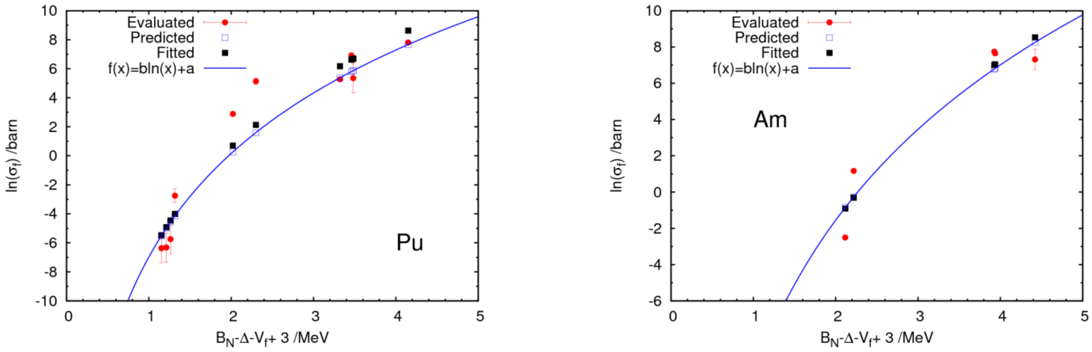

Fig.3 Comparison of predicted values with evaluated and fitted for Pu and Am

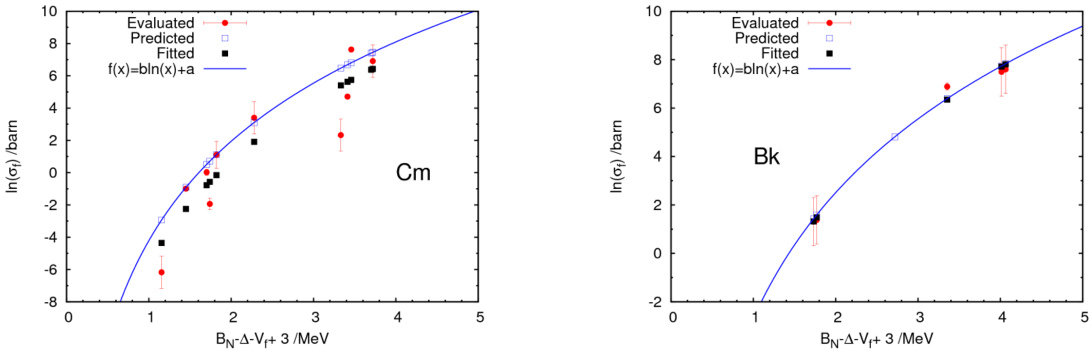

Fig.4 Comparison of predicted values with evaluated and fitted for Cm and Bk

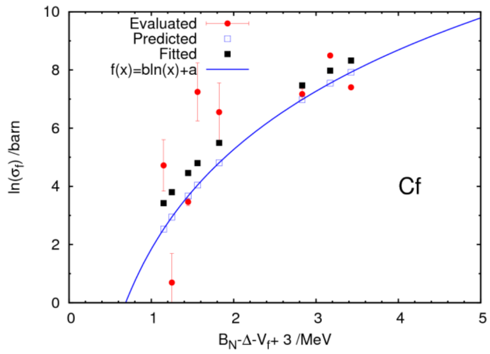

Fig.5 Comparison of predicted values with evaluated and fitted for Cf

fitted values, the solid line is the results calculated from this systematics.

The results indicate that the agreement between the calculation and experiment for the thermal neutron fission cross sections of Th, Pa, U, Np and Bk except Pu, Cm and Cf. The improvement is expected to obtain in future.

REFERENCES

[1] H. Diamond. J.Inorg.Nucl.Chem., 1968, 30: 2553.

[2] GU FUHUA, LIU JICAI. Some systematic characteristics of thermal neutron fission cross sections for actinides[J], ATOMIC ENERGY SCIENCE AND TECHNOLOGY, 1985, 39(1): 39-46 (in Chinese).

[3] WANG SHUNUAN. The theory of nuclear reaction [M]. The press of atomic energy, 2007 (in Chinese).

[4] MAGHABGHAB S F. Atlas of neutron resonances[M]. NNDC: Elsevier Science, 2006.

[5] CHADWICK M B, OBLOZINSKY P, HERMAN M, et al. ENDF/B-VII.0: Next Generation Evaluated Nuclear Data Library for Nuclear Science and Technology[R]. Nuclear Data Sheets,2006, 107(12): 2931-3060.

[6] GE ZHIGANG, ZHUANG YOUXIANG, LIU TINGJIN, et al. The Updated Version of Chinese Evaluated Nuclear Data Library (CENDL-3.1)[R]. Journal of Korean Physical Society, 2011, 59(2): 1052-1056.

[7] SHIBATA K, IWAMOTO O, NAKAGAWA T, et al. JENDL-4.0: A New Library for Innovative Nuclear Energy Systems[R]. International Conference on Nuclear Data for Science and Technology, Jeju Island, Korea, 2010.

[8] PETER MOLLER, ARNOLD J SIERK, AKIRA IWAMOTO. Five-Dimensional Fission-Barrier Calculations from ^{70}Se to ^{252}[J]. Phys. Rev. Lett., 2004, 92(7): 072501- 072505.

[9] CAPOTE R, HERMAN M, OBLOZINSKY P, et al. RIPL – Reference Input Parameter Library for Calculation of Nuclear Reactions and Nuclear Data Evaluations[S]. Nuclear Data Sheets, 2009, 110: 3107–3214

Overview of Nuclear Structure and Decay Data Evaluation Activities at KAERI

Jaegwon Yoo
Korea Atomic Energy Research Institute
jgyoo@kaeri.re.kr

Recently initiated project on Nuclear Structure and Decay Data Evaluation at Korea Atomic Energy Research Institute (KAERI) is overviewed. After introducing the work scope of the project, we briefly discuss applications of the data to nuclear reactor dynamics and decay heat calculations with rate equations.

I. Introduction

At KAERI, we initiated a project on Nuclear Structure and Decay Data Evaluation in which we deal with the most important nuclear structure and decay data, such as isomeric states, spin, parity, half-life, decay modes, branching ratios, characteristic energy spectra from various transitions, and averaged energies emanating from radiations. The project is currently focusing on evaluation and assessment of those nuclear data to enhance basic science capabilities in nuclear safety regulations and nuclear waste management as well as other application areas such as nuclear medicine and national security.

Accurate estimation of decay heat and radioactivity of actinides, fission products, delayed-neutron sources and structural material is very demanding in various nuclear industries. To meet those demands, the nuclear structure and decay data has been compiled in two standard library formats; Evaluated Nuclear Structure Data File (ENSDF) [1] for use in nuclear structure studies, and Evaluated Nuclear Data File (ENDF) [2] for nuclear power plant applications including design and operation. As far as the fuel burn-up and decay heat calculations are concerned, there are plant-type specific data libraries processed on the bases of engineering models under controlled scenarios. However, we feel that we need to prepare for uncontrollable situations to handle them effectively and efficiently with proper physics models based on accurate nuclear data.

The perspective of the project would be extended to cover rare isotopes that will be produced from RAON, a system of two accelerators that is under construction in two phases in Korea. We would expect that high-resolution measurements of the rare isotope beams from RAON will provide a tremendous amount of new data in a working format of Experimental Unevaluated Nuclear Data List (XUNDL) [3]. Evaluation of those new data will expand the horizon of the neutron/proton drip line further and will significantly improve the accuracies in nuclear structure and decay data currently complied.

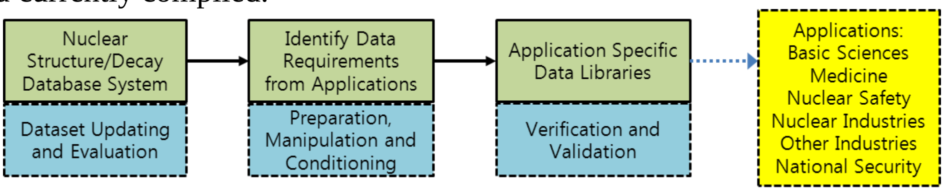

Figure 1. A schematic work scope of KAERI project.

II. Work Scope of the Project

The goal of the project is to enhance the nuclear safety in the power reactor related issues, such as reactor operation and spent fuel managements. Up to now, about 3,100 nuclides have been found and their structure/decay data sets are compiled including ~275 stable nuclides. Setting up a database system with the nuclear data sets, we are going to identify the required data for applications. Then we will build specific nuclear data libraries from the nuclear data sets. The work scope of the project is summarized in Fig. 1.

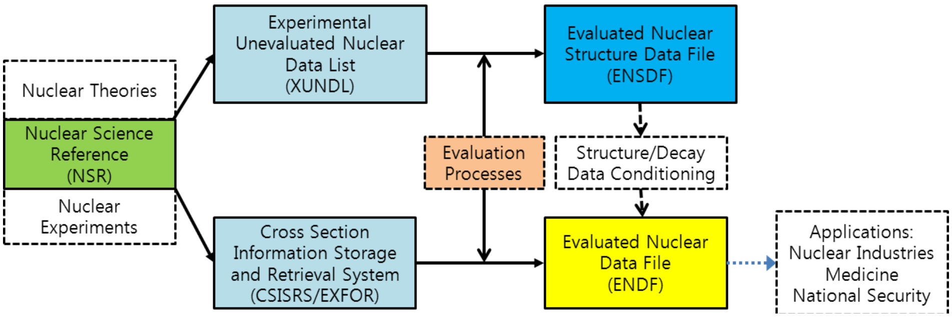

Figure 2. A work flow of nuclear data evaluation.

The work flow of the nuclear data evaluation is summarized in Fig. 1, where the evaluation processes of ENSDF are paralleled with those of ENDF. As far as the nuclear structure/decay data sets are concerned, most of them have been acquired by experimental measurements. Since these are dealing with a quantum many-body system in discrete states, there are not many parameters that can be related to the theoretical predictions. Even though ENSDF analysis and utility codes [4] are available, they play only auxiliary roles. Thus the whole evaluation processes are heavily relying on the evaluator's expertise. Notice that the renowned package of RADLST [5] is very useful in calculating the dose rates from ENSDF data sets and in producing the structure/decay data sets in ENDF format.

III. Application of Nuclear Data to Reactor Dynamics and Decay Heat

Some of the fission products undergo β-decays from which delayed neutrons are released comparatively long after the fission as shown in Fig. 3. Because of a large number of the precursor nuclides, it is impractical to accommodate all of them. Instead, we group those nuclides in manageable ways.

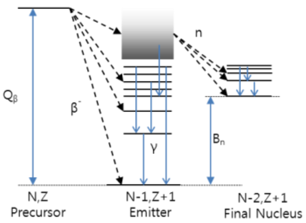

Table 1. Delayed-neutron Fractions		
Nuclide	Thermal	Fast
^{232}Th	-	0.0203
^{233}U	0.0026	0.0026
^{235}U	0.0065	0.0064
^{238}U	-	0.0148
^{239}Pu	0.0021	0.0020

Table 2. 6-Group Delayed Neutron Parameters					
Group	Half-Life (s)	Decay Constant (s^{-1})	Energy (keV)	Yields (n/fission)	Fraction
1	55.72	0.0124	250	0.00052	0.000215
2	22.72	0.0305	560	0.00546	0.001424
3	6.22	0.111	405	0.00310	0.001274
4	2.30	0.301	450	0.00624	0.002568
5	0.614	1.14	-	0.00182	0.000748
6	0.230	3.91	-	0.00066	0.000273

Figure 3. A schematic of delayed neutron emissions.

The rate equation for the total neutron population n(t), in the nuclear reactor can be written down after taking into account of the contribution from the i^{th} group precursors $c_i(t)$, and feedback effects if any,

$$\frac{dn(t)}{dt} = \frac{\rho-\beta}{\ell} n(t) + \sum_{i=1}^{6} \lambda_i c_i(t), \qquad \frac{dc_i(t)}{dt} = \frac{\beta_i}{\ell} n(t) - \lambda_i c_i(t),$$

where ρ, β, ℓ are the reactivity, the total delayed neutron fraction, the average lifetime of neutrons, respectively [6]. The β_i and λ_i are the i^{th} group fraction and the decay constant for delayed-neutron precursors, respectively. The 6-group parameters are shown in Table 2.

We investigated the reactor dynamics with the two operational scenarios; (i) oscillatory reactivity insertion, $\rho(t) = \rho_o + \mu\sin(\omega t)$, and (ii) reactivity insertion with temperature feedback effect, $\rho(t) = \rho_o + a\int_0^t n(\tau)d\tau$, where ρ_o denotes critical reactivity. The results of the computation are plotted in Fig. 4.

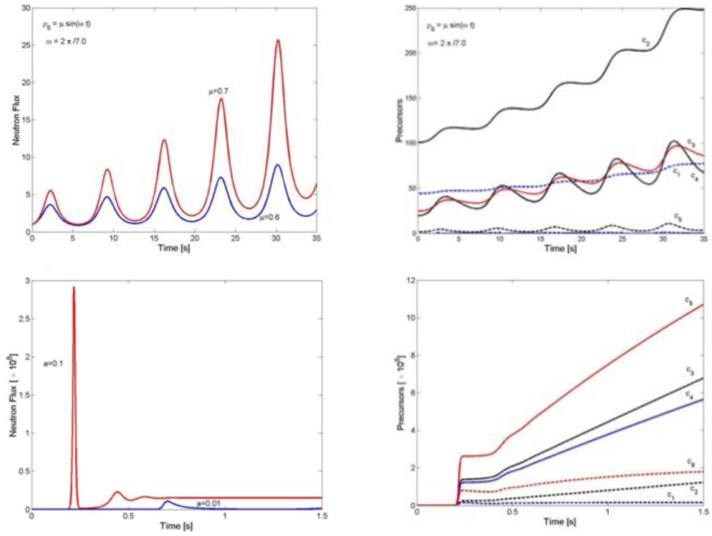

Figure 4. Simulation results of nuclear reactor dynamics with oscillatory reactivity insertion (top two figures) and with temperature feedback effect (bottom two figures).

In general, we can compute the fission energy from the above rete equation, which accounts for about 92.5% of the recoverable energy. The remainder of the energy comes from the decay heat of the fission products, which can be obtained from mean decay energies of radionuclides,

$$\mathrm{r(t)} = \Sigma_i\left(\bar{E}_{\beta,\mathrm{i}} + \bar{E}_{\alpha,\mathrm{i}} + \bar{E}_{\gamma,\mathrm{i}}\right)\lambda_i\, N_i(t).$$

To compute the decay heat of the fission products in the nuclear reactor, we are supposed to calculate the radioactivity in a neutron environment that can be carried out by employing a set of following rate equations of nuclides N_i [7],

$$\frac{dN_i}{dt} = -(\lambda_i + \sigma_i\phi)N_i(t) + \Sigma_j f_{j\to i}\,\lambda_j\, N_j + \Sigma_k\, \mu_{k\to i}\,\sigma_k\, N_k + \mathrm{y}_i\ \mathrm{F},$$

$$y_i = \Sigma_j\, \Sigma_{g=1}^{G}\, \sigma_{j,g}\ \phi_g\ A_j(t)\ Y_{j,g}^{i},$$

where F is the fission rate and σ_i, $f_{j\to i}$, $\mu_{k\to i}$, y_i are the average capture cross section, the branching ratio, the production rate, the independent fission yield of nuclide i.

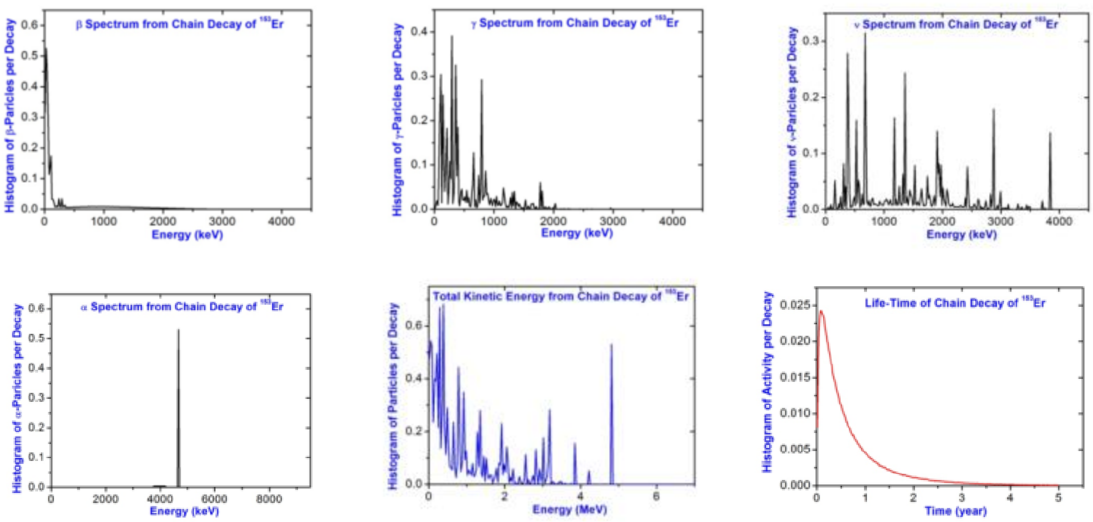

Figure 5. The results of the Geant4 simulation of the decay chain of ^{153}Er.

When the nuclear fuel is discharged from the reactor, the neutron flux is nearly absent and the rate equations become very simple. We carried out numerical simulation of the rate equation for the decay chain of ^{153}Er with the Geant4 that is a very versatile tool for simulating various nuclear phenomena [8]. The simulation results are plotted in Fig. 5.

IV. Summary and Perspectives

Many challenges in theoretical and experimental nuclear many-body physics would expand humankind's knowledge horizon further. To address nuclear safety issues in nuclear waste treatments, radiation shielding and protection, we need to update and evaluate the nuclear data timely. In various areas, preparation and conditioning the nuclear data play important roles in dealing with the specific applications. Also, checking the verification and validation of those data is required, if possible, to secure reliabilities in critical situations.

In Korea, nuclear data measurements and compilations would be continuing at various experimental facilities; a research reactor (KAERI), a proton accelerator (KAERI), cyclotrons (MC, KAERI), electron accelerators (PAL, KAERI), a heavy-ion cyclotron with ISOL/IFF (Phase I) and a radioisotope/heavy-ion linear accelerator (Phase II) under the Rare Isotope Science Project (RISP) at the Institute of Basic Sciences (IBS). We feel that systematic coordination of domestic collaborations is desirable in the evaluation works as well as in the experimental campaigns. Also, we are very interested in international collaborations, since the nuclear data measurements are very time/resource-intensive work and the evaluated data should be freely shared for the enhancement of humankind's well-being.

REFERENCES

[1] Evaluated Nuclear Structure Data file, http://www.nndc.bnl.gov/ensdf.

[2] Evaluated Nuclear Data File, http://www.nndc.bnl.gov/endf.

[3] Experimental Unevaluated Nuclear Structure Data List, http://www.nndc.bnl.gov/xundl.

[4] J.K. Tuli, "Evaluated Nuclear Structure Data File, a Manual for Preparation of Data Sets," BNL-NCS-51655-01.02-Rev, NNDC, BNL (2001); T.W. Burrows, "ENSDF Analysis and Utility Codes," INDCNDS)-0533, IAEA (2008).

[5] Thomas W. Burrows, RADLST v5.5, NNDC, BNL (1988).

[6] David L. Hetrick, Dynamics of Nuclear Reactors, (ANS, 1993); M. Johnson, S. Lucas, and P. Tsvetkov, Modeling of Reactor Kinetics and Dynamics, INL/EXT-10-19953 (2010).

[7] V.E. Schrock, Prog. Nucl. Energy, 3, 125 (1979); A. Tobias, Prog. Nucl. Energy, 5, 1 (1980).

[8] J. Allison et al., Geant4 developments and applications, IEEE Trans. Nucl. Sci., 53, 270 (2006).

Measurement of neutron induced fission cross sections by surrogate methods

V.V. Desai, B.K. Nayak, and A. Saxena

Nuclear Physics Division, Bhabha Atomic Research Centre, Mumbai-400 085, India

Abstract

Heavy ion reaction studies around Coulomb barrier energies have been usually used to investigate projectile/target structure effects on reaction dynamics. Other than providing the basic physics understanding of the reaction dynamics, some of these reactions have been used as a tool to serve as surrogates for determining neutron induced compound nuclear fission reaction cross-sections involving unstable targets. We present results on determination of ^{234}Pa(*n,f*), ^{239}Np(*n,f*), and ^{240}Np(*n,f*) cross sections in the equivalent neutron energy range 10.0 to 16.0 MeV by successfully employing a new surrogate reaction method.

INTRODUCTION:

Nuclear reaction data play an important role in nuclear physics applications. Cross sections for reactions of neutrons and light, charged particles with target nuclei across the isotopic chart, taking place at energies from several keV to tens of MeV, are required for nuclear astrophysics, national security, and nuclear-energy applications [1]. Not all relevant data can be directly measured in the laboratory or accurately determined by calculations. Direct measurements may encounter a variety of difficulties: many of the nuclei of interest are too difficult to produce with currently available experimental techniques or too short lived to serve as targets in a present day experimental setup. Also, the sufficient flux of neutron beams of the required energy regime is often inaccessible. Therefore it becomes necessary to develop indirect methods for determining the relevant reaction cross-sections. The surrogate reaction approach is such an indirect method and first used in the 1970s for estimating neutron induced fission cross sections [2, 3]. In recent years the surrogate reaction methods in improved forms such as the surrogate ratio method (SRM) [4–7], and the hybrid surrogate ratio method (HSRM) [8, 9] have been recognized as a potentially powerful tool for a wide range of applications that involve compound-nuclear reactions. In SRM the ratio of the fission probabilities of two compound-nucleus reactions for the same excitation energy are determined experimentally. Knowing the cross section for one of the compound-nuclear reaction (reference reaction) then allows one to extract the other (desired reaction) by using the ratio $R(E_{ex})$ as follows:

$$\frac{\sigma_f^{n+A}(E_{ex})_{(desired)}}{\sigma_f^{n+B}(E_{ex})_{(reference)}} = \mathrm{R}(E_{ex}) = \frac{\sigma_{CN}^{n+A}(E_{ex})}{\sigma_{CN}^{n+B}(E_{ex})} \times \frac{P_f^A(E_{ex})}{P_f^B(E_{ex})}. \qquad (1)$$

Where $\frac{P_f^A(E_{ex})}{P_f^B(E_{ex})}$ is the ratio of the decay probability of the two compound systems at the same excitation energy, which can be experimentally measured, and ratio of the neutron capture cross section for the corresponding target nuclei in the neutron induced reaction at the same excitation energies, $\frac{\sigma_{CN}^{n+A}(E_{ex})}{\sigma_{CN}^{n+B}(E_{ex})}$, is calculated by using an optical model, thereby enabling one to find out the neutron-induced fission cross section for an unknown system.

More recently, the HSRM has been developed and employed by Nayak *et al.* [8] to determine the ^{233}Pa(*n, f*) cross sections in the equivalent neutron energy range of 11.5– 16.5MeV. In the SRM the two compound nuclei corresponding to "desired" and "reference" reactions are populated by performing the same surrogate reaction on two different targets, whereas in the HSRM one performs two surrogate reactions on the same target *in situ* in two different transfer reactions, where two compound nuclei corresponding to the "desired reaction" and the "reference reaction" are populated with similar excitation energy. The relative fission decay probabilities of the compound nuclei are measured experimentally to determine the cross sections of the desired compound nuclear reaction by using Eq. (1). In the HSRM, thus by taking a ratio of two reactions on the same target, systematic uncertainties due to target thickness, beam current, and dead time in the determination of the ratio of fission decay probabilities corresponding to "desired" and "reference" reactions are eliminated [8,10].

In the present work, we report our recent results on determination of ^{234}Pa(n,f), ^{239}Np(n,f), and ^{240}Np(n,f) compound nuclear cross sections by measuring the ratio of fission decay probabilities in [^{232}Th(^{7}Li,α)^{235}Pa / ^{232}Th(^{7}Li,t)^{236}U],[^{238}U(^{6}Li,α)^{240}Np / ^{238}U(^{6}Li,d)^{242}Pu], and [^{238}U(^{7}Li,α)^{241}Np / ^{238}U(^{7}Li,t)^{242}Pu] transfer reactions respectively employing HSRM.

EXPERIMENTAL DETAILS

Measurements were carried out using ^{6,7}Li beams obtained from the Bhabha Atomic Research Centre–Tata Institute of Fundamental Research (BARC-TIFR) Pelletron Accelerator Facility in Mumbai. The two silicon surface barrier ΔE-E detector telescopes $T1$ and $T2$ with ΔE detectors of thicknesses of 150 and 100 μm, respectively, and with identical E detectors of thicknesses of 1.0 mm were mounted in a reaction plane at angles of 85° and 105° with respect to the beam direction to identify projectile-like fragments (PLFs). Aluminum foil of thickness of 3.86 mg/cm^2 was placed in front of the particle telescopes to stop the fission fragments and thereby protect the ΔE detectors from radiation damage. The PLFs (protons, deuterons, tritons and α particle) are uniquely identified by plotting the partial energy loss in the ΔE detector against the residual energy (E_{res}) in the E detector. A large-area (450 mm^2) solid state detector was kept at an angle of 160° with respect to the beam direction and subtended a solid angle of 63msr with an angular opening of 16° to detect fission fragments in coincidence with PLFs. The telescopes were energy calibrated by using a ^{228,229}Th source and in an in-beam experiment that made use of the discrete α-particle peaks corresponding to ^{15}N* states from the ^{12}C(^{7}Li, α)^{15}N* reaction at a ^{7}Li beam energy of 18.0 MeV.

RESULTS AND DISCUSSION

(a) Determination of ^{234}Pa(n, f) cross sections

The compound nuclei ^{235}Pa and ^{236}U are formed in situ in ^{232}Th(^{7}Li,α)^{235}Pa* and ^{232}Th(^{7}Li,t)^{236}U* transfer reactions are identified by outgoing alpha and triton PLFs, respectively. The ground state Q-values (Q_{gg}) for the above reactions is 5.642 and -7.040 MeV, respectively. The ^{7}Li beam energy of E_{lab}=39.5 MeV was chosen, so that the ^{235}Pa and ^{236}U compound systems are populated at overlapping excitation energies. The excitation energy spectra for the ^{235}Pa and ^{236}U compound systems are obtained by employing two-body kinematics for the outgoing PLFs alpha and triton respectively. The excitation energy spectra of ^{235}Pa and ^{236}U compound systems for PLF-fission coincidence and PLF singles are shown in Fig.1 below.

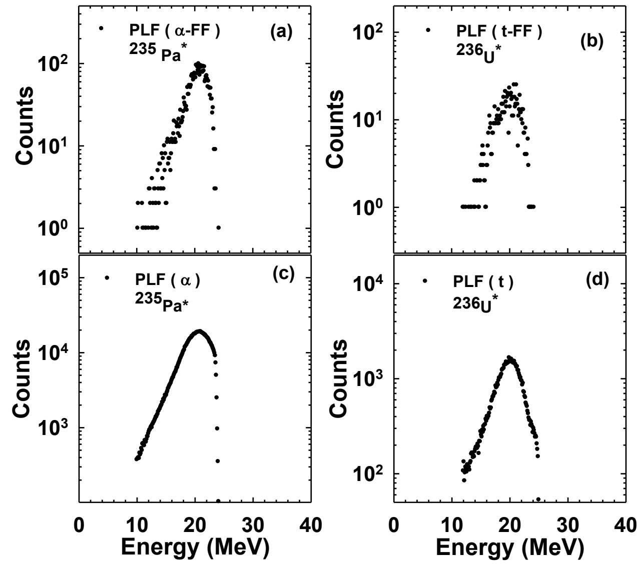

Fig.1: Excitation energy spectra of target like fragments in $^{6}Li+^{232}Th$ reaction with (bottom) and without (upper) coincidence with fission fragments.

The fission decay probabilities of ^{235}Pa and ^{236}U compound systems are determined in steps of 1.0 MeV excitation energy bin by taking the ratio of number of coincidence events between the outgoing PLF-fission fragment to the number of PLF singles, using the relation Eq.(2) as follows:

$$P_f(E_{ex}) = \frac{N_{i-f}}{N_i}, \qquad (2)$$

where, *i* denotes the alpha or triton PLF channels. For each excitation energy bin of 1.0 MeV, the ratio of fission decay probability of the ^{235}Pa and ^{236}U compound nuclei is determined. The relative fission probabilities of the compound nuclei are then multiplied with the ratio of the corresponding neutron induced compound nucleus formation cross section $\sigma_{CN}^{n+^{234}Pa}(E_{ex})$ and $\sigma_{CN}^{n+^{235}U}(E_{ex})$, to obtain the ratio of the compound nuclear reaction cross section at the excitation energies of n $+^{234}Pa \rightarrow ^{235}Pa^* \rightarrow$fission and n $+^{235}U \rightarrow ^{236}U^* \rightarrow$fission reactions using Eq.(1). The well measured n + $^{235}U \rightarrow ^{236}U \rightarrow$ fission cross section in the neutron energy range of 0 - 30.0 MeV are taken from ENDF/B-VII.1 [11] and used as the reference reaction with energy scale converted to excitation energy by adding the neutron separation energy of ^{236}U (S_n=6.545 MeV). The neutron induced compound nuclear formation cross sections for ^{234}Pa and ^{235}U nuclei have been calculated at corresponding excitation energy using EMPIRE- 3.1 code [13] with optical model potential parameters (OMP) taken from RIPL catalog number 2408 for Capote *et al.* [13]. The ^{234}Pa(n, f) cross sections as a function of excitation energy are obtained over the energy range of 14-20 MeV, using Eq.(1). Finally the excitation energies are scaled down by subtracting the ^{235}Pa neutron separation energy (S_n = 6.123) to obtain the ^{234}Pa(n, f) cross sections at the appropriate equivalent neutron energies. The present experimental results for the ^{234}Pa(n, f) cross sections in the equivalent neutron energy are shown in Fig.2 along with the predictions of EMPIRE-3.1 code for the fission barrier heights obtained from BF [9, 14,15] and RIPL-3 [16]. The present experimental data agree very well with the calculated neutron induced fission cross sections for the fission barrier heights obtained from BF. The predictions of EMPIRE-3.1 for the RIPL-3 fission barriers are only in agreement with the data for the neutron energies below 12 MeV. For the neutron bombarding energies above 12 MeV, the EMPIRE-3.1 calculations for RIPL-3 over predicts the experimental data.

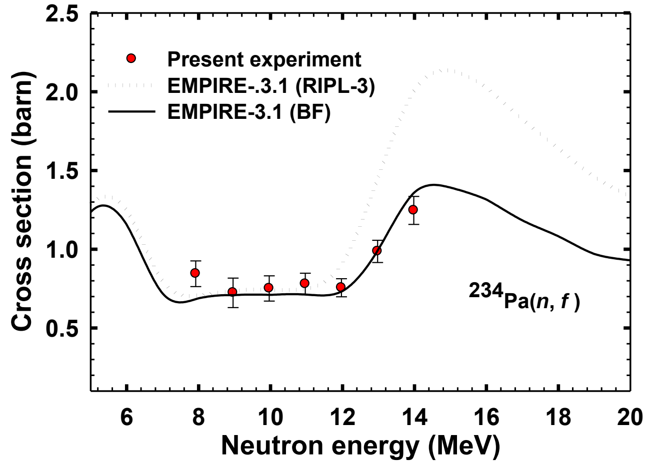

Fig.2: Experimental results on ^{234}Pa(n,f) cross sections along with EMPIRE-3.1 code predictions.

(b) Determination of ^{239}Np(*n,f*) and ^{240}Np(*n,f*) cross sections

The ^{238}U(^{6}Li,αf)^{240}Np* (surrogate of n+^{239}Np→^{240}Np*) and ^{238}U(^{6}Li, *df*)^{242}Pu* (surrogate of n+^{241}Pu→^{242}Pu*) transfer reactions at E_{lab} = 39.6MeV has been used to produce ^{240}Np* and ^{242}Pu* compound nuclei at overlapping excitation energy range of 16.5 - 22.5 MeV. Hence the ratio of fission decay probabilities $\frac{P_f^{240Np}(E_{ex})}{P_f^{242Pu}(E_{ex})}$ of the compound systems ^{240}Np and ^{242}Pu is determined. Similarly, the ^{238}U(^{7}Li, αf)^{241}Np* (surrogate of n+^{240}Np→^{241}Np*) and ^{238}U(^{7}Li, *tf*)^{242}Pu* (surrogate of n+^{241}Pu→^{242}Pu*) transfer reactions at E_{lab} =41.0 MeV have been used to populate ^{241}Np* and ^{242}Pu* compound nuclei at the overlapping excitation energy range of 15.0 - 22.0 MeV. Hence the ratio of fission decay probabilities $\frac{P_f^{241Np}(E_{ex})}{P_f^{242Pu}(E_{ex})}$ of the compound systems ^{241}Np and ^{242}Pu is determined. The ratios of fission decay probabilities $\frac{P_f^{240Np}(E_{ex})}{P_f^{242Pu}(E_{ex})}$ and $\frac{P_f^{241Np}(E_{ex})}{P_f^{242Pu}(E_{ex})}$ are then multiplied by the ratio of the corresponding neutron-induced compound nucleus formation cross section, $\frac{\sigma_{CN}^{n+^{239}Np}(E_{ex})}{\sigma_{CN}^{n+^{241}Pu}(E_{ex})}$ and $\frac{\sigma_{CN}^{n+^{240}Np}(E_{ex})}{\sigma_{CN}^{n+^{241}Pu}(E_{ex})}$ to obtain the compound nuclear reaction cross section ratios $\frac{\sigma_f^{n+^{239}Np}(E_{ex})}{\sigma_f^{n+^{241}Pu}(E_{ex})}$ and $\frac{\sigma_f^{n+^{240}Np}(E_{ex})}{\sigma_f^{n+^{241}Pu}(E_{ex})}$ at similar excitation energies using Eq. (1). The neutron-induced compound nucleus formation cross sections for the present reactions have been determined using the EMPIRE-3.1 code. The $\sigma_{CN}^{n+^{241}Pu}(E_{ex})$ cross-section values as a function of excitation energy were used as the reference reaction in both the cases; these have been derived from Tovesson and Hill [17] by using the neutron separation energy of ^{242}Pu (S_n = 6.545 MeV). The ^{239}Np(*n, f*) and ^{240}Np(*n, f*) cross sections as a function of excitation energy were obtained over the excitation energy ranges of 16.5–22.5 and 15.0–22.0 MeV, respectively, using Eq. (1). The ^{239}Np(*n, f*) and ^{240}Np(*n, f*) cross sections as a function of excitation energy are then converted to the equivalent neutron energy ranges of 10.5–16.5 and 9.0–16.0 MeV by using neutron separation energies of ^{240}Np (S_n = 5.066 MeV) and ^{241}Np (S_n = 6.13 MeV), respectively. The present experimental data have been compared with the recently reported ^{239}Np(n, f) cross sections by Czeszumska *et al.* [18], and adopted cross-section data from JENDL-4.0 [19] are shown in Fig. 3 along with the calculated cross sections using the EMPIRE-3.1 code for fission barrier parameters obtained from BF. The present experimental results for the ^{239}Np(n, f) cross sections are found to be somewhat higher than the predictions of the EMPIRE-3.1 code. It can be also seen from Fig. 3 that the ^{239}Np(n, f) cross sections of the present work follow closely the recently reported ^{239}Np(n, f) cross sections by Czeszumska *et al.* [18] in the neutron energy range of 13.0–16.0 MeV; however, the ^{239}Np(n, f) cross-section values deduced by Czeszumska *et al.* in the neutron energy range of 10.0–13.0 MeV are different from the present results. The trend of the JENDL-4.0 data is much lower as compared to the present values of experimental ^{239}Np(n, f) cross sections. However, it is observed that, by reducing the inner and outer barrier heights of the ^{239}Np isotope from the BF predicted values of 5.84 and 5.56 MeV to 5.10 and 5.25 MeV, respectively, the EMPIRE-3.1 code calculations, a better comparison with the present experimental ^{239}Np(n, f) cross sections data is obtained, as shown in Fig. 3 denoted as "best fit". The present experimental ^{240}Np(n, f) cross sections are found to compare reasonably well with the EMPIRE-3.1 calculations in the neutron energy range of 9.0–16.0 MeV, as shown in Fig. 4, for default BF barriers and also for the best fit of ^{239}Np(n, f) barriers.

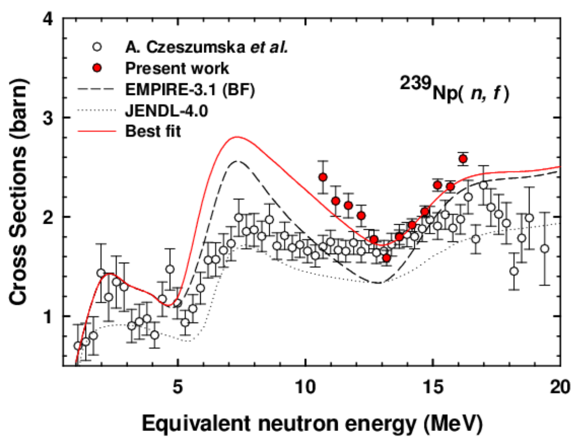

Fig.3: Experimental ^{239}Np(n, f) cross sections, present measurements (solid circles), and the work of Czeszumska *et al.* [18] (open circles). Calculated results are from the EMPIRE-3.1 code for fission barriers obtained from the barrier formula (BF) (short dashed line). The adopted data from the JENDL-4.0[19] nuclear data library (dotted line) and the best fit (solid line) are also shown.

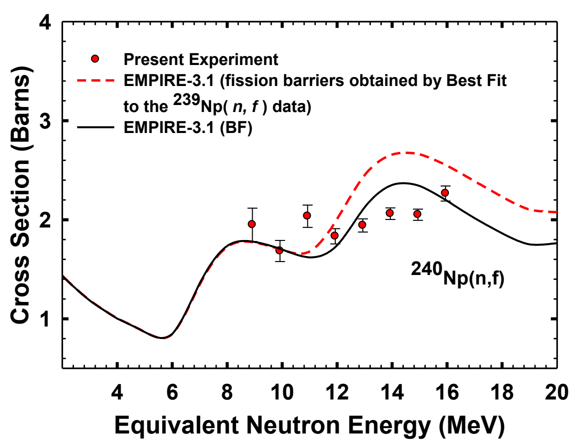

Fig.4 : Experimental ^{240}Np(n, f) cross sections and calculated results using the EMPIRE-3.1 code.

SUMMARY AND CONCLUSION

In summary, we have employed a new surrogate approach to determine the ^{234}Pa(n,f), ^{239}Np(n,f), and ^{240}Np(n,f) cross sections in the equivalent neutron energy range 10.0 MeV to 16.0 MeV using ^{7}Li+^{232}Th and ^{6,7}Li+^{238}U transfer-fission coincidence measurements. Present experimental data have been compared with the predictions of EMPIRE-3.1 for fission barrier heights corresponding to RIPL-1, and Barrier Formula.

REFERENCES:

[1] J. E. Escher, J. T. Burke, F. S. Dietrich, N. D. Scielzo, I. J. Thompson, and W. Younes, Rev. Mod. Phys. **84**, 353 (2012).

[2] J. D. Cramer and H. C. Britt, Phys. Rev. C **2**, 2350 (1970).

[3] H. C. Britt and J. D. Cramer, Phys. Rev. C **2**, 1758 (1970).

[4] C. Plettner *et al.*, Phys. Rev. C **71**, 051602(R) (2005).

[5] J. T. Burke *et al.*, Phys. Rev. C **73**, 054604 (2006).

[6] V. V. Desai *et al.*, Phys. Rev. C **87**, 034604 (2013).

[7] J. J. Ressler *et al.*, Phys. Rev. C **83**, 054610 (2011).

[8] B. K. Nayak *et al.*, Phys. Rev. C **78**, 061602(R) (2008).

[9] V.V. Desai, B.K. Nayak, A. Saxena *et al* Phys. Rev**. C 88**, 014613 (2013).

[10] B. F. Lyles *et al.*, Phys. Rev. C **78**, 061602(R) (2008).

[11] M. B. Chadwick *et al.*, Nucl. Data Sheets **107**, 2931 (2006).

[12] M. Herman *et al.*, Nucl. Data Sheets **108**, 2655 (2007).

[13] R. Capote *et al.*, J. Nucl. sci. and Tech. (Japan), Vol.**45**, No.4, p.333340 (2008).

[14] S. K. Gupta and A. Saxena, in *Proceedings of 8th International Workshop on Nuclear Data Production and Evaluation (NDPE), Pohang Accelerator Laboratory (PAL)* (Pohang University of Science and Technology (POSTECH), Korea, 2005).

[15] S. K. Gupta and L. Satpathy, Z. Phys. **A 326**, 221 (1987).

[16] R. Capote et al., Nucl. Data Sheets **100**, 3107 (2009).

[17] F. Tovesson and T. S. Hill, Nucl. Sci. Eng. **165**, 224 (2010).

[18] A. Czeszumska *et al.*, Phys. Rev. C **87**, 034613 (2013).

[19] K. Shibata *et al.*, J. Nucl. Sci. Technol. **48**, 1 (2011).

Spatiotemporal Distribution of Nuclear Showers Generated By Super-High Energy Cosmic Radiation

R.U.Beisembayev[(1)], Ye.A.Beisembayeva[(1)], Yu.N.Vavilov[(1)], N.G.Vildanov[(1)], M.I.Vildanova[(1)], O.D.Dalkarov[(1)], V.V.Zhukov[(1)], V.P.Pavluchenko[(1)], V.A.Ryabov[(1)], N.O.Saduyev[(2)], T.Kh.Sadykov[(3)], A.V.Stepanov[(1)], Zh.S.Takibayev[(2)], N.Zh.Takibayev[(2)], S.B.Shaulov[(1)].

[(1)] *The P.N. Lebedev Physical Institute under Russian Academy of Sciences, Moscow, Russia.*
[(2)] *Al-Farabi Kazakh National University, Almaty, Kazakhstan.*
[(3)] *Institute of Physics and Technology, Almaty, Kazakhstan.*

Primary cosmic rays (PCR) are represented by five groups of nuclei ranging from protons to iron nuclei. This understanding was formed is a series of experiments at artificial satellites at energies $E \leq 10^{15}$ eV. Nuclear composition of cosmic radiation (CR) at super-high energies $E \geq 10^{17}$ eV is still undisclosed and remains an object of modern research. The ambiguity in CR composition is related to a range of other unsolved problems in astrophysics; so, the processes which form the energy spectrum of super-high energy CR are still unknown.

For over fifty years the Tyan-Shan High-Altitude Scientific Station of the Lebedev Physical Institute (TShHASS) has been one of the world's leading centers for studies of cosmic radiation. The station is located in vicinity of Almaty in Zailiisky Alatau Mountains at the altitude 3,340m above the sea level. Horizon-T installation is located at TShHASS. There is a novel instrument for complex studies of spatiotemporal characteristics of nuclear showers generated by super-high energy cosmic radiation in the Earth's atmosphere.

The installation Horizon-T can register in the nuclear showers the shower discs of charged particles and shower discs of Vavilov-Cherenkov radiation in the range of zenith angles 0-85° at nanosecond precision rate. Geometry factor of the installation is 1 $km^2 \cdot sr$; registration threshold is estimated to be $4 \cdot 10^{16}$ eV.

Experimental data obtained at Horizon-T installation demonstrated existence of two new phenomena in the nuclear showers generated in the Earth atmosphere by super-high energy cosmic radiation:

1. For the showers coming at zenith angles more than 70°, the shower disk of Vavilov-Cherenkov radiation reached the installation prior, simultaneously with or later than the shower disk of charged particles. Calculation analysis showed that in the first case the nuclear showers are generated by protons, in the second – by alpha-particles, and in the third case – by CNO nuclei, aluminum or iron nuclei.

2. Among the registered events are hundreds of those with multi-peak pulses. We suppose such events with several peaks are generated by groups of particles which simultaneously reached the atmosphere. We also suppose that these groups of particles are the daughter products at decay of a massive single particle with the mass considerably exceeding mass of any known particle.

TRITIUM AND HELIUM FORMATION IN A BERYLLIUM SLAB, LOCATED IN THE NEUTRON FLUX

Kunakov S., Takibayev N., Kenzhebayev N.

Faculty of Physico-Technical, al-Farabi Kazakh National University, Almaty, Kazakhstan

Abstract

Energy needs accelerate the development of methods for producing electricity , the most promising of which is , of course , nuclear power . In the nuclear power industry , such restrictions often associated with materials research , most of the problems which is either a justification for extending the life of the materials used in nuclear and thermonuclear devices or choice of materials or the creation of new materials with physical properties superior to the known use . Recently, increasing attention has been paid to such reactor materials like beryllium. Beryllium has a good set of neutron-physical characteristics : low neutron absorption cross section , high retarding capacity due to low atomic weight and high neutron scattering cross-section , so it is widely used in the nuclear industry as a material for reflectors , moderators , neutron sources , as well as the recent beryllium time began to attract interest in the use as a breeder , the first wall or limiter in fusion devices .

1. Accumulation of helium in beryllium under neutron irradiation

Irradiation of beryllium by fast particles contributes to the formation and accumulation of radiation defects in it, and the nuclei of helium and tritium from nuclear reactions in the beryllium atoms. Damage to the beryllium neutron irradiated is the result of two known in radiation physics processes - the elastic interaction of neutrons with nuclei and nuclear reactions ((n, 2n), (n, α)) []. In elastic interaction of neutrons with nuclei of atoms is shifted out of their seats. The total number of displacements during the irradiation is estimated by the formula

However, beryllium is subject to significant radiation damage under the influence of neutron radiation. Irradiation of beryllium by fast particles contributes to the formation and accumulation of radiation defects in it , and the nuclei of helium and tritium from nuclear reactions in the beryllium atoms . In certain irradiation parameters , these effects can cause significant changes in the physical and mechanical properties of the material , the main of which practical application is the density , thermal conductivity, strength and ductility. Possible duration of the work in this case is determined by the neutron fluence , at which the maximum permissible reduction in the quality of beryllium. Now the world is already a considerable amount of irradiated beryllium , which can not be used further without additional processing and clearing it from the radioactive products (major sources of beryllium are such a research nuclear reactors and some thermonuclear installations , for example , JET). After the commissioning of ITER and DEMO total number of irradiated beryllium significantly increase. Currently, irradiated beryllium goes to waste , but the high cost and the potential risk of making radio-ecological disposal of irradiated beryllium highly undesirable procedure:

$$n + Be^9 \rightarrow He^4 + He^6,\ E \geq 0,71 MeV \rightarrow {}^6Li + n_{th} \rightarrow {}^3H + {}^4He \qquad (0.1)$$

$$n + Be^9 \rightarrow 2He^4 + 2n,\ E \geq 2.71 MeV \qquad (0.2)$$

$$^6He \xrightarrow[T_{1/2} \approx 0,85c]{\beta^-} {}^6Li \qquad (0.3)$$

$$n + Li^6 \rightarrow He^4 + H^3 \qquad (0.1)$$

2. The algorithm for calculating the distribution function of the neutron energy distribution

The calculation program was built on the processing circuit branching process for generations. The algorithm of the calculation.

The calculation program was built on the processing circuit branching process for generations. After each act of neutron traced with more energy, and the energy born of an neutronic memory. Then there are the neutron trajectories simulated future generations. Tracking the trajectory of the primary neutrons energy was carried out to 10 MeV down 1ev. In the code FDN *N* simulated particles were taken inti consideration with energy E_0 (mono-energetic source.) If the neutron energy $E > E_{gr}$ = 20 eV, the electron mean free path was played by the formula:

$$t = ln\ \xi\lambda(E) \qquad (0.7)$$

where λ - uniformly distributed in the interval [0,1] random number, λ (E) - mean free path is equal to

$$\Sigma\ (E) = (\Sigma_1(E) + \Sigma_2(E) + \cdots + \Sigma_i(E))^{-1} \qquad (0.8)$$

where $\Sigma_i(E)$ - macroscopic scattering cross-section *i*-th channel. Then scattering channel was played by the formula

$$\xi < (\Sigma_1 + \Sigma_2 + \cdots + \Sigma_i)/(\ \Sigma_1 + \Sigma_2 + \cdots + \Sigma_n) \qquad (0.9)$$

In the case of elastic scattering differential cross sections at the corner of the angle of the scattered neutrons was played out on the screened nucleus. The loss of energy in the elastic collision was calculated by the formula

$$\Delta E = (2m/M) \times (E - E_T\ ) \times (1 - cos\ \upsilon\ ) \qquad (0.10)$$

where *m* and *M* - the mass of the neutron and the scattering center, E_m - the thermal energy of the target atom, υ - scattering angle. In the case of nuclear reactions ((n, 2n), (n, α)) it was assumed that the energy of the ejected neutron with $E = E - E_b$ (E_b is the binding energy) is less than the energy of the scattered. Its coordinates, direction and energy are remembered for future follow-up. The energy of the scattered neutron played out similarly to from the distribution.

The new coordinates the interaction of the electron considered when calculating the neutron mean free path *t* - by (4.3.1) and the cosine of the scattering angle $cos\ \upsilon_i$. For the three-dimensional coordinates (x_i, y_i, z_i) conversion formulas have the form

$$x_{i+1} = x_i + t \cos \upsilon_x \quad (0.13)$$

$$y_{i+1} = y_i + t \cos \upsilon_y \quad (0.14)$$

$$z_{i+1} = z_i + t \cos \upsilon_z \quad (0.15)$$

Here, the vector ($\cos \upsilon_x$, $\cos \upsilon_y$, $\cos \upsilon_z$) with the coordinate axes. Recalculation formulas of spherical trigonometry vector angles of the direction cosines of the particle of new directions after scattering angle υ is well-known.

To calculate the neutron distribution function is summed up time during which the neutrons and the secondary neutrons generated by them $d\tau\Sigma = \Sigma\tau^1$in the interval $d\xi$. Number traces the history should not be much large, since proportionally increase the cost of computer time, but it should provide the statistical reliability of the calculated distributions. The following technics were also realized inthe code FDN:

- Determine which isotope the interaction is with
- Determine which interaction type for that isotope
- Determine the energy & direction of the exiting particle
- Determine if secondary particles were produced
- Biasing + weight adjustments
- Tallies of quantities of interest

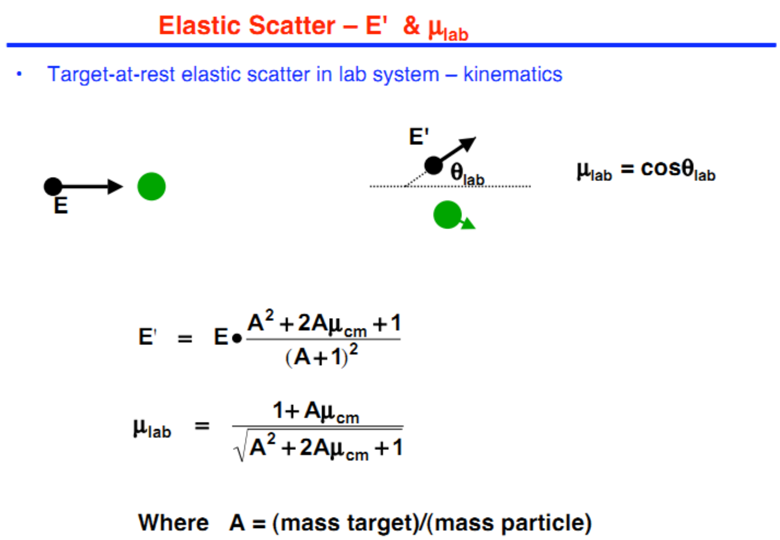

Figure 1: Target-at-rest elastic scatter in lab system – kinematics

3. Helium formation in a beryllium slab, located in the neutron flux

As part of the settlement of the problem includes the modeling of the finite spectrum of thermal neutrons incident irradiated beryllium (neutron-physical calculations), the generation of helium:

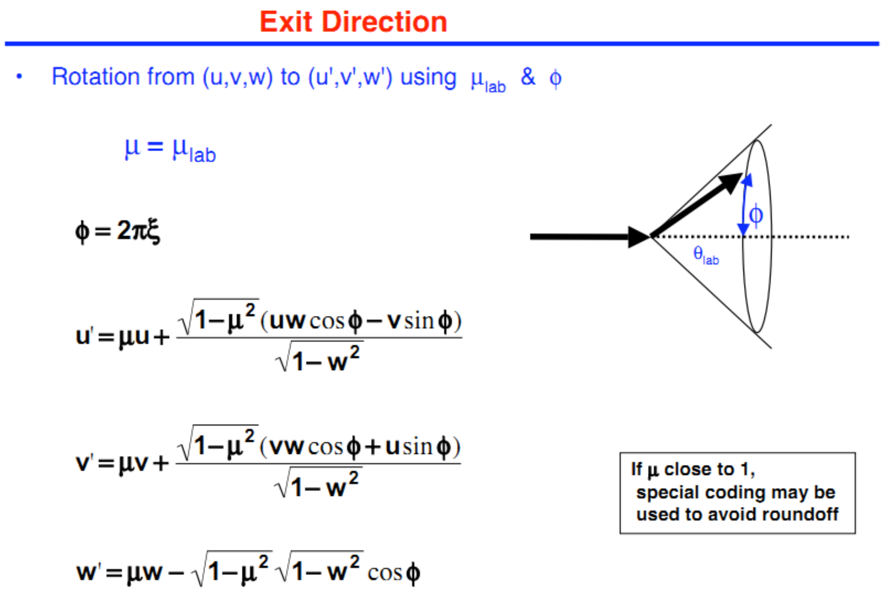

Figure 2: Rotation from (u,v,w) to (u',v',w') using μ_{lab} and tritium in a reactor irradiation within the set of geometry, as well as modeling of diffusion processes of tritium in the irradiated beryllium.

The fig.3 presents the neutron spectra within berillium slab:

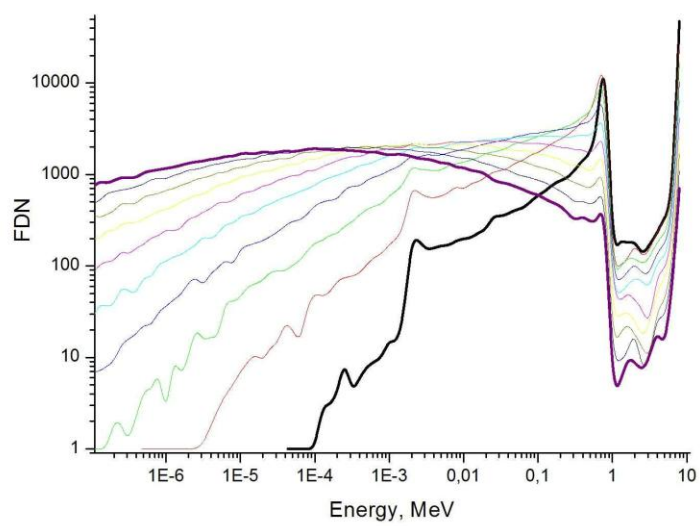

Figure 3: Time degradation of neutron energy spectra in the berillium sample for initial monochromatic neutron flux

The accumulation of tritium atoms in beryllium is shown on the fig 4. and in the fig 5. The presented results are to be discussed and should be compared with experimental data. However the programming code is very perspective in calculation of some definite reactor geometry containing beryllium materials and is to be on the further development.

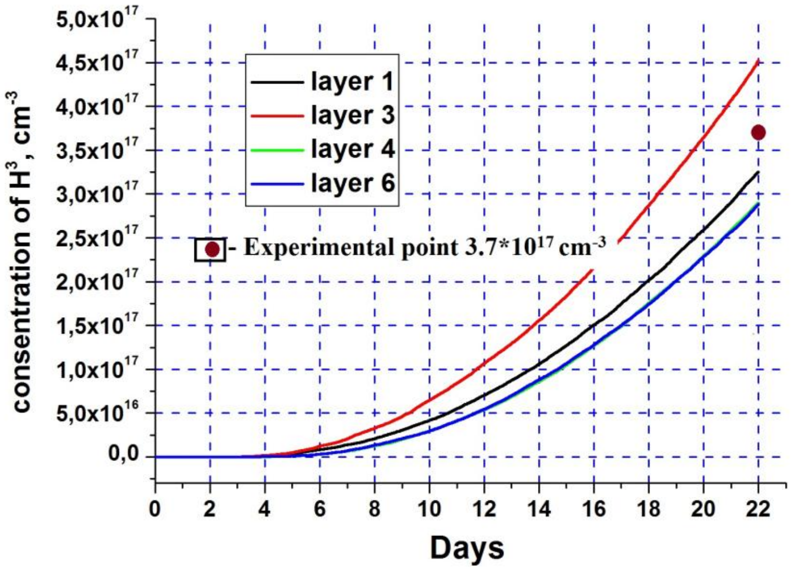

Figure 4: Accumulation of tritium atoms in beryllium slab

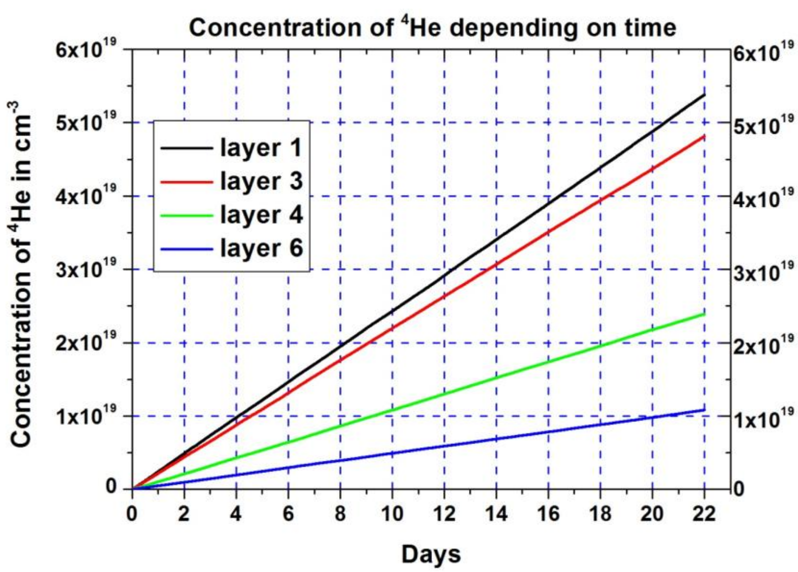

Figure 5: Accumulation of helium atoms in beryllium slab

The project (E-13) is supported by the fund of Ministry of Education and Sciences of Republic of Kazakhstan.

1. J. Lieberoth, "A Monte Carlo Technique to Solve the Static Eigenvalue Problem of the Boltzmann Transport Equation," Nukleonik 11,213 (1968).

2. M. R. Mendelson, "Monte Carlo Criticality Calculations for Thermal Reactors," Nucl. Sci Eng. 32, 319-331 (1968).

3. H. Rief and H. Kschwendt, "Reactor Analysis by Monte Carlo," Nucl. Sci. Eng., 30, 395 (1967)

4. Chikhray, Y.Measurement system for in-pile tritium monitoring from Li2TiO3 ceramics at WWRK reactor .Journal of Nuclear Materials , 1 August 2007. – Volumes 367-370, Part 2. – Pp. 1028-1032.

5. Y. Chikhray, H. Kawamura and K. Tsuchiya// Journal of Nuclear Materials, 30 April 2009. - Volumes 386-388. – Pp. 286-289.

List of Participants

1. Medeu Abishev
   Physico-Technical Faculty, al-Farabi Kazakh National University, Almaty, Kazakhstan
   abishevme@mail.ru

2. Masayuki Aikawa
   Nuclear Reaction Data Centre, Faculty of Science, Hokkaido University, Sapporo, Japan
   aikawa@sci.hokudai.ac.jp

3. Yuriy.Arkhipov
   Physico-Technical Faculty, al-Farabi Kazakh National University, Almaty, Kazakhstan
   Yuriy.Arkhipov@kaznu.kz

4. Erlan Batyrbekov
   National Nuclear Center of the Republic of Kazakhstan, Kurchatov, Kazakhstan
   nnc@nnc.kz

5. Muhammedkali Burkitbayev
   al-Farabi Kazakh National University, Almaty, Kazakhstan
   Mukhambetkali.Burkitbayev@kaznu.kz

6. Nasrulla Burtebayev
   Institute of Nuclear Physics, Almaty, Kazakhstan
   burteb@inp.kz

7. Leonid Chechin
   Fesenkov Astrophysical Institute
   chechin-lm@mail.ru

8. Vladimir Dzhunushaliev
   Physico-Technical Faculty, al-Farabi Kazakh National University, Almaty, Kazakhstan
   v.dzhunushaliev@gmail.com

9. Alnur Duysebayev
   Institute of Nuclear Physics, Almaty, Kazakhstan

10. Shuichiro Ebata
    Meme Media Laboratory, Hokkaido University, Sapporo, Japan
    ebata@nucl.sci.hokudai.ac.jp

11. A.Ermylov
    al-Farabi Kazakh National University, Almaty, Kazakhstan

12. Feruzjon Ergashev
Institute of Nuclear Physics, Academy of Sciences, Tashkent, Uzbekistan
ergashev@inp.uz

13. Maratbek Gabdullin
Nonalaborotory of the al-Farabi Kazakh National University, Almaty, Kazakhstan
gabdullin@physics.kz

14. Kenzhina Inesh
Physico-Technical Faculty, al-Farabi Kazakh National University, Almaty, Kazakhstan

15. Kyoshi Kato
Nuclear Reaction Data Centre, Faculty of Science, Hokkaido University, Sapporo, Japan
kato@nucl.sci.hokudai.ac.jp

16. Venera Kurmangalieva
Physico-Technical Faculty, al-Farabi Kazakh National University, Almaty, Kazakhstan
venera_baggi@mail.ru

17. Manas Khassanov
Physico-Technical Faculty, al-Farabi Kazakh National University, Almaty, Kazakhstan
manas_hasanov@mail.ru

18. Nurzat Kenzhebayev
Physico-Technical Faculty, al-Farabi Kazakh National University, Almaty, Kazakhstan
nurzat.kenzhebaev@gmail.com

19. Serik Kumekov
Institute of High Technologies of the Kazakh National Technical University. Almaty, Kazakhstan
skumekov@mail.ru

20. Sandybek Kunakov
International of IT University, Almaty, Kazakhstan
sandybeck.kunakov@gmail.com

21. Oleg Lavrishev
Research Institute of Experimental and Theoretical Physics, Almaty, Kazakhstan
lavr@physics.kz

22. Ayano Makinaga
Faculty of Science, Hokkaido University, Sapporo, Japan
makinaga@nucl.sci.hokudai.ac.jp

23. Meruert Nusipalyeva
Physico-Technical Faculty, al-Farabi Kazakh National University, Almaty, Kazakhstan
mikos_1991@mail.ru

24. Maygmarjav Odsuren
Meme Media Laboratory, Hokkaido University, Sapporo, Japan
odsuren@nucl.sci.hokudai.ac.jp

25. Naohiko Otsuka
Nuclear Data Section, International Atomic Energy Agency, Vienna, Austria
n.otsuka@iaea.org

26. Oleg Prikhodko
Physico-Technical Faculty, al-Farabi Kazakh National University, Almaty, Kazakhstan
Oleg.Prikhodko@kaznu.kz

27. Nurzhan Saduyev
Research Institute of Experimental and Theoretical Physics, Almaty, Kazakhstan
lvcl@mail.ru

28. Turlan Sadykov
Cosmic ray physics laboratories, Physico-Technical Institute, Almaty, Kazakhstan

29. Galya Spanova
Physico-Technical Faculty, al-Farabi Kazakh National University, Almaty, Kazakhstan
galiya.spanova@mail.ru

30. Nurgaly Takibayev
Al-Farabi Kazakh National University, Almaty, Kazakhstan
takibayev@gmail.com

31. Rahim Yarmukhamedov
Institute of Nuclear Physics, Uzbekistan Academy of Sciences, Tashkent, Uzbekistan
rakhim@inp.uz

32. Jaegwon Yoo
Korea Atomic Energy Research Institute, Daejeon, South Korea
jgyoo@kaeri.re.kr

33. Chingis Umarov
Fesenkov Astrophysical Institute
chingis.omarov@gmail.com

34. Sergei Zaitsev
Institute of Microelectronics Technology and High Purity Materials, Chernogolovka,Russia
zaitsev@ipmt-hpm.ac.ru

35. Valery Zhukov
Tien Shan Astronomical Observatory, Almaty, Kazakhstan

36. Venera Zhumabekova
Physico-Technical Faculty, al-Farabi Kazakh National University, Almaty, Kazakhstan
zh.venera@mail.ru

Nuclear Data Section
International Atomic Energy Agency
Vienna International Centre, P.O. Box 100
A-1400 Vienna
Austria

e-mail: nds.contact-point@iaea.org
fax: (43-1) 26007
telephone: (43-1) 2600-21710
Web: http://www-nds.iaea.org/